IPPJ-AM-59

ATOMIC AND MOLECULAR PROCESSES IN EDGE PLASMAS INCLUDING HYDROCARBON MOLECULES

EDITED BY H. TAWARA

INSTITUTE OF PLASMA PHYSICS
NAGOYA UNIVERSITY

NAGOYA, JAPAN

IPPJ-AM-59

ATOMIC AND MOLECULAR PROCESSES IN EDGE PLASMAS INCLUDING HYDROCARBON MOLECULES

Edited by H. Tawara

Institute of Plasma Physics, Nagoya University
Chikusa-ku, Nagoya 464-01, Japan

April 1988

Forewords

This volume is a proceedings of a workshop which was held at Institute of Plasma Physics, Nagoya University, on January 18, 1988. This workshop was intended to bring plasma and atomic and molecular physicists together in order to discuss the relevant problems related to the use of graphites and carbon layers coated on the plasma facing materials which is used for reduction of the impurities, in particular of high z metallic ions, and reduction of the radiation losses from them. Although our understanding of phenomena related to graphites and cabon layers seems to be primitive, some AM data are found to be already available. During this workshop, it was stressed that the contribution of higher order hydrocarbon molecules, which are produced from these carbon wall materials under intense hydrogen beam bombardment through chemical sputtering processes but were neglected up to now, should be taken into account properly in order to simulate the plasma processes including carbon atoms originated from graphite and related materials. Also it was suggested that some molecules such as $(CN)_2$, C_4H_2 or $C_4(CN)_2$ can be usable for coating the first wall which might result in the reduction of hydrogen contents in the coated carbon layers, compared with CH_4 gases, most widely used presently and some of them might have good sticking on the surfaces.

Finally the editor would like to thank the contributors to this volume and also both the speakers and the participants of this workshop for making the workshop fruitful.

H.Tawara (the editor), IPP/Nagoya

CONTENTS

1. N.Nishino, H.Kubo, A.Sakasai, Y.Koide, T.Sugie, H.Takeuchi and JT-60 Team : Light impurity behavior during NBI in JT-60 with carbon wall.....p.1
2. K.Kondo, K.Okazaki, T.Oda, N.Noda, K.Akaishi, H.Kaneko, T.Mizuuchi, F.Sano, O.Motojima and A.Iiyoshi : Spectroscopic Studies on carbon coating.....p.25
3. S.Amemiya : Carbonization and hydrogen concentration profile in the films.....p.41
4. H.Sugai : Carbonization processes and hydgrogen plasma interactions.....p.45
5. R.Yamada : C_2 and C_3 hydrocarbon release due to interaction of protons and graphite.....p.52
6. Y.Horino : Chemical sputtering of graphite under hydrogen ion irradiation.....p.60
7. H.Tawara : The present status of atomic and molecular data for edge plasmas.....p.80

Light Impurity Behavior during NBI in JT-60 with Carbon Wall

N.Nishino, H.Kubo, A.Sakasai, Y.Koide

T.Sugie, H.Takeuchi and JT-60 Team

ABSTRACT

Light impurity behavior during NBI is considered in JT-60 with carbon wall.

Two features are observed from recent experiments during OH and NBI in JT-60 plasma. First, metal impurities, mainly Ti and Mo, are reduced after carbonization meanwhile light impurities increase. Therefore the effective charge of plasma, Z_{eff}, at the wall temperature of 300°C is found to be larger than that before carbonization. However, Z_{eff} can be decreased to the same value as that before carbonization by lowering the wall temperature. Second, two types of light impurity behavior during NBI are observed depending on discharge mode. One is that the time evolution of the line intensity of CVI (1s-2p) is similar to that of OVIII (1s-2p) during NBI. The other is that the carbon line increases during NBI, meanwhile, the oxygen line decreases. This latter type occurs only in a limiter discharge with a high power of NBI and small gas puff rate during NBI. The spectroscopic measurement shows that the influx of carbon impurity increases with decreasing that of oxygen impurity in this type.

These results indicate the release mechanism of carbon and

oxygen impurity from graphite wall relates closely to the wall temperature and the plasma-wall interaction, especially, to the chemical sputtering.

1. INTRODUCTION

Impurities cool the plasma by their radiation emission. Moreover, they decrease the proton ratio and may affect plasma confinement and disruption through Z_{eff}.

Metal impurities (high Z) have a large cooling-rate. Therefore, they enhance the total radiation in spite of a little quantity in a plasma. On the contrary, light impurities (low Z) affect mainly Z_{eff}, since their quantities are much larger than those of metal impurity.

In 1987, the first wall of JT-60 was changed from TiC-coated Mo to graphite in order to reduce metal impurity. Thus the metal impurity, mainly Ti and Mo in JT-60 plasma, are successfully reduced by a factor of 5-10. On the other hand, Z_{eff} determined from visible bremsstrahlung increases and becomes larger than that when the TiC-coated Mo first wall is used.

Therefore, it is important to know the detailed mechanisms of light impurity release from graphite in order to control Z_{eff}.

2. EXPERIMENTAL DEVICE AND IMPURITY DIAGNOSTICS

2.1 Tokamak device JT-60

JT-60 is a large tokamak device [1] (major radius = 3.03 m, minor radius = 0.95 m) in Japan. Figure 1 shows the cross-sectional view of JT-60 vacuum chamber. The graphite tiles are located at the inner wall, the near divertor throat and outer divertor plate. The graphite tiles covers about 40% area of the whole surface. The two kinds of graphite tiles are used, one is ETP-10 (IBIDEN Ltd.) for the first wall and the other is HCB-18S (Hitachi Chem. Ltd.) for the divertor plate. The thermal characteristics of both graphites are similar. Before experiment, in order to quickly release impurities from the wall, the vacuum vessel is baked out up to 350℃, and TDC (Taylor discharge cleaning) and GDC(glow discharge cleaning) were carried out by several thousands of the main shots. The time variation of the residual gas pressures of each impurity are shown in Fig. 2. They decreased about two orders of magnitude after several tens hours of pumping.

2.2 Impurity measurement systems

It is important to study impurity behavior in a plasma. A number of spectrometers are installed in JT-60 for diagnostics. They are identified as A4x systems, x being denoted from A to F depending on their location. Their arrangements are shown in Fig. 3, and the characteristics of each system are summarized in table 1. In these impurity measurement systems, A4A and A4D systems have several multi-spectrum spectrometers. The lines of sight of these systems are different. A4A system views the upper half of plasma

by four multi-spectrum spectrometers, and A4D system views the area of the crossing point near the divertor (see Fig.9 for example) by two. The same unit-type spectrometers were used in both systems to be installed easily. Table 2 shows the characteristics of these four different unit-type spectrometers. Each spectrometer observes the photons in VUV region corresponding to the spectra of impurities in a high temperature plasma, especially for, the spectra of metal impurities and highly ionized light impurities.

3. RESULTS AND DISCUSSION

The experimental period after carbonization of JT-60 is spanned from June to October in 1987. In this period about 1500 discharges were carried out including 400 discharges of NBI experiment.

First, the reduction effect of the metal impurity by carbon wall was examined. Figure 4 and 5 show the spectra before and after carbonization. After carbonization, practically no spectral lines of metal impurities were observed in non-disruptive discharges. The impurity content and Z_{eff} were obtained by the absolute sensitivity calibrated systems as A4E and A4F. The metal impurities in JT-60, mainly Ti and Mo, are reduced by a factor of 5-10, meanwhile Z_{eff} increase. Figure 6 shows the dependence of Z_{eff} on the electron density before and after carbonization. These results were obtained at the wall temperature of 300°C. They indicate that light impurities, carbon and oxygen, increase when the carbon wall is used. In fact, the observed line intensities

of light impurities after carbonization are larger than that before carbonization.

However, it is found that Z_{eff} can be decreased to the same value as that before carbonization by lowering the wall temperature to 150°C. Figure 7 shows the dependence of Z_{eff} on the electron density at various wall temperatures.

Second, the two types of light impurity behavior were observed during NBI. Figure 8 shows the time evolution of line intensities of light impurity. The upper is identified as type A, where the time evolution of the line intensities of carbon and oxygen are similar. The lower is identified as type B, where the line intensities of carbon increase during NBI, meanwhile those of oxygen decrease. Figure 9 and 10 show that the time evolution of the line intensities of each type measured with A4A and A4D systems. In type A, the time evolution of carbon lines measured with A4A and A4D are similar to that of oxygen. Therefore, the time evolution of the influx of carbon and oxygen should be similar. On the other hand, in type B, different features are observed for carbon and oxygen ions. The spectral lines from carbons increase relatively slowly at the beginning and, then, increase rapidly. This increments (A in Fig.10) of carbon lines measured with A4D are larger than those with A4A. On the other hand, the line intensities of oxygens increase at the beginning and, then, decrease: the decrements (A in Fig.10) of oxygen lines measured with A4A are larger than those with A4D. Therefore in type B the influx of carbon increase, meanwhile the influx of

oxygen decrease during NBI. Type A often occurs in a divertor discharge, while type B often occurs under a limiter discharge with a high power of NBI and a little gas puffing during NBI. Figure 11-13 show the occurrence frequency of each type for different discharge conditions. Moreover, the transformation from type A to B during NBI is observed as in Fig. 14. In this figure, first, type A is observed at a low power of NBI; then, when the power of NBI increases up to 20MW, type B occurs; and lastly by introducing gas puff type B disappears.

Type B is observed only since the first wall was changed to the graphite tiles. Therefore, it is believed that type B relates to the plasma-wall interaction and the characteristics of graphite. The mechanisms of impurity release from graphite under irradiation of the intensive flux of hydrogen have been studied[2-17] recently. It was reported that the chemical sputtering of graphite is large within the temperature range of 500*K* - 1200*K*. In both types, the wall loading increases by NBI power and the wall temperature increases during NBI. In type A of the limiter discharges, the high energy (a few *keV*) protons decrease at the periphery owing to large gas puffing because of the electron capture and collision. Therefore, only low energy (a few hundreds of *eV*) protons can strike to the graphite wall, meanwhile in type B, the high energy protons do not decrease therefore low and high energy protons hit onto the graphite wall. In divertor discharges, type B rarely occurs, and it can be understood from the fact that the temperature rise of divertor plates is not so large owing to

remote cooling as to trigger the chemical sputtering. Thus, it is thought that the increase of carbon is due to the chemical sputtering, although, it can not account for the decrease of the influx of oxygen. Up to now, the change of mechanism of oxygen release from graphite under irradiation with the intensive hydrogen flux have not been reported. As far as oxygen release is concerned, the outflux of molecular contained oxygen from graphite is found to change[16,17] after irradiation with high energetic hydrogen beam. Figure 15 shows some experimental results. These depend on the characteristics of the graphite targets themselves. Some graphite target has characteristics of oxygen release which change after irradiation with hydrogen beams. It is not clear for us if ETP-10 (graphites of JT-60 first wall) has similar characteristics. Therefore, it is to be hoped that the outflux of oxygen from graphite would be investigated in details.

SUMMARY

Light impurity behavior during NBI in JT-60 plasmas with carbon wall was considered. The two results were obtained through recent NBI experiments of JT-60.

First, metal impurity are successfully reduced by changing the wall materials from TiC-coated Mo to graphite. However, light impurities increase and, then, Z_{eff} is found to be larger than that before carbonization. When the wall temperature was lowered, Z_{eff} decreased to the same value as that before carbonization.

Second, the two types of light impurity behavior were observed during NBI. One was that the time evolution of line intensity of carbon is similar to that of oxygen, and the other was that the line intensity of carbon increases meanwhile that of oxygen decreases. From spectroscopic measurement, it is found that these features are caused by the changes of the light impurity influx during NBI. As far as the erosion process of graphite is concerned, it is concluded that the influx of carbon increases owing to the chemical sputtering and it is expected that the influx of oxygen decrease by changing the mechanism of oxygen release from graphite due to energetic hydrogen flux.

References

1. JT-60 team : in Plasma Physics and Controlled Nuclear Fusion Research (Proc. 11th Conf. Kyoto, 1986), IAEA, Vienna, Vol.1, 1987 p11

2. K.L.Wilson and W.L.Hsu
: J. Nucl. Mater. 145&147 (1987) 121

3. J.Roth : J. Nucl. Mater. 145&147 (1987) 87

4. J.Roth, J.Ehrenberg, et al
: J. Nucl. Mater. 145&147 (1987) 383

5. C.H.Wu : J. Nucl. Mater. 145&147 (1987) 448

6. A.A.Haasz and J.W.Davis
: J. Nucl. Mater. 145&147 (1987) 77

7. R.Yamada and K.Sone : J. Nucl. Mater. 120 (1984) 119

8. A.A.Haasz, J.W.Davis, et al
: J. Nucl. Mater. 145&147 (1987) 412

9. R.Beutler, A.A.Haasz and P.C.Stangeby
: J. Nucl. Mater. 145&147 (1987) 280

10.E.Vietzke, T.Tanabe, et al
: J. Nucl. Mater. 145&147 (1984) 425

11.R.Yamada, K.Makamura, et al
: J. Nucl. Mater. 95 (1980) 278

12.R.Yamada, and K.Sone : J. Nucl. Mater. 116 (1983) 200

13.J.Roth J.Bohdansky and K.L.Wilson
: J. Nucl. Mater. 111&112 (1982) 775

14.A.A.Haasz, O.Auciello and P.C.Stangeby
: J. Vac. Sci. Technol.A4(1986) 1179

15.J.Roth : Sputtering by Particle Bombardment II, Topics Applied Physics, Vol.52 (Springer-Verlag, New York 1983) p93

16.T.Hino and T.Yamashina : TANSO 130 (1987) 118

17.T.Hino : private communication

Table 1. A-4 Impurity Measuring System

Symbol Diagnostics	Specification	Feature	Volume of Data
A-4-a Light Impurity Spectrometer (Spatial Resolution)	λ: 0.5~50 nm (0.02~50 nm) Δt ≳ 20ms Z_j: 2 points, ΔZ = 7 cm (15 points)	Holographic grating, Flat field, (Crystal grating) 1024 ch and 512 ch array detectors, Real time	800KW for MDR (12 MW) 128 KW for ISP
A-4-b Light Impurity Spectrometer (Doppler)	λ = 100~235nm (0~900nm) Δt ≳ 1 ms, X_j : 1 point	Concave grating, 32 ch array detector Photograph	320KW for MDR (1.6 MW) 128 KW for ISP
A-4-c Heavy Impurity Spectrometer (Doppler)	λ = 0.15~0.27nm Δt ≳ 1 ms, X_j : 1 point	Crystal grating, (Si, SiO_2) 32 ch array detector Real time	320KW for MDR (1.6 MW) 128 KW for ISP
A-4-d Spectrometer for Divertor	λ = 2 ~ 120 nm, Δt ≳ 10 ms X_j : 1 point	Holographic grating, Flat field, 1024 ch and 512ch array detectors	1.6 MW for MDR 128KW for ISP
A-4-e Visible Spectrometer for Absolute Callbration	λ = 200~700 nm, Δt ≳ 0.05ms X_j : 1 point	Photomultiplier & Photograph	128 KW for ISP
A-4-f Grazing Incidence Spectrometer for Absolute Calibration	λ = 1 ~ 130 nm (0~130nm) Δt ≳ 0.05ms X_j : 1 point	Same as above	128 KW for ISP
A-4-g A-4 System Calibration Devices		Light source etc.	

( ) indicates plan.

Table 2. Characteristics of unit-type spectrometers

Unit	Type-1	Type-2	Type-3	Type-4
Wavelength Region (nm)	0.5~5	0.5~50	2~50	50~122
Angle of Incidence (°)	89	89	88	85
Grooves (mm^{-1})	1200	300	300	300
Distance from Entrance Slit to Grating (mm)	238	238	238	238
Distance from Grating to Detector (mm)	250 (at 5nm)	256 (at 50nm)	234 (at 50nm)	245 (at 120nm)
Length of Flat Focal Plane (mm)	20	39	31	23

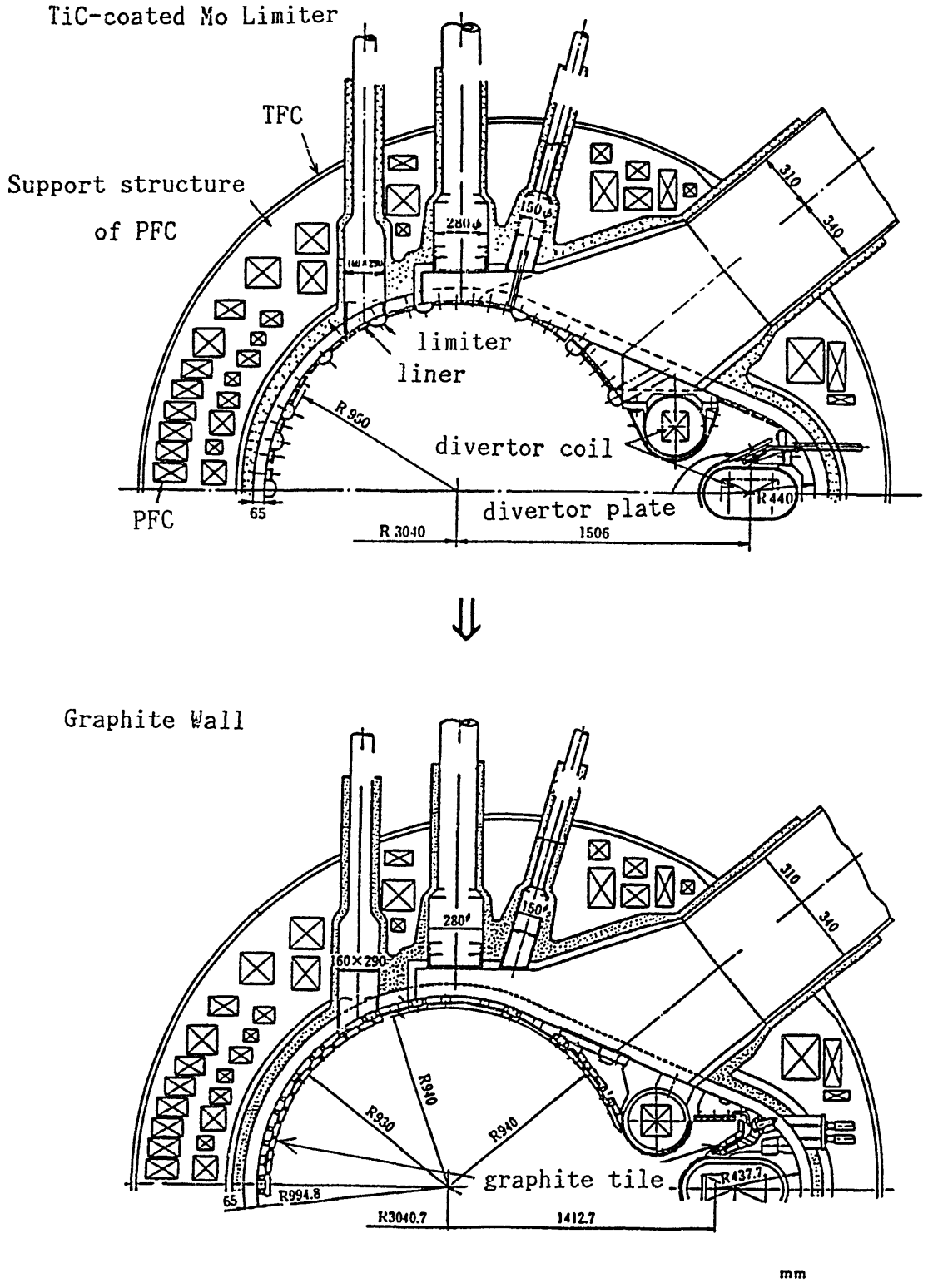

Fig. 1. Cross-sectional view of JT-60 before (the upper) and after (the lower) carbonization. 40 percent of the whole surface area is covered with graphite tiles.

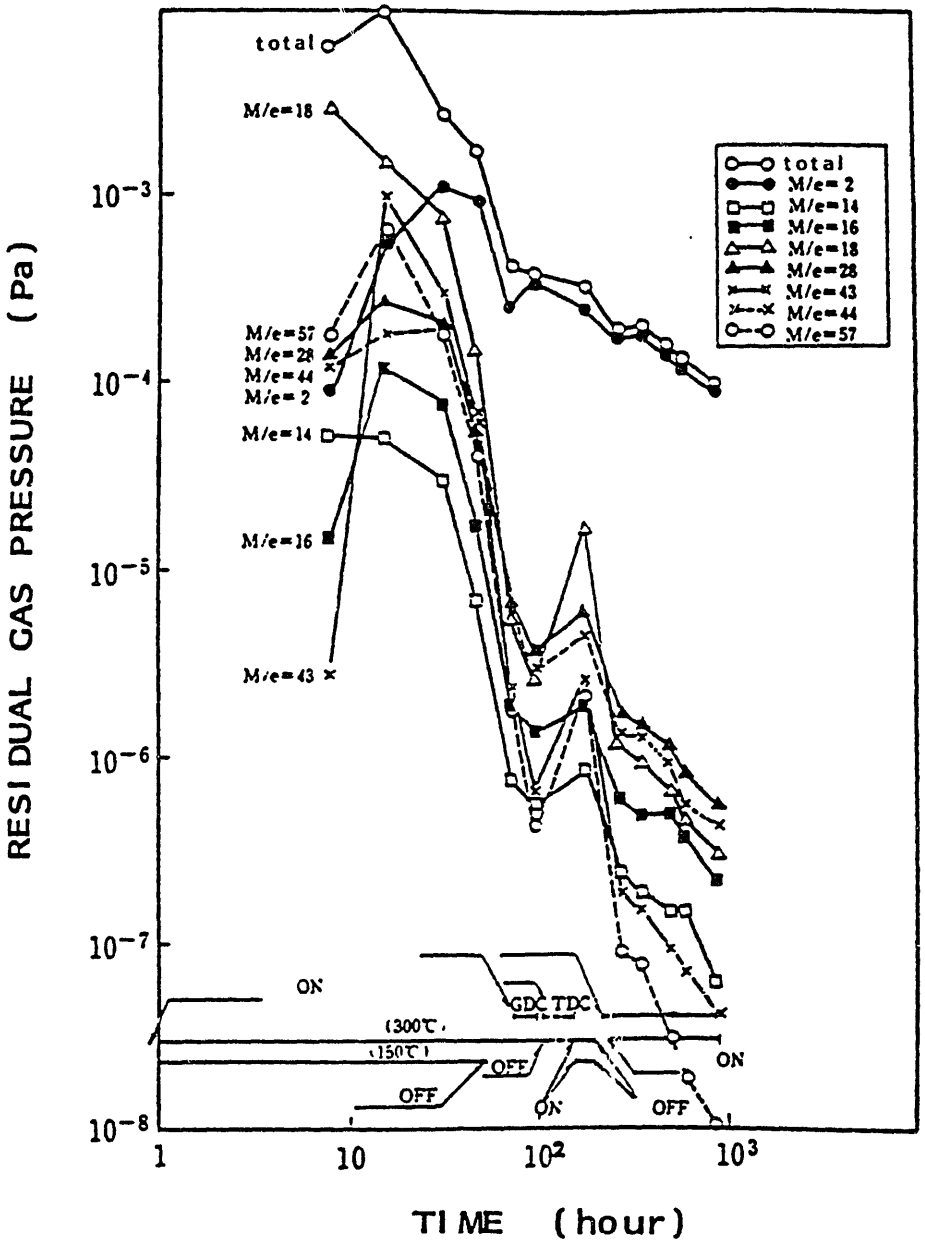

Fig. 2. Time evolution of the residual gas pressure in JT-60 vacuum chamber. Vacuum chamber was baked out up to 350°C for the wall conditioning before experiment.

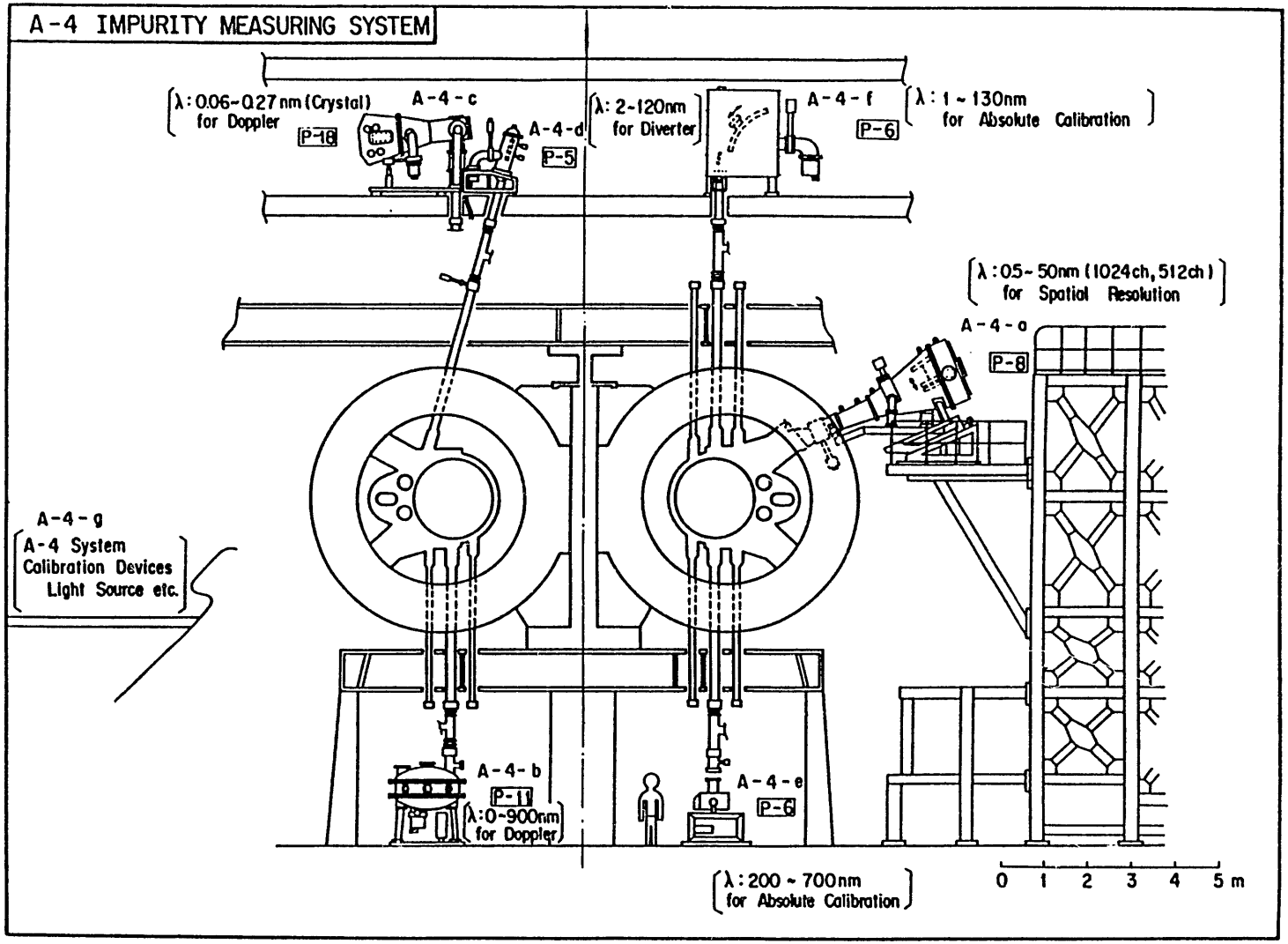

Fig. 3. Arrangement of impurity measurement systems in JT-60. Each system is installed at different toroidal section except for A4E and A4F systems.

Comparison of Impurity Spectra

Before and After Carbonization

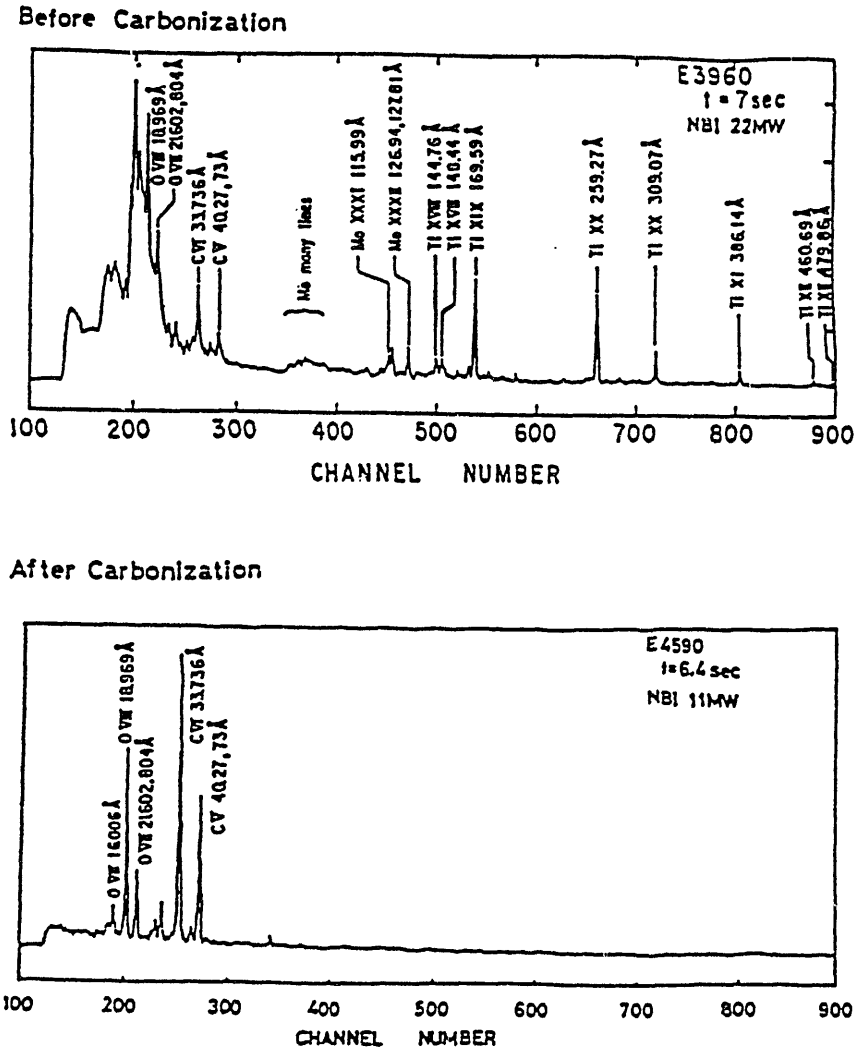

Fig. 4. Comparison of impurity spectra before (the upper) and after (the lower) carbonization by the limiter discharge during NBI.

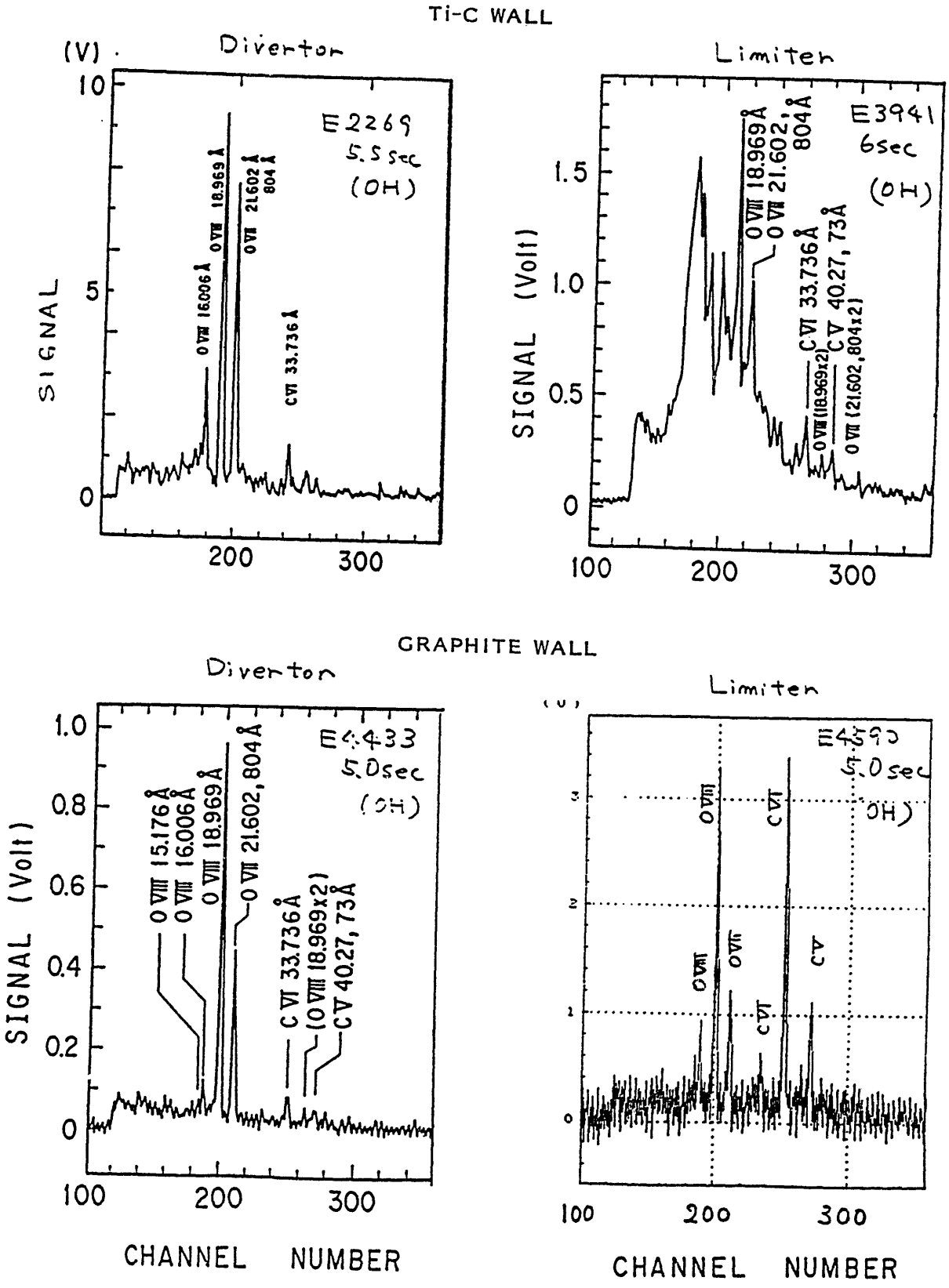

Fig. 5. Comparison of impurity spectra before (the upper) and after (the lower) carbonization by the limiter (left side) and the divertor (right side) ohmic discharges.

The detector bias was changed in each case.

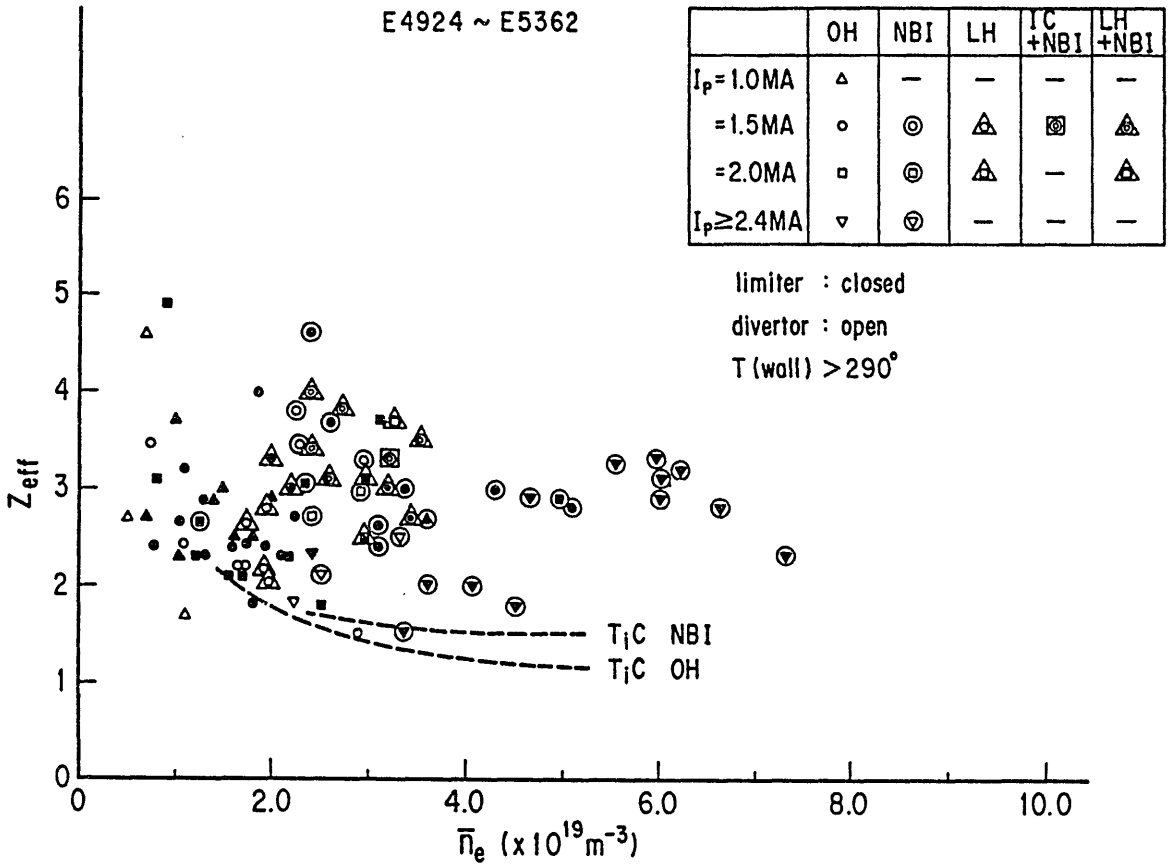

Fig. 6. Dependence of Z_{eff} on the electron density. The wall temperature is 300°C.

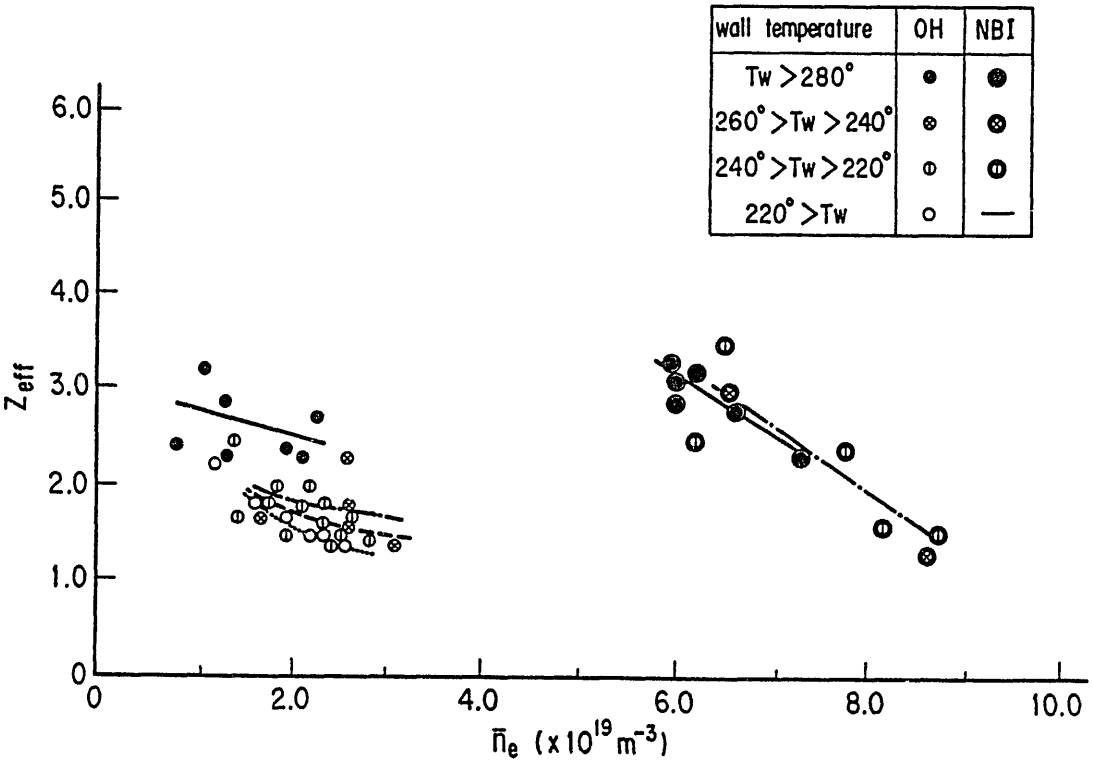

Fig. 7. Dependence of Z_{eff} on the electron density. The wall temperature is varied from 280 to 200°C.

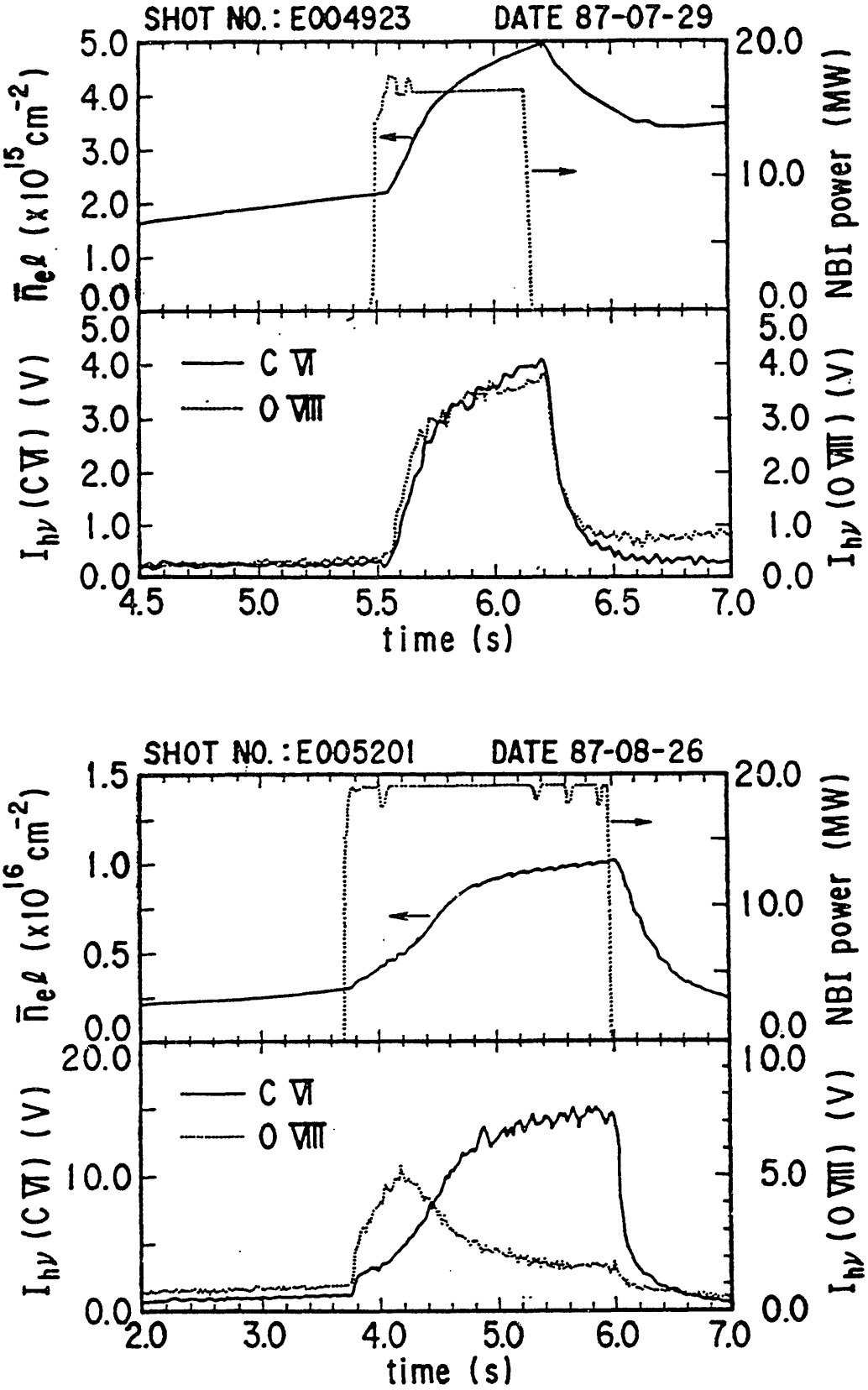

Fig.8. Two types of light impurity behavior during NBI in JT-60 plasmas. The upper shows the type A, and the lower the type B.

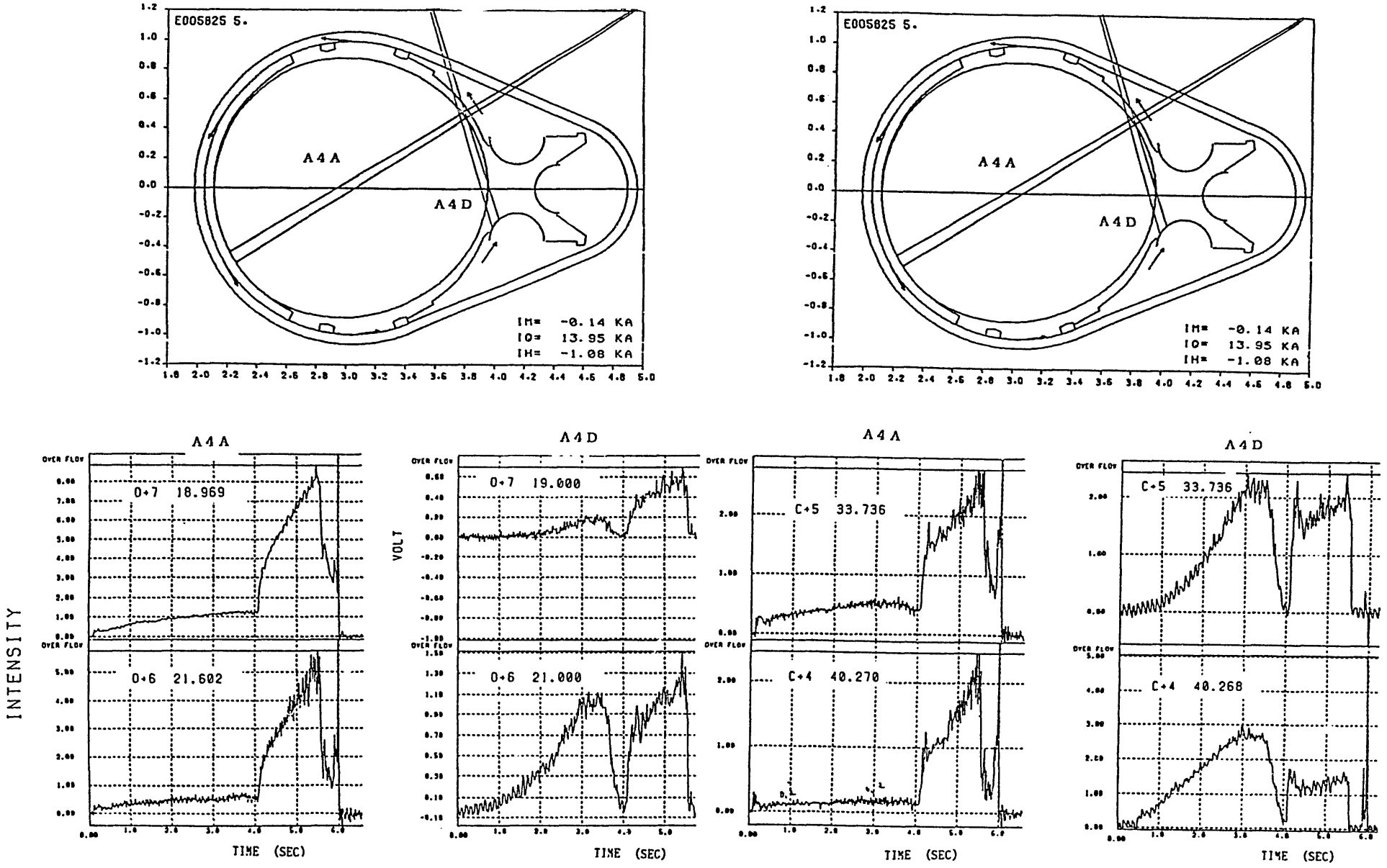

Fig. 9. Time evolution of each impurity line from different cords. The lines of CV, CVI, OVII and OVIII are observed under type A mode by A4A and A4D.

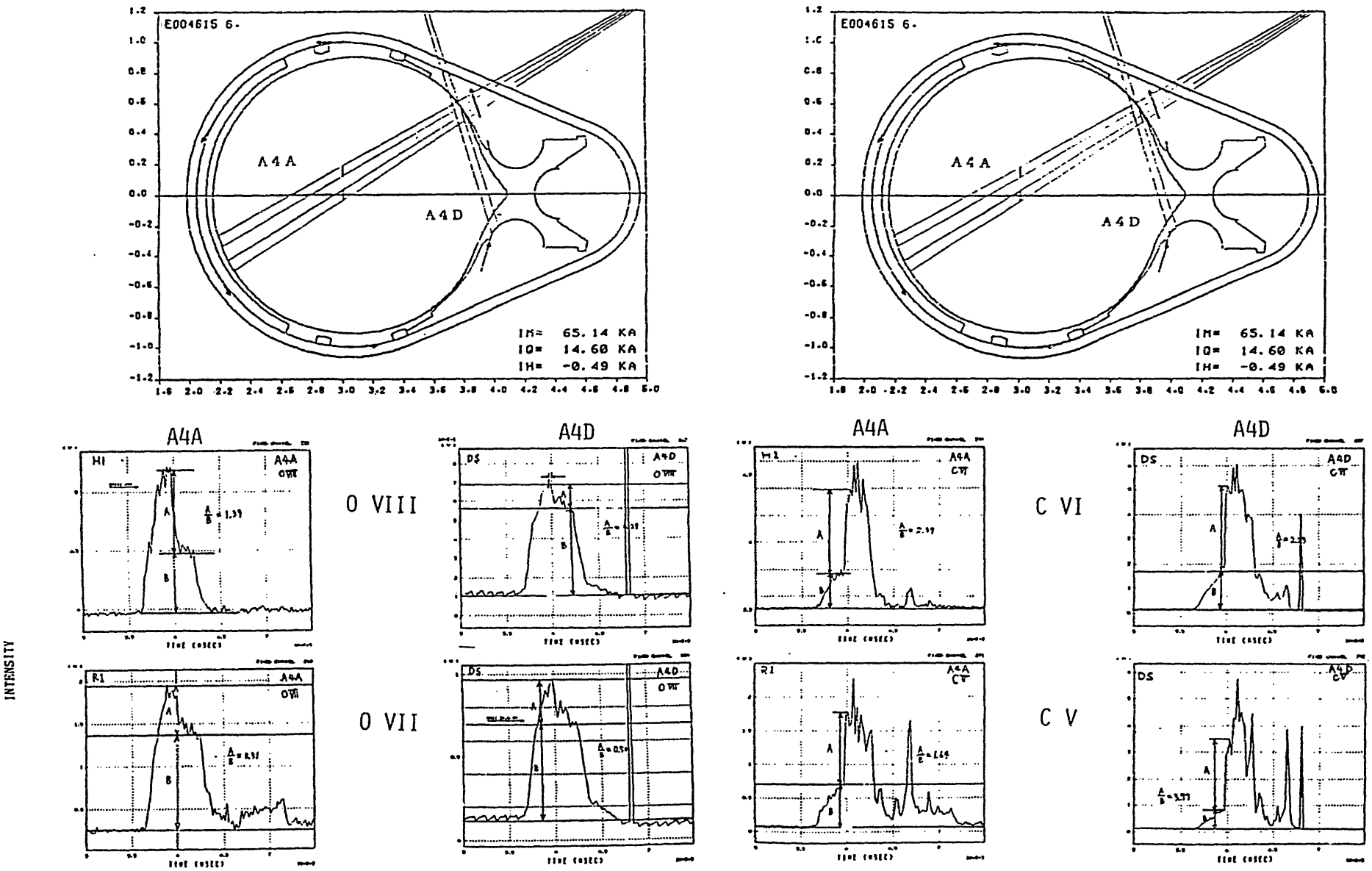

Fig. 10. Time evolution of each impurity line from different cords. The lines of CV, CVI, OVII and OVIII are observed under type B mode by A4A and A4D.

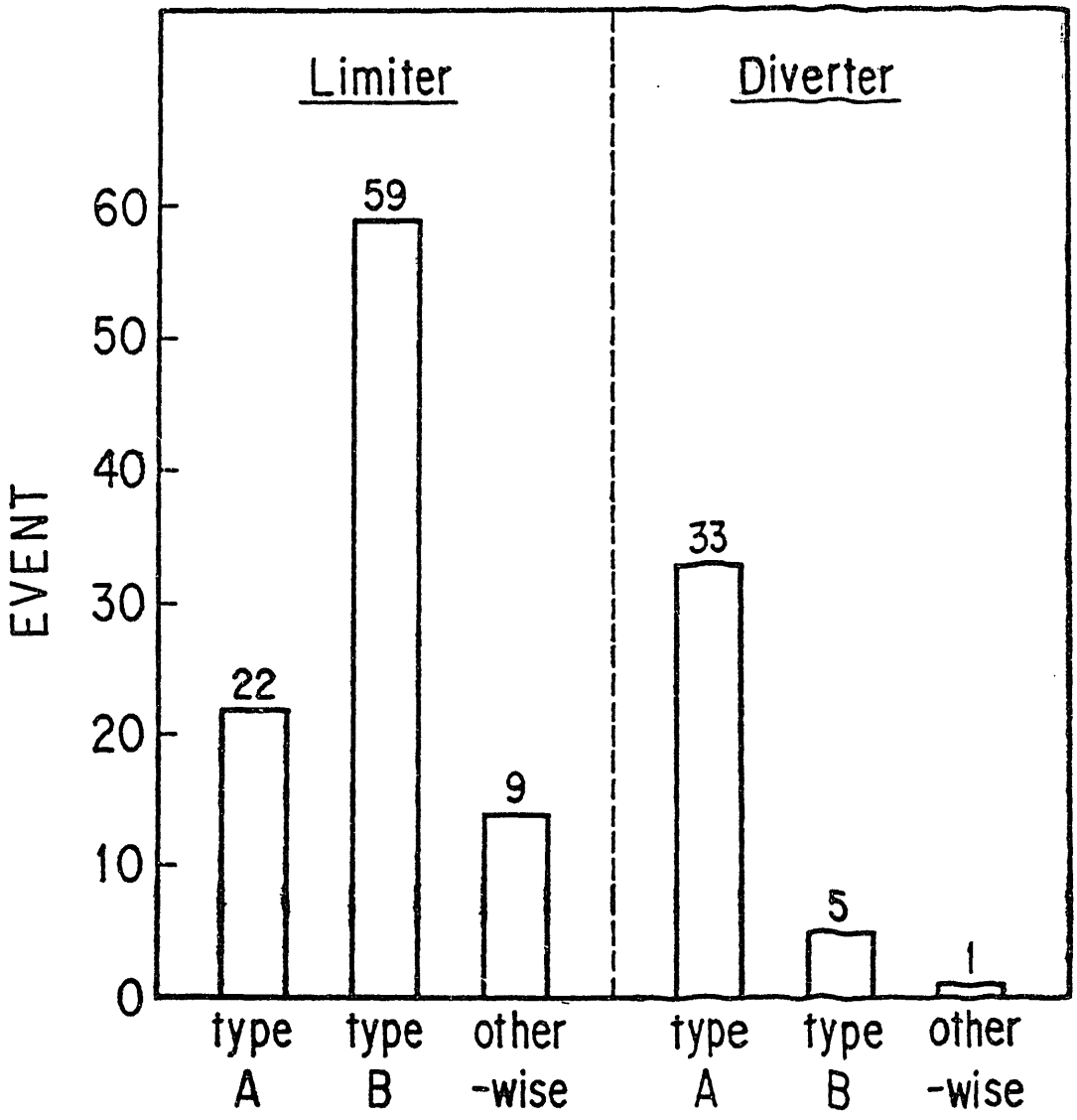

Fig. 11. Number of occurrence of each type in the limiter and divertor discharges. The type A and B represent the same as shown in Fig. 8. The "otherwise" means other types.

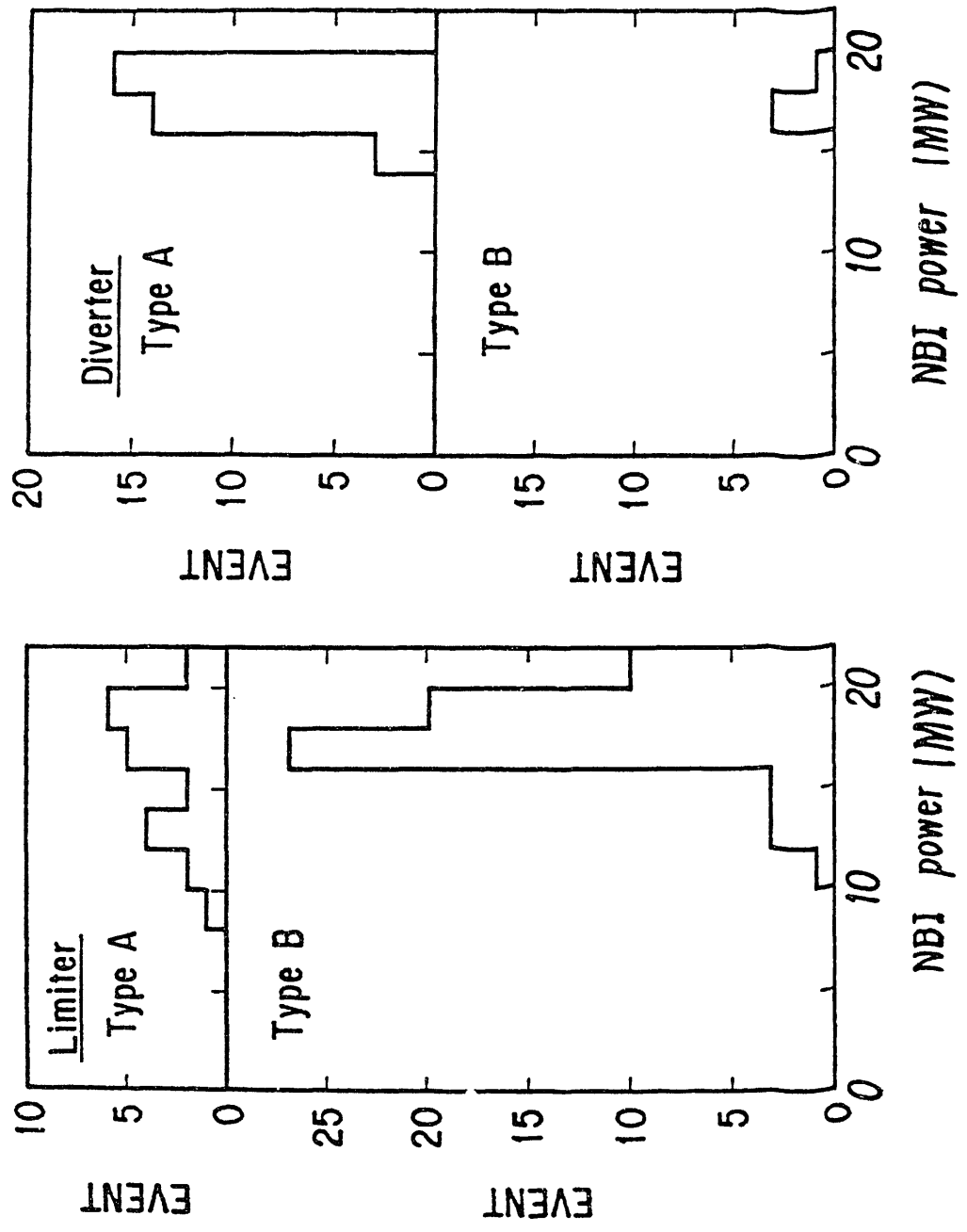

Fig. 12. Dependence of the occurrence of each type on NBI power.

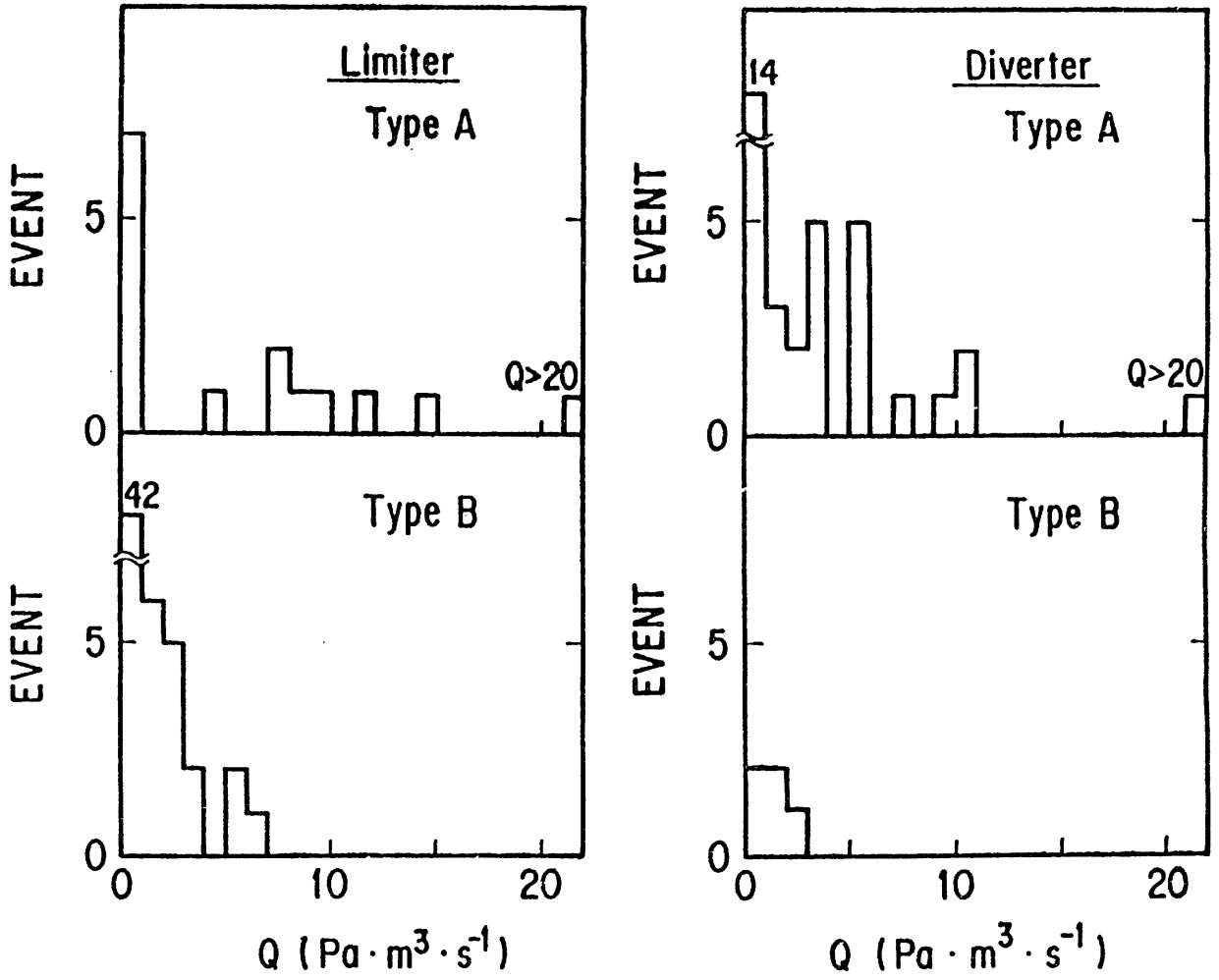

Fig. 13. Dependence of the occurrence of each type on gas puff rate Q.

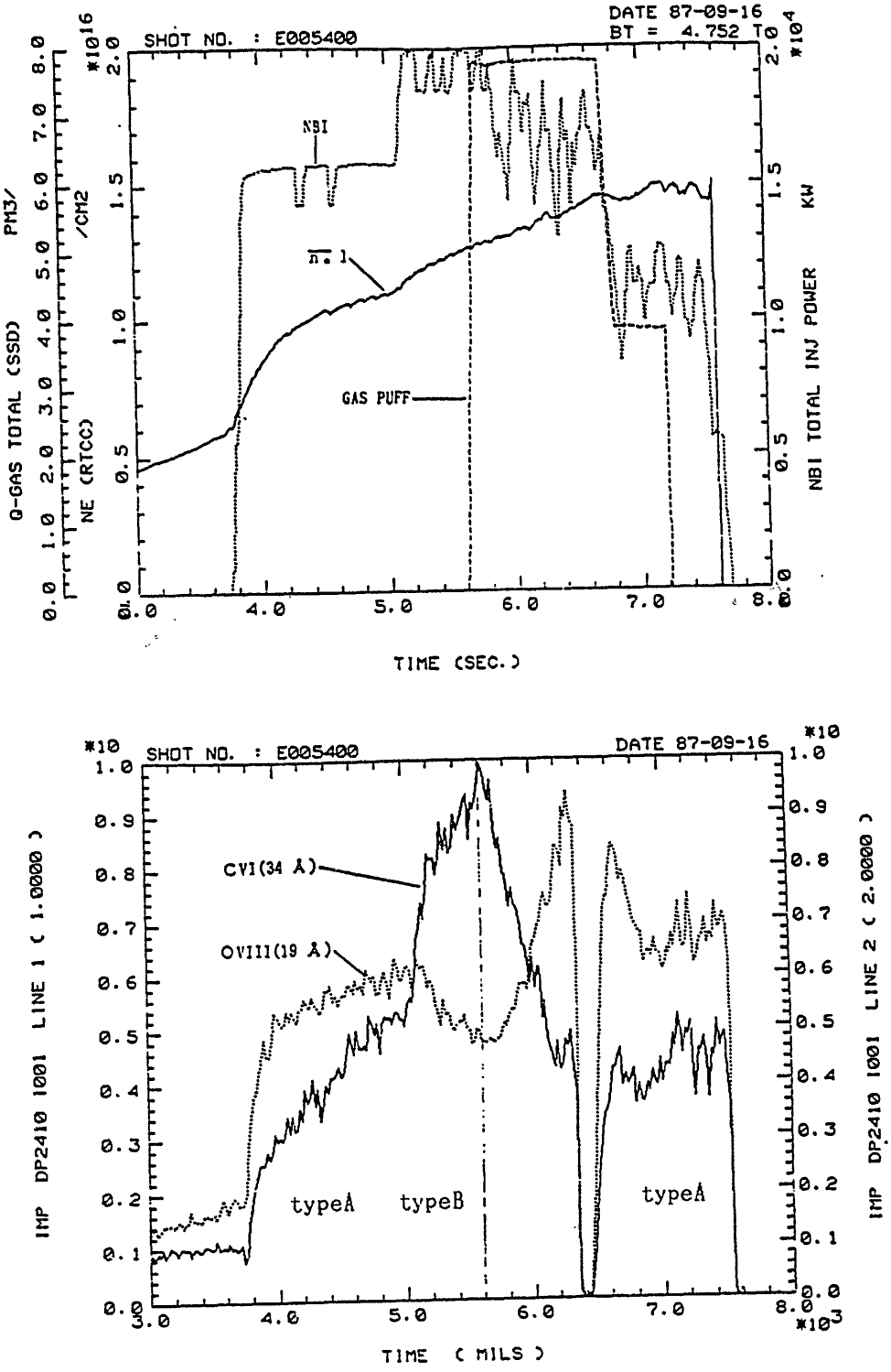

Fig. 14. Change of light impurity behavior during NBI. First, it changes from type A to B by NBI power up, and, second, changes from type B to A by additional gas puffing.

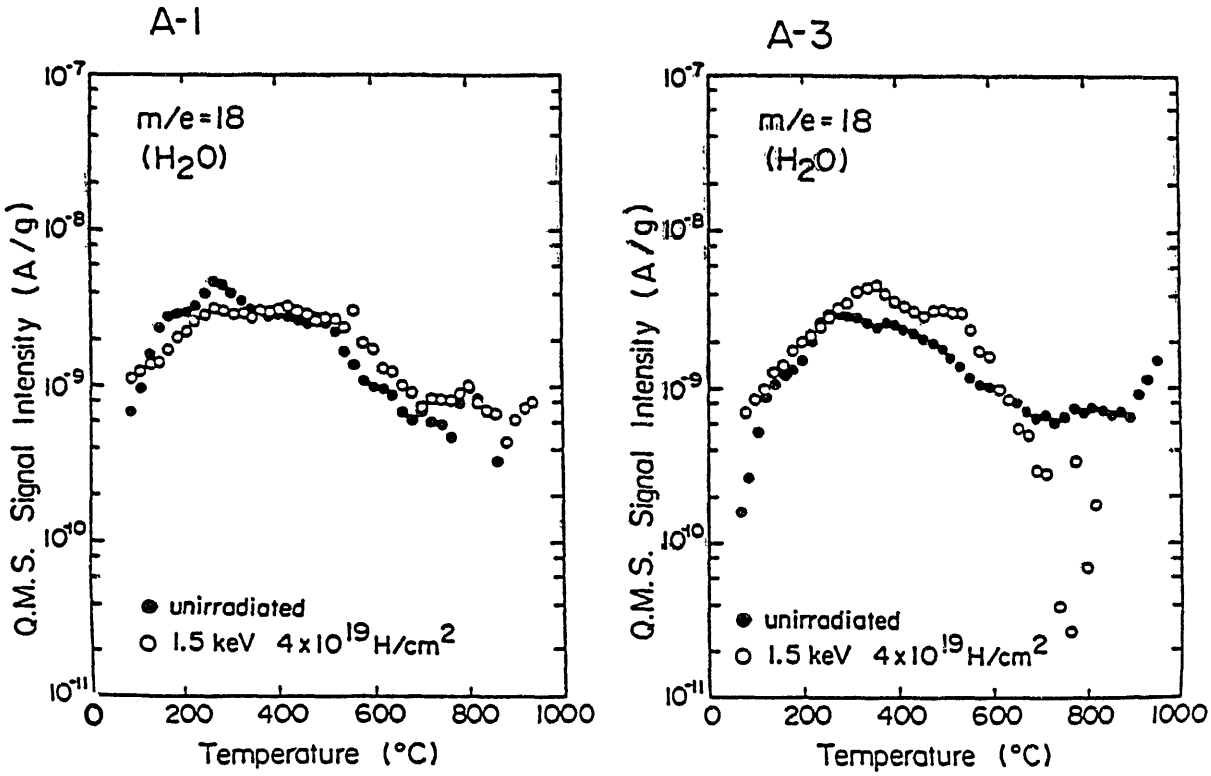

Fig. 15. Dependence of the outgas from graphite on the temperature. The closed and open circles represent data before and after irradiation, respectively.

Spectroscopic Studies on Carbon Coating

K.Kondo, K.Okazaki*, T.Oda**, N.Noda, K.Akaishi, H.Kaneko,
T.Mizuuchi, F.Sano, O.Motojima, and A.Iiyoshi

Plasma Physics Laboratory, Kyoto University, Uji, Kyoto, Japan
*The Institute of Physical and Chemical Research, Wako, Saitama, Japan
**Faculty of Engineering, Hiroshima University, Higashi-Hiroshima, Japan

Abstract

Visible and vacuum ultraviolet (VUV) spectroscopic studies on carbon coating are described. In Heliotron E, carbon coating was performed on the vacuum chamber wall to reduce metallic impurities. The carbon layer was deposited on the wall using glow discharge with CH_4 and H_2 mixture gases. The spectra of $CH(A^2\Delta - X^2\Pi)$ and H_2 were identified in the visible region. The excitation mechanism of CH emission is discussed. The changes of the brightness of multiply ionized iron ions were measured by a vuv monochromator. The reduction of the iron impurity was observed in plasmas, heated by neutral beams, after carbon coating. The behavior of the retained hydrogen in the carbon layers was also studied observing H_α emission.

§1. Introduction

Metallic ions are unwanted impurities on obtaining high temperature plasmas. They are released from the walls of the vacuum vessel by physical sputtering of ions and charge exchange neutral particles [1]. To reduce the contents of the metallic impurities in plasmas, a technique of in-situ carbon coating has been established. The carbon layer, deposited on the walls, protects the walls from the physical sputtering, and reduces the metallic impurity generation. The carbon coating was already applied to tokamaks [2,3]. In Heliotron E , glow discharge, with CH_4 and H_2 mixture gases, was used for carbon coating on the wall [4].

In this report, spectroscopic studies on carbon coating are presented. In the visible region, spectrum identification of the glow plasma was performed. Lines from H_2 molecule were identified. The CH band($A^2\Delta$ - $X^2\Pi$) was observed in the CH_4 + H_2 glow discharge.

The dependence of the CH intensity on the discharge current and pressure ratio of CH_4 to H_2 was investigated. The emission mechanism of CH is discussed.

The effect of the carbon coating to reduce the metallic impurities in the plasmas was studied in the neutral beam heated plasmas. The brightness of multiply ionized iron ions, measured by an absolutely calibrated grazing incidence monochromator in the vuv wavelength region, was found to decrease after the carbon coating, A 1.26 m visible spectrometer was also used to measure the H/D ratios in the ICRF experiments.

In section 2, the experimental setup is described. In section 3, the

spectra of H_2 and CH observed in the glow discharge are shown. In section 4 is presented the changes of the line emissions from multiply ionized iron ions after carbon coating. In section 5, the behavior of the retained hydrogen and deuterium is shown. Section 6 contains the conclusions.

§2. Experimental Setup

A schematic of carbon coating on Heliotron E is shown in Fig.1. The carbon layer was deposited using glow discharge with CH_4 and H_2 mixture gases. The stainless steel limiter, located at # 6.5 port, was used as an anode and the vacuum chamber wall was a cathode.

The discharge current and voltage were 1 - 2 A and 300 - 380 V, respectively. Typical current density at the wall was 6 $\mu A/cm^2$. The total gas pressure of $CH_4 + H_2$ was 10 - 20 mTorr. The pressure ratio of CH_4 to H_2 was varied from 0 to 0.2.

The electrostatic probes were located at # 6.5 port. The electron density and temperature were 10^8 - 10^9 cm^{-3} and 0.2 - 1 eV, respectively. A surface deposition probe was inserted through #29.5 port to measure the thickness of the carbon layer deposited on the sample pieces. The growing rate of carbon layer was analyzed by Auger spectroscopy. Under these conditions, the growing rate was about 200 Å/hour. Usually, carbon layers coated were 500 Å in thickness. Figure 2 shows the typical composition of the sample piece made of stainless steel. From the surface to 400 Å depth, the main composition is carbon, and iron and chromium are not observed near the surface [5]. In this

figure, the retained hydrogen concentration is not shown because Auger spectroscopy is inadequate to measure hydrogen.

A visible scanning monochromator with a 0.25 m focal length (Nikon P-250) was used to observe the spectra over the wavelength from 3800 Å to 6570 Å through the port located at the manifold for pumping system. In the vuv region, the grazing incidence monochromator (McPerson 247V) was used to measure the brightness of impurity lines, which are distributed in 100 - 1250 Å region.

Pure D_2 glow discharge was made after CH_4 and H_2 discharge to exchange the retained hydrogen to deuterium in the carbon layer, when ICRF minority heating experiments were scheduled. The time behaviors of H_α and D_α were observed by the visible spectrometer with a multichannel detector.

§3. Spectra of H_2 and CH

Figures 3(a) and (b) show the spectra of three kinds of glow plasmas with $CH_4 + H_2$, H_2 and D_2 gases. Comparing two spectra of $CH_4 + H_2$ and H_2 discharges, the band spectrum degraded to violet near the Balmer γ (4340.47 Å) was clearly noticed in the $CH_4 + H_2$ discharge. This band spectrum with band head at 4314 Å is attributed to CH radical. The electronic transition is $A^2\Delta - X^2\Pi$ and the vibrational transition is (0,0). The line-like emission at 4324 Å is a piled Q branch of the same electronic transition with the (2,2) rotational transition (see Fig. 4) [6]. Other lines attributed to H_2 molecules also appeared in both discharges [7]. The Balmer series, H_α , H_β , H_γ , H_δ and H_ϵ were considered to be originated from the dissociative excitation of H_2 and

CH_4 molecules. The identified lines are listed in Table 1. The spectra of CH_2(6532, 6226, 5906, 5375 Å), CH^+(4237, 4225 Å), and C_2 (SWAN band, 5165, 4737, 4715 Å) [6] were not enough to be measured above the background. Figure 4 shows the observed fine structure of CH band ($A^2\Delta - X^2\Pi$). The peaks degraded to violet are R-branches. The rotational temperature can be estimated, from the R-branches, to be about 300°K, as shown in Fig.5.

Figure 6 shows the dependence of the intensities of H_α, H_2(Fulcher α system, $d^3\Pi_u - a^3\Sigma_g$, Q-1 branch of the 1,1 vibrational transition) and of CH on the discharge current I_d. The intensities of these emissions are roughly proportional to the electron density, since the electron density increases as the discharge current increases.

Figure 7 shows the dependence of these emission intensities on the CH_4 to H_2 pressure ratio, with H_2 pressure kept constant. From the dependence on I_d and pressure ratio of CH_4 to H_2, the most important emission mechanism of CH radical is considered due to direct dissociative excitation of CH_4 by electron impact collision.

The H_α intensity also changes as the pressure ratio of CH_4 to H_2 is varied, indicating that the H_α emission is due to the dissociative excitation of both CH_4 and H_2 molecules. The emission cross sections for these dissociative excitations were given by Mohlmann et al.[8]. The emission cross section for the Fulcher α system of H_2 molecule was also given by Mohlmann et al.[9]. Using these atomic data, it is possible to estimate the densities of CH_4 and H_2 from the line intensities.

The CH emission is important to understand the plasma wall interactions in high temperature plasmas. In the JET tokamak, CH

emission was observed after heavy carbon coating on the walls [10]. This was explained as due to the fact that the charge exchange neutral hydrogens penetrated into the carbon layer and first formed CH, and, then, successively followed by CH_2, CH_3, and CH_4. Finally, CH_4 was released from the carbon layer because of its low sticking coefficient. The released CH_4 molecules dissociated immediately by the electron collision. The emission of CH indicated that the chemical sputtering occured at the carbon layer.

§4. Changes of Iron Emission from Neutral Beam Heated Plasmas after Carbon Coating

The wall of the Heliotron E device is made of stainless steel (YUS 170), and iron is the main component. The changes of the brightness of multiply ionized iron emissions were measured by the grazing incidence vuv monochromator in order to evaluate the effect of the carbon coating. The plasmas were produced by 53.2 GHz gyrotrons and heated further by energetic neutral beams. Typical electron density was $3 - 10 \times 10^{13}$ cm^{-3}. The electron and ion temperatures were about 300 eV.
Figure 8 shows the changes of the brightness of Fe IX (171 Å) and Fe XVI (335 Å) before and after carbon coating as a function of the average electron density in plasmas. The power of the neutral beams was about 1.7 MW. The brightness of the iron ions with different ionization stages decreases simultaneously which indicates that iron impurities in the plasmas decrease.

§5 The Retained Hydrogen in the Carbon Layer

The glow discharge, with CH_4 and H_2 mixture gases, forms the carbon layer and at the same time hydrogen atoms are retained in the layer. Typical concentration of H/C is about 0.2 [5]. These hydrogens are released by the bombardment of the particle fluxes escaping from the high temperature plasmas when the main discharge is initiated. Then, in the ICRF minority experiments, the important parameter of H/D ratios may shift significantly to unoptimized values. Figure 9 shows the time behavior of D_α and H_α emissions in the ICRF heated plasmas which is different before and after carbon coating. The measurements were made using SPEX 1269 spectrometer with 512 channel detector. Single spectrum was obtained with 10 msec integration time. The ratio of H/D was controlled by gas puffing before carbon coating, where the initial peak observed of D_α emission was entirely due to D_2 gas puffing. After carbon coating, additional pure D_2 glow discharge was made in order to replace H by D and to investigate the effect of the retained hydrogen. There, only hydrogen was puffed, which can be noticed by intense H_α peak at the beginning of discharge. Since no D_2 gas was puffed, the continuously observed D_α emissions indicate that deuterium is released from the carbon layer by the particles escaped from the main discharge.

§6 Conclusions

The spectra of $CH(A^2\Delta - X^2\Pi)$ and H_2 molecules were identified in the glow discharge for carbon coating. The emission mechanisms of CH was analyzed, and the dissociative excitation from CH_4 is considered to

be the most probable process. It was also shown that the CH emission is important to understand the plasma-wall interactions in the high temperature plasmas. From the present vuv spectroscopy, it was concluded that the iron impurity decreases by the carbon coating on the vacuum chamber wall. The control of the retained hydrogens in the carbon layer is, however, still unsolved in the carbon coating technique.

Acknowledgements

The authors would like to thank professors K.Uo, T.Yamashina and Y.Sakamoto for their interest toward the present work. They also acknowledge the members of the carbon coating experiment from Hokkaido University, the Institute of Physical and Chemical Science, and Nagoya University for their help.

The author (K.K) also wish to thank Professor H.Tawara for a critical reading of the manuscript.

References

[1] K.Kondo, H.Okada, H.Zushi, et al., J.Nucl.Mater. 145 - 147(1987) 501

[2] J.Winter, F.Waelbroeck, P.Wienhold, et al., J.Nucl.Mater. 128 & 129 (1984) 841

[3] N.Noda, Y.Ogawa, K.Masai, et al., Jpn.J.Appl.Phys. 25 (1986)397

[4] K.Uo, A.Iiyoshi, T.Obiki, et al., 11th Int.Conf.on Plasma Physics and Controlled Nuclear Fusion Research,(Kyoto 1986) IAEA-CN-47/D-I-1

[5] H.Minagawa, T.Hino, T.Yamashina, et al., submitted to 8th Int.Conf. on Plasma-Surface Interactions,(Julich 1988)

[6] R.W.B.Pearse and A.G.Gaydon, The Identification of Molecular Spectra (Chapman and Hall, London, 1984)

[7] H.M.Crosswhite, The Hydrogen Molecule Wavelength Tables of Gerhard Heinrich Dieke (John Willy & Sons, New York, 1972)

[8] G.R.Mohlmann and F.J.De Heer, Chem.Phys. 19 (1977) 233

[9] G.R.Mohlmann and F.J.De Heer, Chem.Phys.Letters 43 (1976) 240

[10] K.H.Behringer, W.W.Engelhart, L.Horton et al., Proc.of the XIII Symposium on the Physics of Ionized Gases 1986, p241

Table I. Identified Spectrum of H, H_2 and CH

	Wavelength (Å)	Transition		
H	3970.07	7 - 2 (ϵ)		
	4101.74	6 - 2 (δ)		
	4340.47	5 - 2 (γ)		
	4861.33	4 - 2 (β)		
	6562.85	3 - 2 (α)		
H_2	3871.59	$p^3\Sigma_g - b^3\Sigma_u$	0 - 1	R2
	4205.09	$g^3\Sigma_g - b^3\Sigma_u$	1 - 0	R2
	4233.83	$k^3\Pi_u - a^3\Sigma_g$	3 - 2	Q1
	4490.45	$k^3\Pi_u - a^3\Sigma_g$	0 - 0	Q1
	4554.16	$k^3\Pi_u - a^3\Sigma_g$	1 - 1	Q1
	4617.52	$k^3\Pi_u - a^3\Sigma_g$	2 - 2	Q1
	4634.02	$g^3\Sigma_g - b^3\Sigma_u$	0 - 0	R2
	4680.43	$k^3\Pi_u - a^3\Sigma_g$	3 - 3	R1
	4719.04	$g^3\Sigma_g - b^3\Sigma_u$	1 - 2	R2
	4742.79	$k^3\Pi_u - a^3\Sigma_g$	4 - 4	Q1
	4934.24	$g^3\Sigma_g - b^3\Sigma_u$	0 - 1	Q2
	5303.11	↑	1 - 0	Q1
	5419.89	↑	2 - 1	Q1
	5537.47	Fulcher α system	3 - 2	Q1
	5655.75	$d^3\Pi_u - a^3\Sigma_g$	4 - 3	Q1

Table I. (continued)

H_2	5975.44	↑	0 - 0	R1
	5994.07		0 - 0	R0
	6018.29		0 - 0	Q1
	6080.78		1 - 1	R1
	6098.24	Fulcher α system	1 - 1	R0
	6121.79		1 - 1	Q1
	6127.25	$d^3\Pi_u - a^3\Sigma_g$	1 - 1	Q2
	6135.40		1 - 1	Q3
	6182.99		2 - 2	R2
	6201.19		2 - 2	R0
	6224.81		2 - 2	Q1
	6238.40		2 - 2	Q2
	6285.38		3 - 3	R1
	6303.48		3 - 3	R0
	6327.06		3 - 3	Q1
	6428.12	↓	4 - 4	Q1
CH	4314	$A^2\Delta - X^2\Pi$	0 - 0	
	4324	$A^2\Delta - X^2\Pi$	2 - 2	Q

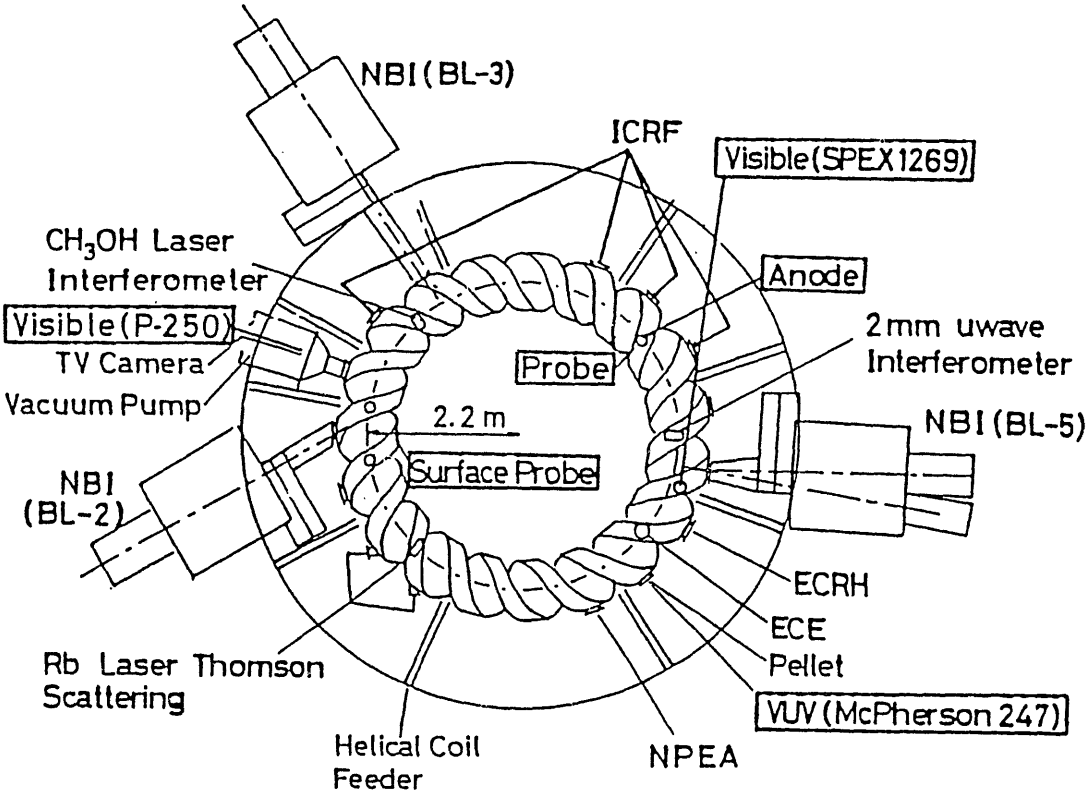

Fig.1. A schematic drawing of carbon coating.

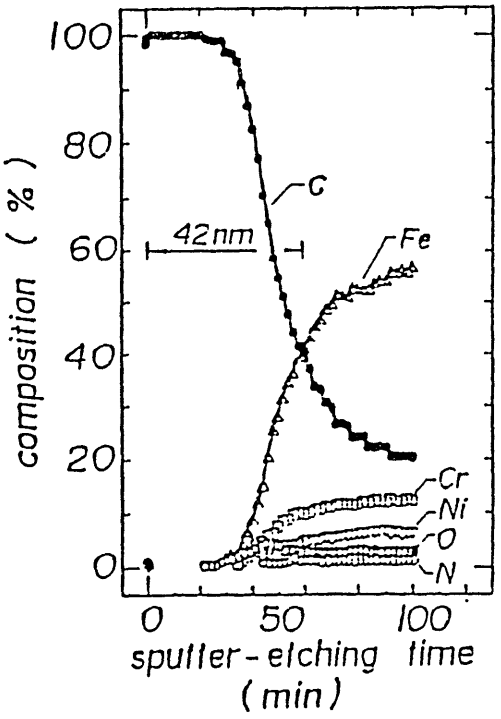

Fig.2. Typical composition of the carbon deposited sample piece.

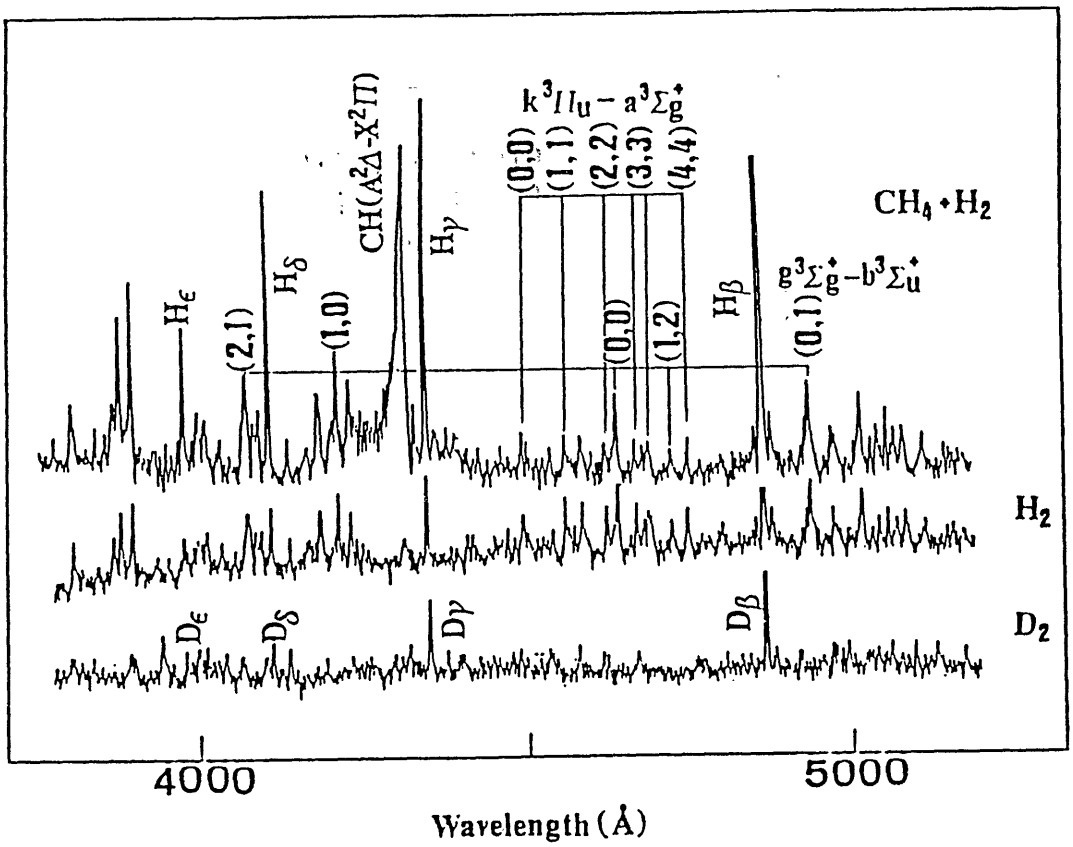

Fig.3(a). Visible spectrum of the glow plasmas from 3800 Å to 4800 Å.

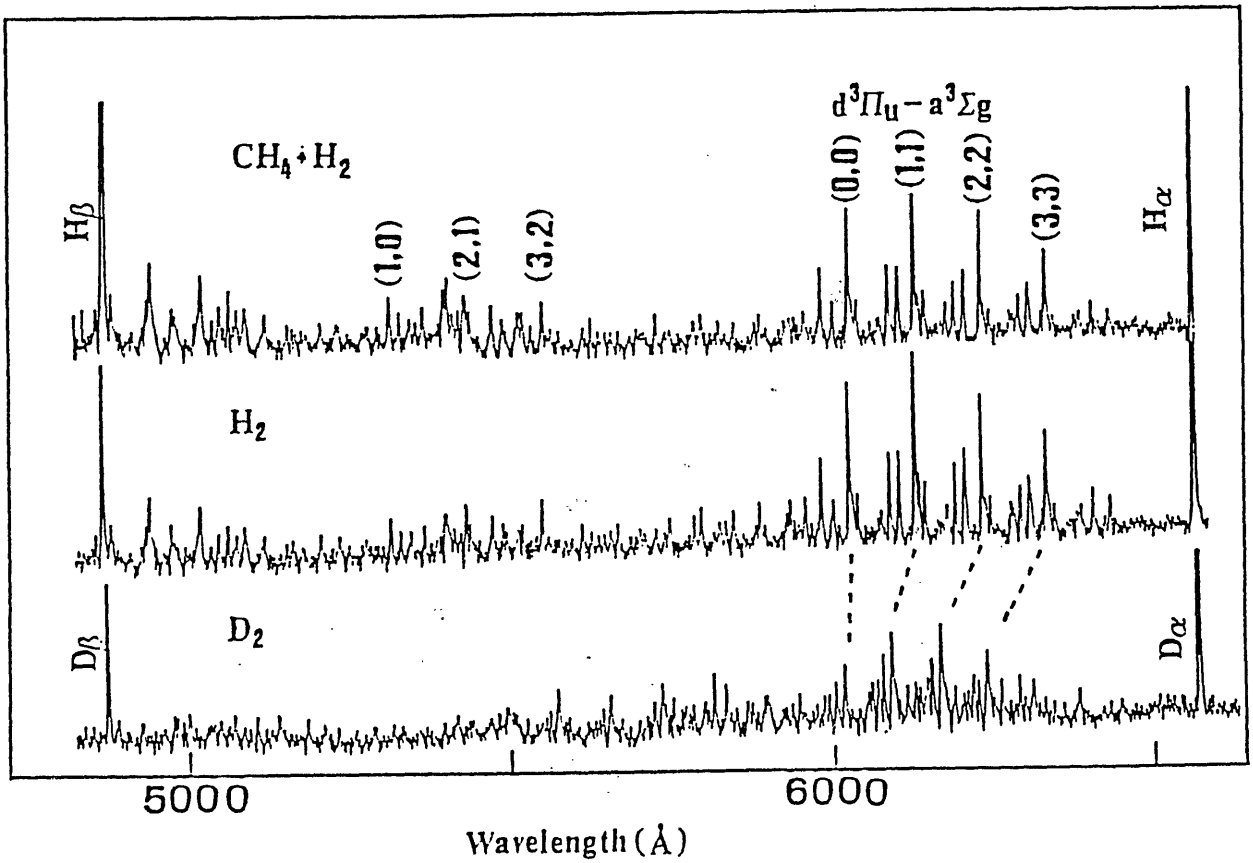

Fig.3(b). Visible spectrum of the glow plasmas from 4800 Å to 6570 Å.

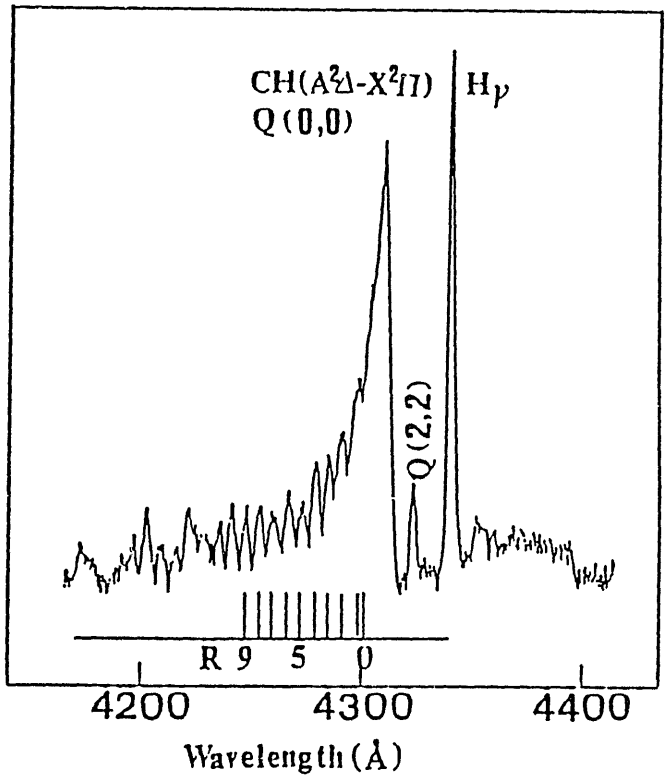

Fig.4. Fine structure of CH band spectrum ($A^2\Delta - X^2\Pi$)

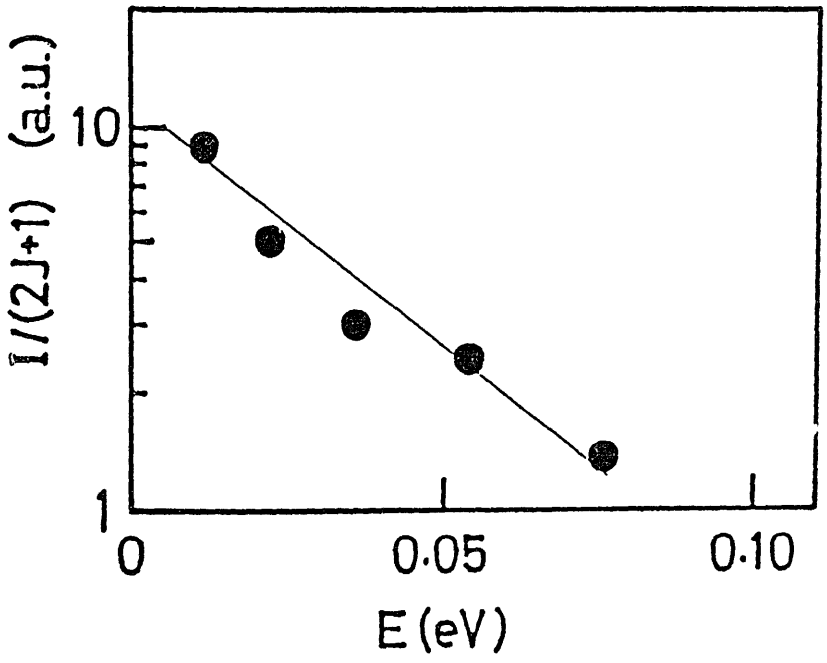

Fig.5. Intensities of the rotational branches to the excitation energy.

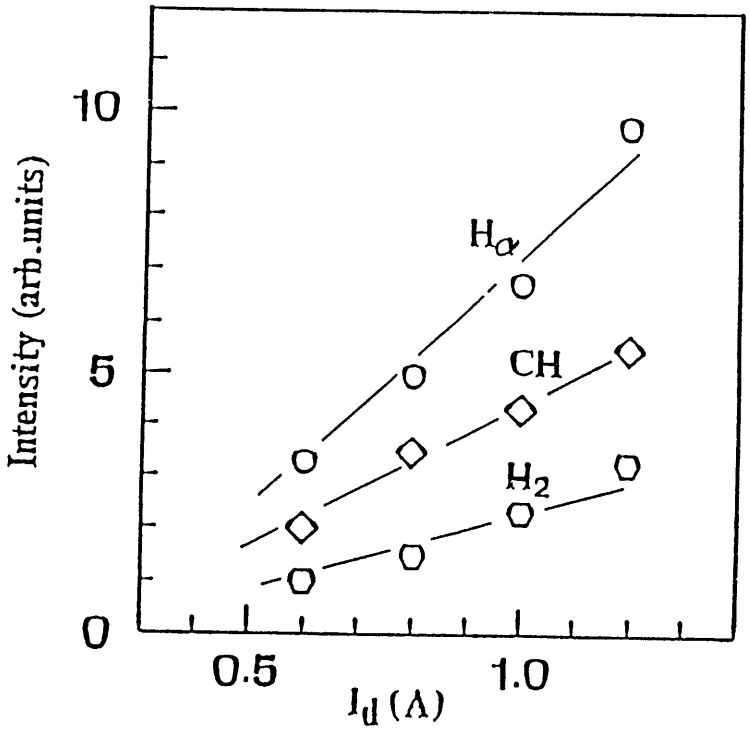

Fig.6. Intensities of CH, H_α, and H_2(Fulcher α) vs. discharge current I_d.

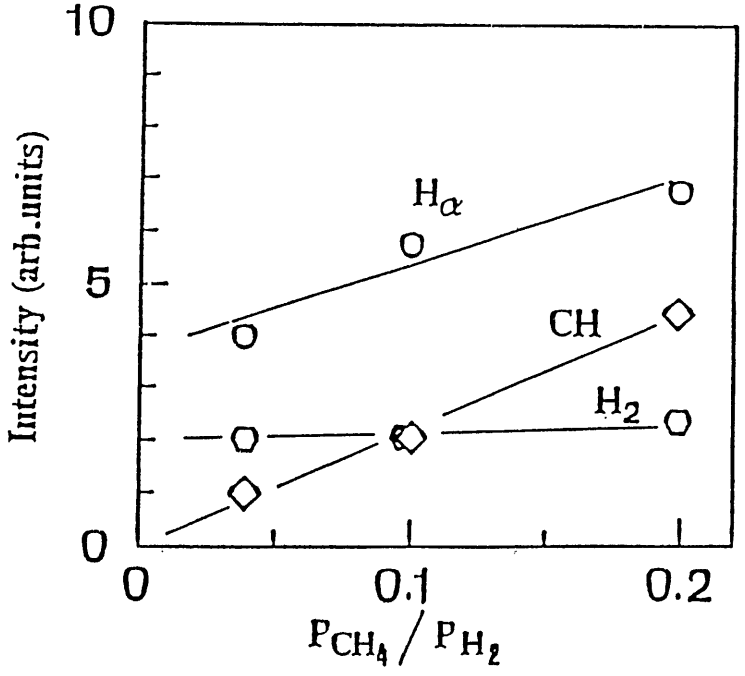

Fig.7. Intensities of CH, H_α, and H_2(Fulcher α) vs. pressure ratio of CH_4 to H_2.

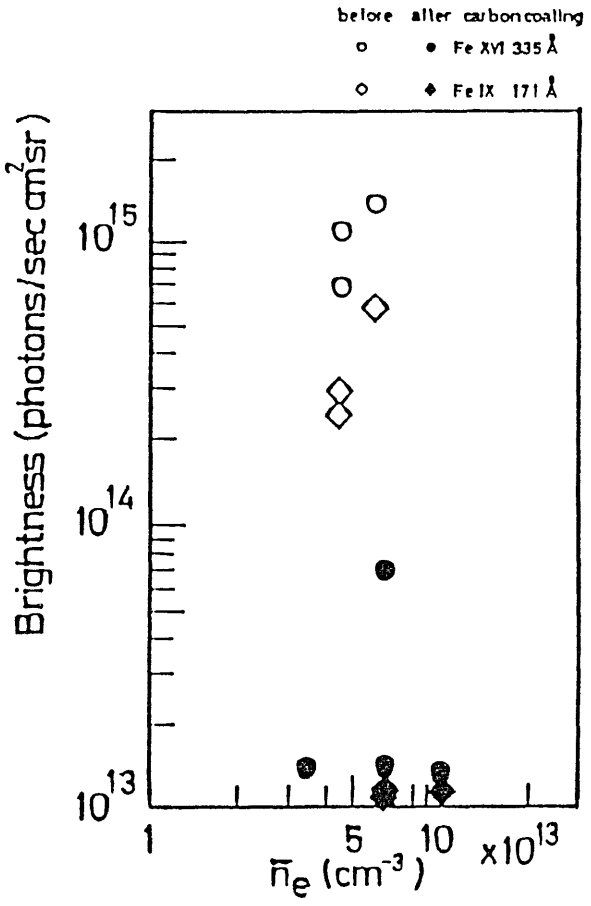

Fig.8. The changes of the brightness of Fe IX and Fe XVI after carbon coating.

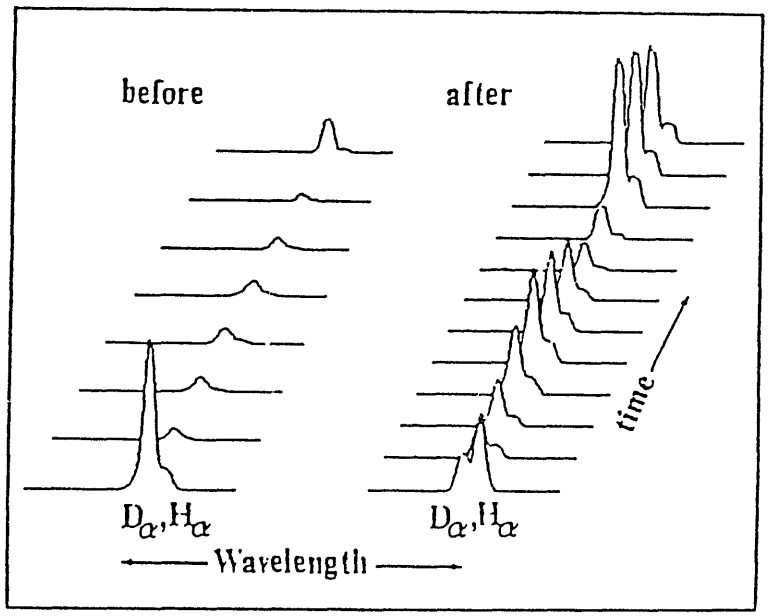

Fig.9. Time behavior of D_α and H_α in the ICRF heated plasmas before and after carbon coating.

Carbonization and Hydrogen Concentration Profile in the Films

Susumu AMEMIYA

Department of Nuclear Engineering, Nagoya University, Nagoya 464

1. Introduction

Introduction of impurity elements into a magnetically confined plasma has been a serious problem in the development of nuclear fusion devices. Metal impurities introduced to a hot plasma emit very strong radiation and lead to large amount of energy loss from the plasma. This radiation becomes particularey pronounced when ICRF heating is applied. As the energy loss due to the radiation out of plasma by impurity element is proportional to Z^2, it is essential to reduce high Z impurities in the plasma, which are mainly generated from the first-wall of the fusion experiment devices by plasma-wall interaction (PWI). Control and reduction of the impurities released from the first-wall are a most important and urgent task to be solved.

First-wall coating with materials of low atomic number (Z) is potential technology for fusion devices to minimize such plasma contamination. Carbon coatings are considered to be one of candidate material for this purpose. Plasma-assisted carbon coating technique has recently been developed and noted as an in-situ carbon coating method for the first-wall(carbonization). The carbonization drastically reduces metal impurities in a main plasma and is very power ful method to improve the various plasma parameters. Inevitably, however, the carbon layers coated by dissociating a hydrocarbon compound gas absorb a large amount of hydrogen. Then, a large amount of hydrogen is desorbed from the coatings, during tokamak discharge, making the H-recycling rates higher. Thus reducing the H atom content of the coatings is a very important and urgent problem to be solved. And the optimization of carbon coating procedure is now required. In conjunction with the optimization of the coating procedure, a precise hydrogen depth profiling in the coatings is becoming very important.

In this experiment, hydrogen concentration profiles in carbon films coated with different gas (CH_4 and C_2H_2) discharges were measured by ^{15}N resonant nuclear reaction method. Carbon films coated in an actual fusion experiment device (Heliotron-E) are also examined.

2. Experimental

2.1. Preparation of carbon films

Two carbon films were prepared by hot cathode dc glow discharge of pure methane or pure acetylene gas. The dc glow discharge was maintained with a negatively biased hot cathode and the discharge chamber wall which was grounded and served as anode. Hydrocarbon gas, pure CH_4 or C_2H_2, was introduced into a discharge chamber. Sample substrates (1cm×1cm×0.1cm) of mechanically polished 304-L stainless steel were inserted into the plasma. After four-hour carbon coating discharges the samples were extracted from the discharge chamber and nuclear analyses were performed using 3.75 MV Van de Graaff accelerator of Nagoya University. Other carbon films coated in-situ in Heliotron-E device of Kyoto University were also examined .

2.2.Hydrogen concentration profiling in the coatings

Nuclear reaction analysis for hydrogen was performed by bombarding the sample with ^{15}N ions. The amount of hydrogen is determined by counting the 4.44MeV γ-rays produced by the nuclear reaction

$$^{1}H + {}^{15}N \rightarrow {}^{4}He + \gamma\,(4.44\ MeV)$$

A depth profile is obtained by increasing the bombarding energy above the resonance energy of 6.385 MeV. This reaction has very narrow and isolated resonance at the energy of 6.385 MeV.
Fig.1 shows the yield function for $^{15}N(p,\alpha\gamma)^{12}C$ obtained by proton bombardment of titanium the surface of which was nitrated with $^{15}N_2$. Generation of doubly charged ^{15}N ions is indispensable to get energy higher than thus resonance energy in a small (3.75 MV) accelerator. Doubly charged ^{15}N ions were generated in a PIG type ion source. $^{15}N^{++}$ ion beams were accelerated up to resonance energy of 6.385 MeV and introduced to the scattering chamber where the hydrogen concentration profilings were performed. In between the accelerator and the scattering chamber, a pair of defining slits, a deflector to eliminate the $^{15}N^{+}$ions, a differential-pumping system and some others are installed. Fig.2 shows a schematic diagram of the experimental set-up used in this study.
The γ-rays were detected with a 60cm^3 Ge(Li) detector which was positioned at an angle of 0° with respect to the incident beam direction and at a distance of about 7 mm apart from the target.

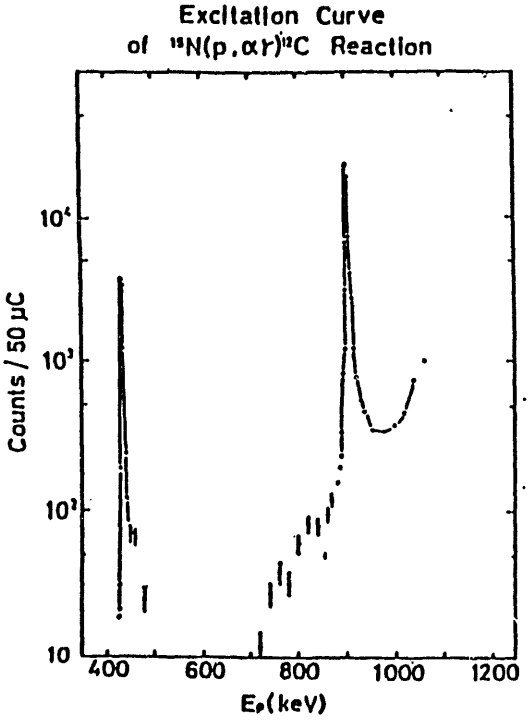

Fig.1 Excitation curve of $^{15}N(p,\alpha\gamma)^{12}C$ reaction.

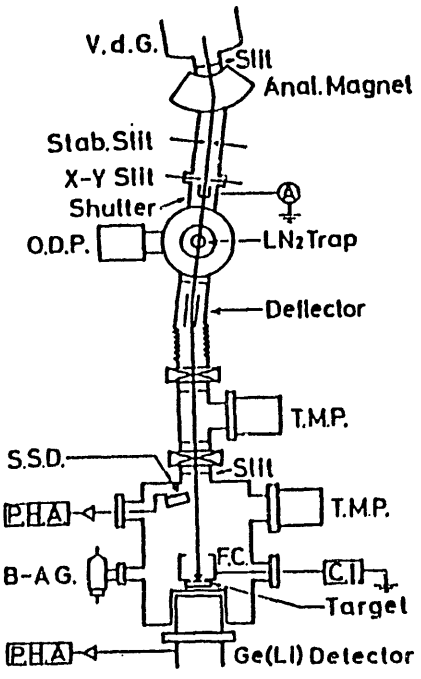

Fig.2 Schematic diagram of experimental set-up for resonant nuclear reaction analysis.

3. Results

Hydrogen concentration profilings in various carbon films were performed by ^{15}N resonant nuclear reaction method. Fig.3 show typical γ-ray spectra from bombarding the carbon films by ^{15}N ions a) on resonance and b) off resonance (back-ground). In the γ-ray spectrum of on-resonance, the characteristic γ-rays of 4.44 MeV and its single and double escape peaks can been seen clearly. In the off-resonace spectrum these γ-ray peaks are completely vanished. These characteristic γ-rays between 4.6 MeV to 3.2 MeV were integrated and plotted as a function of incident ^{15}N ion beam energy.
Fig.4 show the experimental results of hydrogen concentration profiling in two carbon films produced by methane and acetylene discharges. As is evident from Fig.4 the H-concetration decreases from 15% to 9% when the discharge gas changes from CH_4 to C_2H_2. On the other hand, the thicknesses of the film were estimated to be 2.8×10^{18} atoms/cm^2 for C_2H_2 and 1.8×10^{18}atoms/cm^2 for CH_4 discharge as these films were coated under the same conditions (voltage Vd=150V, current Id=0.1A, pressure p=1×10^{-4}Torr) and the same coating time(4hrs), the coating speed for C_2H_2 is higher than that of CH_4 by a factor of 1.5. Actual thicknesses of the carbon film were measured by a surface profiling instrument. From the results of these mesurements, actual thicknesses of the carbon film were determined to be 0.34μm for C_2H_2 and 0.26μm for CH_4 discharge. The density of the carbon film was determined from the measured carbon surface density divided by the actual thickness. This results indicates that the carbon film produced by pure C_2H_2 gases has higher density(1.7g/cm^3) than that of CH_4(1.4g/cm^3).

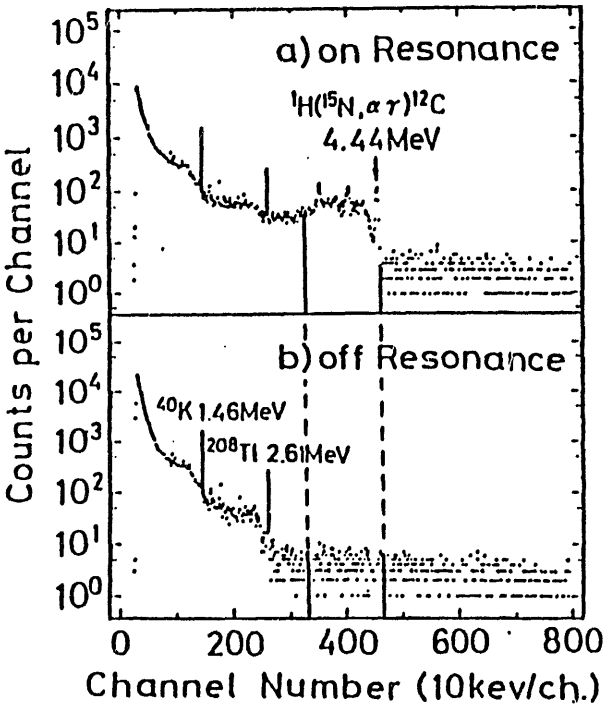

Fig.3 Gammaray spectra from bombardment of carbon films. a) on resonance, b) off resonance.

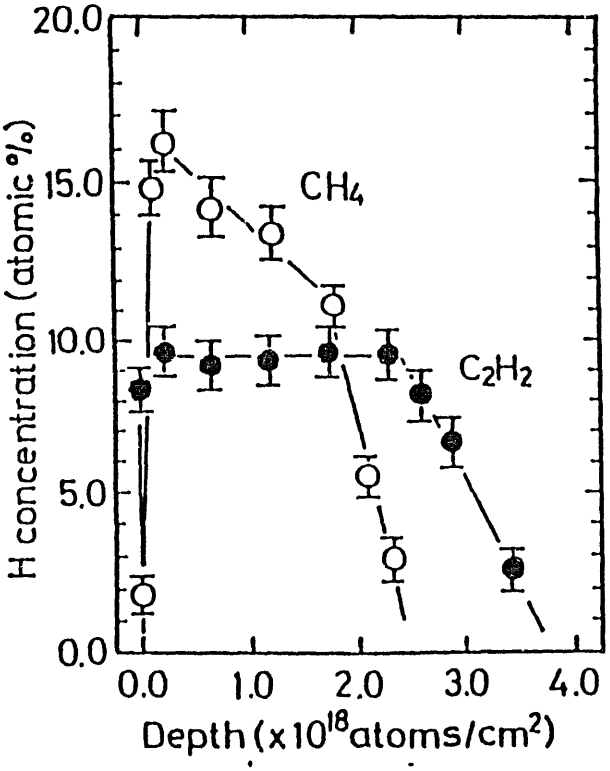

Fig.4 Hydrogen concentration profiles of carbon films deposited by methane and acetylene discharges.

Fig.5 shows the hydrogen concentration profile in Heliotron-E as in-situ coated sample. Hydrogen concentration in the films is about 12% at most, and the thickness of the film is 2.2×10^{17}atoms/cm^2. Fig.6 also shows the H concentration profile of Heliotron-E sample exposed to D_2 glow discharges and 139 shots of the main discharges. After the exposure to D_2 glow and the main discharges, the H concentration profile changed very much. Hydrogen content is decreased roughly by a factor of 2 and the thickness of the film is reduced by one half.

4. Summar

Hydrogen concentration profiles in various carbon films were measured by ^{15}N resonant nuclear reaction method. Carbon films were produced in hot cathode dc glow discharge of pure acetylene or pure methane gases. Compared with a CH_4 discharge, a low hydrogen content carbon film in the case of C_2H_2 discharge was produced with high coating speed. Hydrogen concentration of the films decreased roughly by a factor of 2 when the discharge gas was changed from CH_4 to C_2H_2. The carbon films coated in-situ in an actual fusion experiment device (Heliotron-E) were also examined.

^{15}N resonant nuclear reaction method is preferable and very important technique for hydrogen concentration profiling in the carbon films.

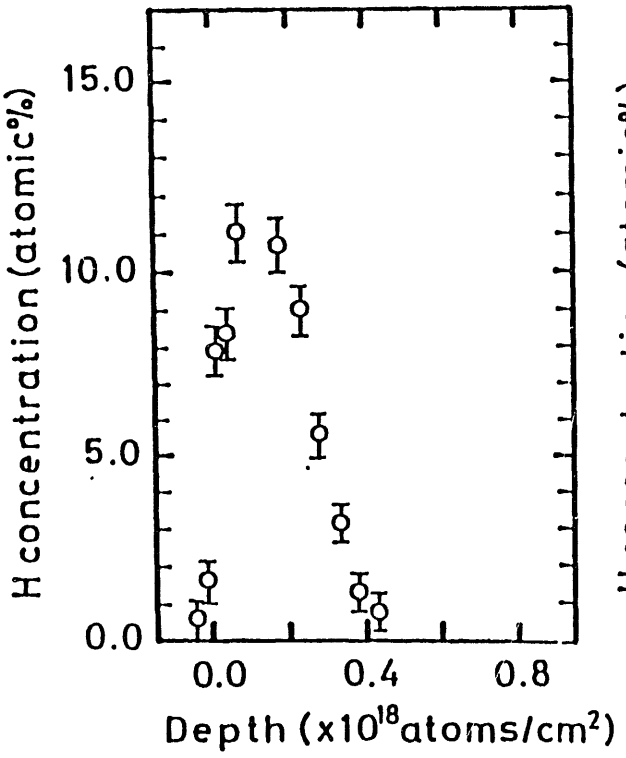

Fig.5 Hydrogen concentration profiles of carbon film coated in Heliotron-E device (as coated).

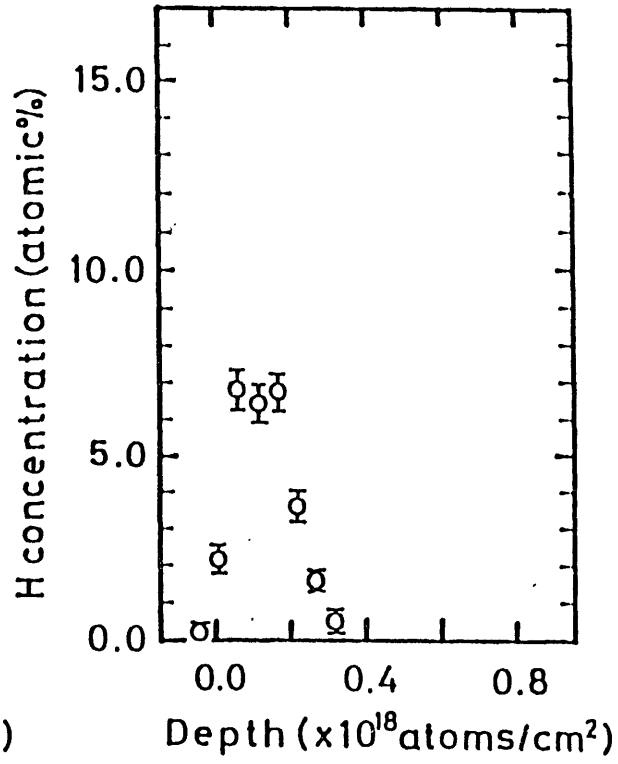

Fig.6 Hydrogen concentration profiles of carbon film coated in Heliotron-E device (after exposure to D_2 glow and main discharges).

Carbonization Processes and Hydrogen Plasma Interactions

H. Sugai
Department of Electrical Engineering
Nagoya University, Nagoya 464, Japan

Abstract

Recent basic studies of carbonization are briefly reviewed, and the necessity of the relevant atomic and molecular data is stressed for understanding the carbonization processes as well as the interaction of carbon with a hydrogen plasma.

Recently, much attention has been given to an in-situ carbon coating of the first wall of nuclear fusion devices.[1] The carbon films typically 300 Å thick protect the metal vessel walls from energetic particle bombardment, and they drastically reduce metal impurities in a high temperature fusion plasma. Compared with pre-coating, the in-situ coating has the following advantages: Firstly, low-Z materials (carbons) can readily be coated onto walls of enormously large area ($\sim$ 100 m^2) without exposure to atmosphere. Secondly, if necessary, the in-situ removal of coated films is available with use of chemical sputtering of hydrogen glow discharges. So far, the experiments with carbon coated walls have indicated favorable results of metal impurity reduction in fusion plasmas. Besides this success, however, there appeared a new problem of hydrogen gas desorption from the coated walls: A great quantity of hydrogen atoms contained in the prepared films are desorbed and deteriorate a magnetic confinement of fusion plasmas. Thus, a reduction of the H atom content in carbon films is an urgent and important subject in the carbon coating of fusion devices.

There has been a growing interest in carbon thin film

formation by the discharge decomposition of hydrocarbon gases.[2] The film properties are strongly dependent on many parameters such as gas pressure, power input, and substrate temperature. The quality of the obtained carbons can be classified to be amorphous carbon (soot), polymers (optically transparent, relatively soft films), graphitic films (dark brown, electrically conductive films), and "diamond-like" films (extremely hard, transparent films). The carbon films formed at a low temperature ($\leq$ 300 ^{0}C) contain a lot of hydrogen atoms; H/C atomic ratio often exceeds 0.4. A recent novel attempt[3] to deposit the diamond-like films showed the clear correlation of H-atom content with the film hardness: The less the H content is, the harder the carbon films .

The hydrogen content of carbon films is a good measure of film properties as well as film growth kinetics. The H-atom content can be reduced by a decrease in the discharge pressure of methane[4], by an increase in the ion bombardment[3], or by an elevated temperature of substrate(wall).[5] Recently, we have found a possibility of hydrogen reduction by acetylene discharges instead of methane discharges.[6] Extending the previous results, we have reported[7] a systematic study of carbon film formations from various species of hydrocarbon gases (methane, acetylene, benzene) admixed with diluting gases(hydrogen and noble gases).

First of all, we compared the carbon films formed by acetylene discharges with those by methane discharges in the hot-cathode discharge mode. To do this,we set the same filling pressure($p=1\times10^{-4}$ Torr) and almost the same n_e(2×10^9 cm^{-3}) and T_e(4 eV) for methane and acetylene. The carbon atom density n_C of the deposited films was evaluated from nuclear reaction, $^{12}C + d \rightarrow {}^{13}C + p$, while the hydrogen atom density of films was measured by elastic recoil detection (ERD). Figure 1 shows the carbon density and the hydrogen density measured as a function of wall(substrate) temperature for (a) methane and (b) acetylene discharges. Compared with the pure(100%) methane discharge, the pure acetylene discharge gives a high C-atom density and low H-atom density of films, as seen in this figure. This result may

be closely related to the triple bond of acetylene. On the other hand, the hydrogen-admixed discharges (15% CH_4/H_2, 15% C_2H_2/H_2) give rise to the reduction in the C density of films although the H density remains almost constant.

The dependence of carbon coatings on gas species was examined also in a cold-cathode discharge mode, which is characterized by the high pressure and high ion bombarding energy. The minimum pressures of CH_4, C_2H_2, and C_6H_6 to obtain the stable discharge were 2 mTorr, 70 mTorr, and 8 mTorr, respectively. The coating speed of carbon films is proportional to the pressure p and the electron density n_e. The speed normalized by p and n_e for the benzene discharge was five times as large as that for the methane and acetylene discharges.

The effect of admixed hydrogen was investigated in the same discharge power at the constant pressure of H_2 ($\sim$15 mTorr), where a trace of CH_4, C_2H_2, or C_6H_6 was admixed. Also, the effect of admixed helium was investigated in the same way. The H density of films deposited at the room temperature was estimated by the IR absorption technique.[4,5] The IR absorption spectra were found near 2900 cm^{-1}, corresponding to sp^3 (single) carbon bonds. No spectrum indicating sp^2 (double) or sp^1 (triple) carbon bonds was recognized even for the films formed by C_2H_2 or C_6H_6 discharges. And we could not detect the spectrum near 1500 cm^{-1} which corresponds to the bond oscillating mode of the benzene ring structure.

Figure 2 shows the H-atom density estimated by the IR absorption data. Three species of hydrocarbon gases are compared with one another for the discharges of pure species (100%), hydrogen dilution, and helium dilution. The datum for 100% C_6H_6 is missing in the figure since the rapid film growth leads to the poor adhesion, making the IR measurement inaccurate. Comparing 100% C_2H_2 discharge with 100% CH_4, it is again found in the cold-cathode mode that acetylene gives rise to the low H content. As shown in Fig.2, diluting the hydrocarbon gas with H_2 or He does not yield a significant variation of H content. If this tendency should hold true also for benzene,the H content for 100% benzene would be higher than that for acetylene.

The growth mechanisms of carbon films have remained unsolved, primarily because the diagnostics of radicals in gas phase is extremely difficult. A number of atomic and molecular processes are involved in a hydrocarbon plasma: The discharge decomposition of hydrocarbon gas takes place by electron impact dissociation and ionization as well as ion-molecule reactions. The resultant ions and neutral radicals are transported onto a solid surface where the surface reactions yield a new solid phase, i.e., carbon films. A few data of the total ionization cross sections can be found for methane, acetylene, and benzene[8], but the partial dissociation cross sections are scarce, which are necessary for modelling and understanding the chemically active plasmas.

The interactions of a hydrogen plasma with carbonized walls are important problems in application to nuclear fusion devices. Recently, Vietzke et al.[9] have investigated the chemical sputtering of amorphous carbon films where hydrogen atoms form a volatile methane via chemical reactions with carbon films. The sputtering yield strongly depends on the temperature, affecting the life time of carbon films. Furthermore, the methane desorbed from the films is decomposed by electrons in the hydrogen plasma, redepositing a new carbon films on the wall. For understanding the redeposition processes, we again need the data of the relevant atomic and molecular processes. Besides the sputtering process, the desorption and adsorption (recycling) of hydrogen are significant problems in carbonizing the first wall of fusion devices. A recent investigation[10] of hydrogen recycling in carbonized environment suggested the importance of the dangling bonds contained in the carbon films, which may be created by ion bombardment.

REFERENCES

(1) J. Winter, F. Waelbroeck et al., J. Nucl. Mater. 122 & 129, 1187(1984); 128 & 129, 841(1984).
(2) J.C. Angus, P. Koidl, and S. Domitz, Plasma Deposited Thin Films (edited by J. Mort and F. Jansen, CRC Press, Florida, 1986), Chap.4.
(3) H. Sugai, H. Kako and T. Okuda, Nucl. Instr. and Methods B23, 552(1987).
(4) H. Kojima, H. Kako, M. Terada, H. Sugai and T. Okuda, Japan. J. Appl. Phys. 24, 1432(1985).
(5) H. Sugai, H. Kojima, H. Kako, S. Urano and T. Okuda, J. Nucl. Mater. 145-147, 751(1987).
(6) H. Sugai, S. Urano, S. Amemiya, K. Ishikawa, N. Noda and T. Okuda, Japan. J. Appl. Phys. 25, L749(1986).
(7) H. Sugai, S. Urano, S. Ohshita and T. Okuda, Proc. of 8th Int. Symp. on Plasma Chemistry (Tokyo, 1987), Vol.3, p.1548.
(8) H. Deutsch, M. Schmidt, Beitr. Plasma Phys. 24, 475(1984).
(9) E. Vietzke et al., J. Nucl. Mater. 145-147, 443(1987).
(10) S. Yoshida, S. Ohshita, H. Sugai and T. Okuda, Kaku-Yugo Kenkyu 58, 402(1987), in Japanese.

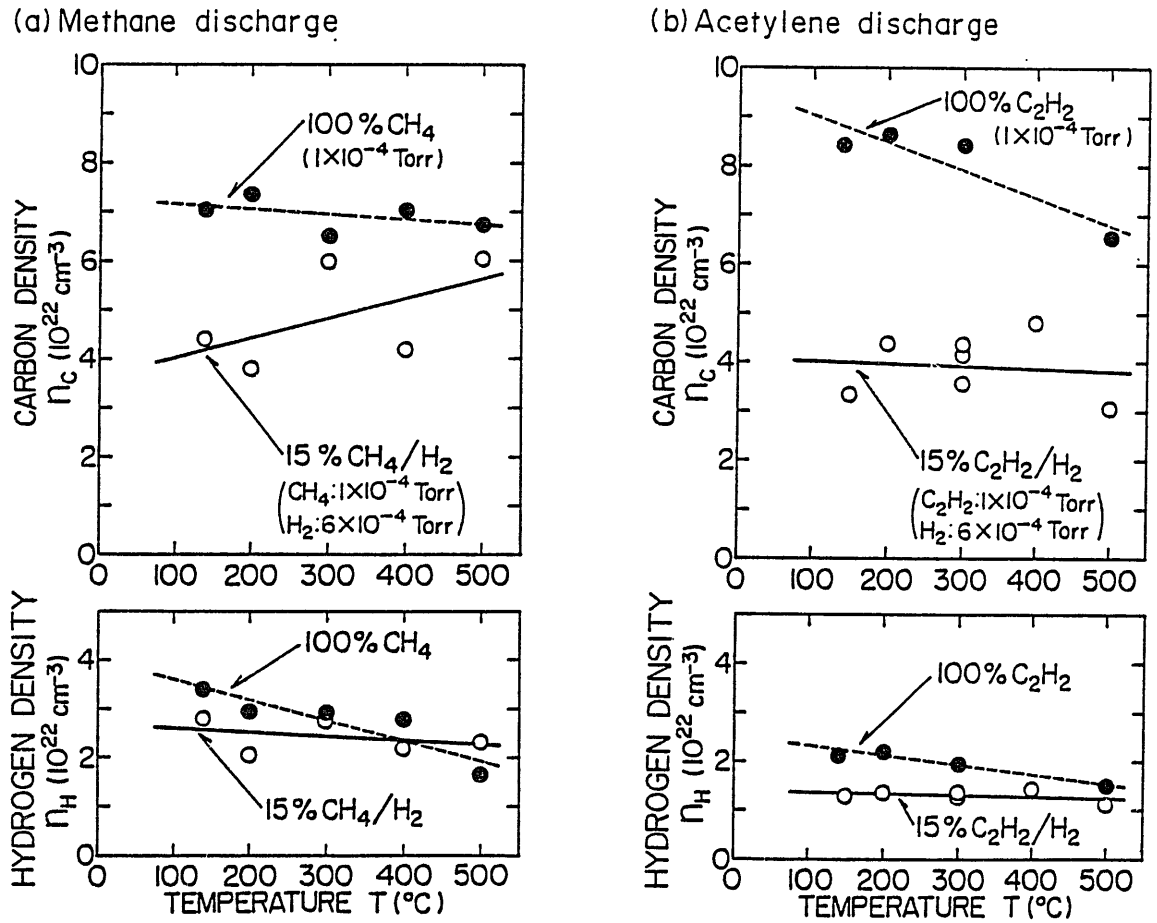

Fig. 1. Carbon density n_C and hydrogen density n_H vs. substrate temperature, for pure and H_2-admixed discharges.

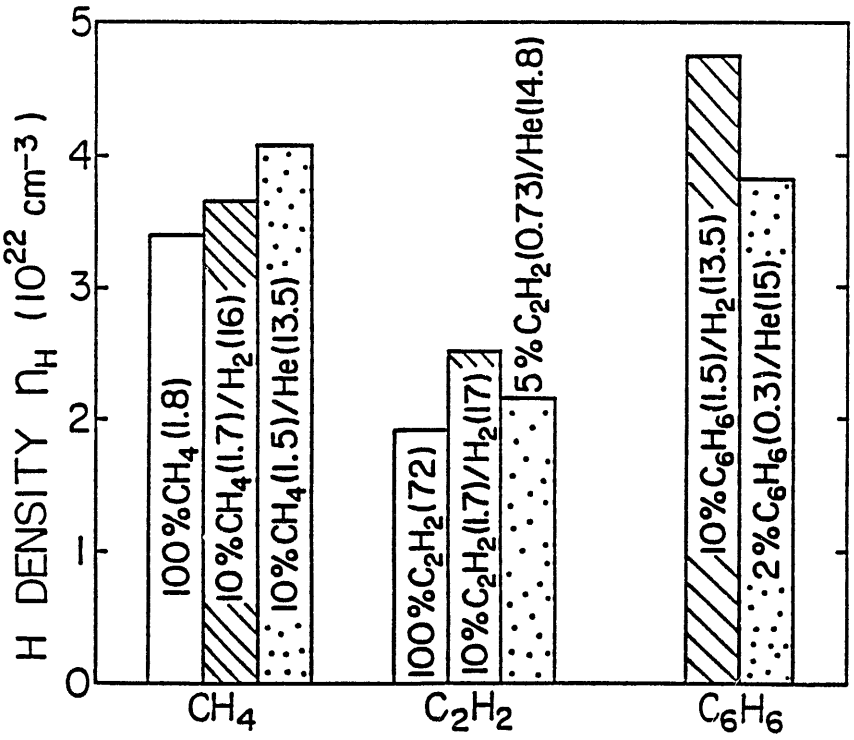

Fig.2. Hydrogen density n_H of films prepared from methane, acetylene and benzen in the mono-species (open columns), in the H_2 dilution (hatched columns), and in the He dilution(dotted columns). The numbers in brackets indicate the pressures in mTorr.

C_2 and C_3 Hydrocarbon Release due to Interaction of Protons and Graphite

Reiji Yamada
Japan Atomic Energy Research Institute, Tokai-mura, Ibaraki-ken, Japan

CH_4 formation due to bombardment of graphite with protons is widely known, whereas C_2 and C_3 hydrocarbon formation is apt to be neglected up to now. Recent works, however, reveal that the heavier hydrocarbon formation plays much more important roles in the chemical sputtering than CH_4 formation does, if the incident energy is less than 500eV. This short note introduces some of those results to underline the need of careful consideration to them for the release of impurities into plasma from graphites.

1. A critical comparison of chemical sputtering yields obtained by different groups

Graphite has been widely used in fusion devices as limiter and divertor materials due to low-Z and high melting point. From a viewpoint of the introduction of carbon impurity into plasma as well as of the lifetime of the walls, the chemical sputtering due to interaction of energetic hydrogen and graphite was intensively investigated at high temperatures.

For measurements of chemical sputtering yields two methods have mainly been used, namely the measurements of weight loss of target and of CH_4 production rate using quadrupole mass spectrometer(QMS). Total erosion yields at high temperatures(around 500 C) measured by the weight loss method were considered as CH_4 production yields, because it was taken

for granted that CH_4 was the predominant product at a temperature around 500 C without further careful consideration. A similar situation occurred in the second method where only signal intensities of mass 15 corresponding to CH_4 were measured by using QMS and, then, from the beginning, assumed to represent the chemical sputtering yields. This is because there was no knowledge about the importance of heavier hydrocarbon products to the chemical sputtering up to a couple of years before.

The above two misleading usages of chemical sputtering are considered to be one of reasons why some discrepancies seem to exist among the data previously reported as chemical sputtering yields by different groups. Let us review them from the above viewpoint. In the case of energy dependence there were discrepancies among JAERI, Garching and Toronto groups[1-5]. Our previous results obtained by using QMS show that the yield, actually to be named as the CH_4 production yield, has a maximum around 1 keV[1], whereas those of Garching group by using the weight loss method show that it has a peak around 200-300 eV[2-4]. This discrepancy should be attributed to whether or not heavier hydrocarbon products are included into the yield as shown in the next section. Using the same method as ours, however, the CH_4 production yields reported by Toronto group[5] had the energy dependence similar to that of Garching group. By making the incident energy intervals smaller, we recently measured more precise energy dependence of CH_4 yields, whose peak occurs at 700-1000eV[6] and becomes a little broader than the previous one[1]. The other two groups also have recently reported new similar results measured by using QMS at peak the temperatures[7,8]. The discrepancy between ours and the previous results of Toronto group is found to come from the fact that those of the former group were obtained at the peak temperatures[1,6] but those by the latter at the constant temperature of 800 K[5,7]. Therefore, we can say now that the results of different groups

about the energy dependence of CH_4 yields at the peak temperatures agree fairly well each other.

It seems that the discrepancy among the results of temperature and flux dependence of CH_4 yields is rather small, i.e., the CH_4 production yield has the peak around 450-600 C and the peak temperature tends to increase with increasing the incident proton flux[6,7,9]. The peak yield depends little on the flux in the range of 10^{14-15} H/cm^2s[6,7], and then decreases with increasing flux, if the flux goes up to 10^{19} H/cm^2s[10]. The slope of decrease, however, is less than the predicted, namely the inverse of flux, by a simple model proposed by Erents et al.[11].

2. Contribution of heavier hydrocarbon products to chemical sputtering yield

Our recent investigation shows that the C_2 hydrocarbon production at 500 C greatly contributes to the chemical sputtering in the low proton energies(200-500 eV), whereas the CH_4 production dominates at higher proton energies[6]. Fig. 1 shows typical temperature dependences of the QMS signals of CH_4(M/e=15), C_2 and C_3 hydrocarbon production. Fig. 2 shows hydrocarbon production yields(C_mH_n/H) at peak temperatures as a function of the incident energy of hydrogen. It is clear that the CH_4 yields are larger than the yields of other heavier hydrocarbons in the whole energy range(0.1-6keV), and that the heavier hydrocarbons have maxima at lower incident energies than CH_4 does. The heavier hydrocarbons production yields, however, should be multiplied by the number of carbon atoms in hydrocarbons to obtain the chemical sputtering yield(C/H), i.e., the number of sputtered carbon atoms per hydrogen. Fig. 3 shows the above results and reveals that the contribution of C_2 hydrocarbons to the chemical sputtering is the largest among total hydrocarbon production in the energy range between 200 and 500 eV, and that the sum of CH_4, C_2 and

C_3 yields has a maximum at 200-300 eV similar to the peak energy of chemical sputtering yield measured by the weight loss method.

The above results are considered to be quite reasonable, since the chemical sputtering yield measured by the weight loss method includes implicitly the heavier hydrocarbon yields, whereas these should be added to the chemical sputtering yield previously measured by using QMS.

The importance of heavier hydrocarbons to the chemical erosion of carbon materials was also observed by Vietzke et al.[12] and Davis et al.[13] using sub-eV atomic hydrogens and low energy protons. Their results show that the sub-eV atomic hydrogen impact makes the formation of heavier hydrocarbons dominate the total carbon erosion process much more than the energetic proton bombardment does.

It is clear from the above results that when the ionization and dissociation processes are analyzed in plasmas facing carbon wall/limiters in fusion devices, not only total chemical sputtering yield but also each yield of hydrocarbons should be included. It should be noted here that these heavier hydrocarbon yields cannot be directly obtained from QMS measurement and require a rather complicated fitting procedure[14], which causes inevitably large errors in the estimation of these yields. This would be one of the main reasons that the summed yields of hydrocarbons are higher than those obtained from the weight loss method.

References

[1] R. Yamada, K. Nakamura, K. Sone and M. Saidoh, J. Nucl. Mater. 95 (1980) 278.

[2] J. Roth, in: Sputtering by Particle Bombardment II, Topics in Applied Physics, Vol. 52, Ed. R. Behrisch (Springer-Verlag, New York, 1983) p.21.

[3] J. Roth , in: Physics of Plasma-Wall Interactions in

Controlled Fusion, NATO Advanced Science Institutes Series B Physics, Vol.131, Ed. D. E. Post and R. Behrisch (Plenum Press, New York, 1986) p.389.

[4] J. Roth, in Data Compendium for Plasma-Surface Interactions, Nucl. Fusion, special issue (1984) p.72.

[5] A. A. Haasz, O. Auciello and P. C. Stangeby, Rad. Effects 89 (1985) 63.

[6] R. Yamada, J. Nucl. Mater. 145-147 (1987) 359.

[7] J. W. Davis, A. A. Haasz and P. C. Stangeby, J. Nucl. Mater. 145-147 (1987) 417.

[8] J. Roth and J. Bohdansky, Nucl. Inst. Meth. B23 (1987) 549.

[9] J. Roth, J. Bohdansky and K. L. Wilson, J. Nucl. Mater. 111-112 (1982) 775.

[10] J. Roth, J. Nucl. Mater. 145-147 (1987) 87.

[11] S. K. Erents, C. M. Braganza and G. M. McCracken, J. Nucl. Mater. 63 (1976) 399.

[12] E. Vietzke, K. Flaskamp, V. Philipps, G. Esser, P. Wienhold and J. Winter, J. Nucl. Mater. 145-147 (1987) 443.

[13] J. W. Davis, A. A. Haasz and P. C. Stangeby, Proc. Int. Conf. Fusion Material held in Karlsruhe (1987) to be published in J. Nucl. Mater.

[14] R. Yamada, J. Vac. Sci. Technol. A5 (1987) 305.

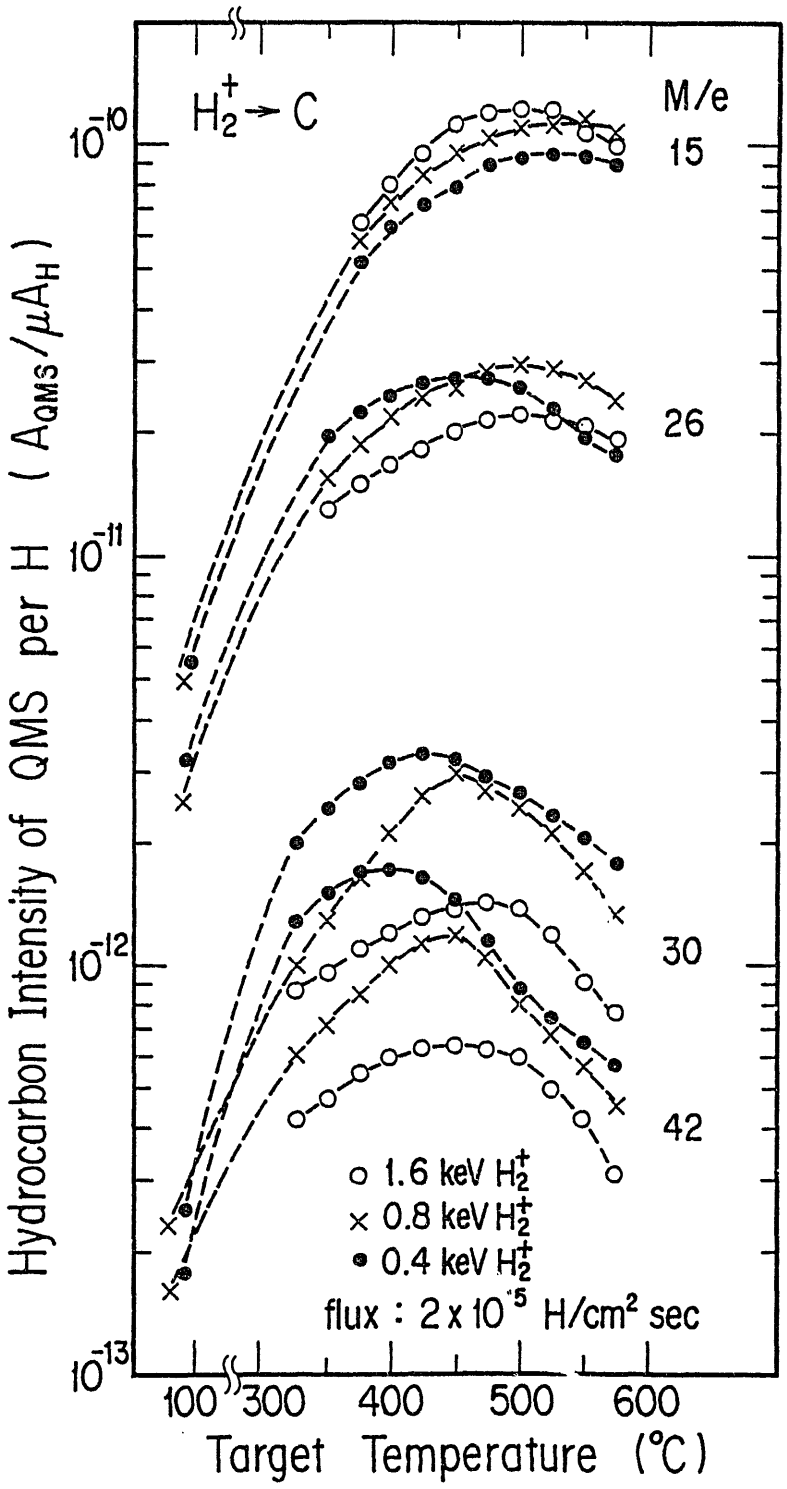

Fig. 1 Typical temperature dependences of the QMS signals of CH_4(M/e=15), C_2 and C_3 hydrocarbon production. From ref.6

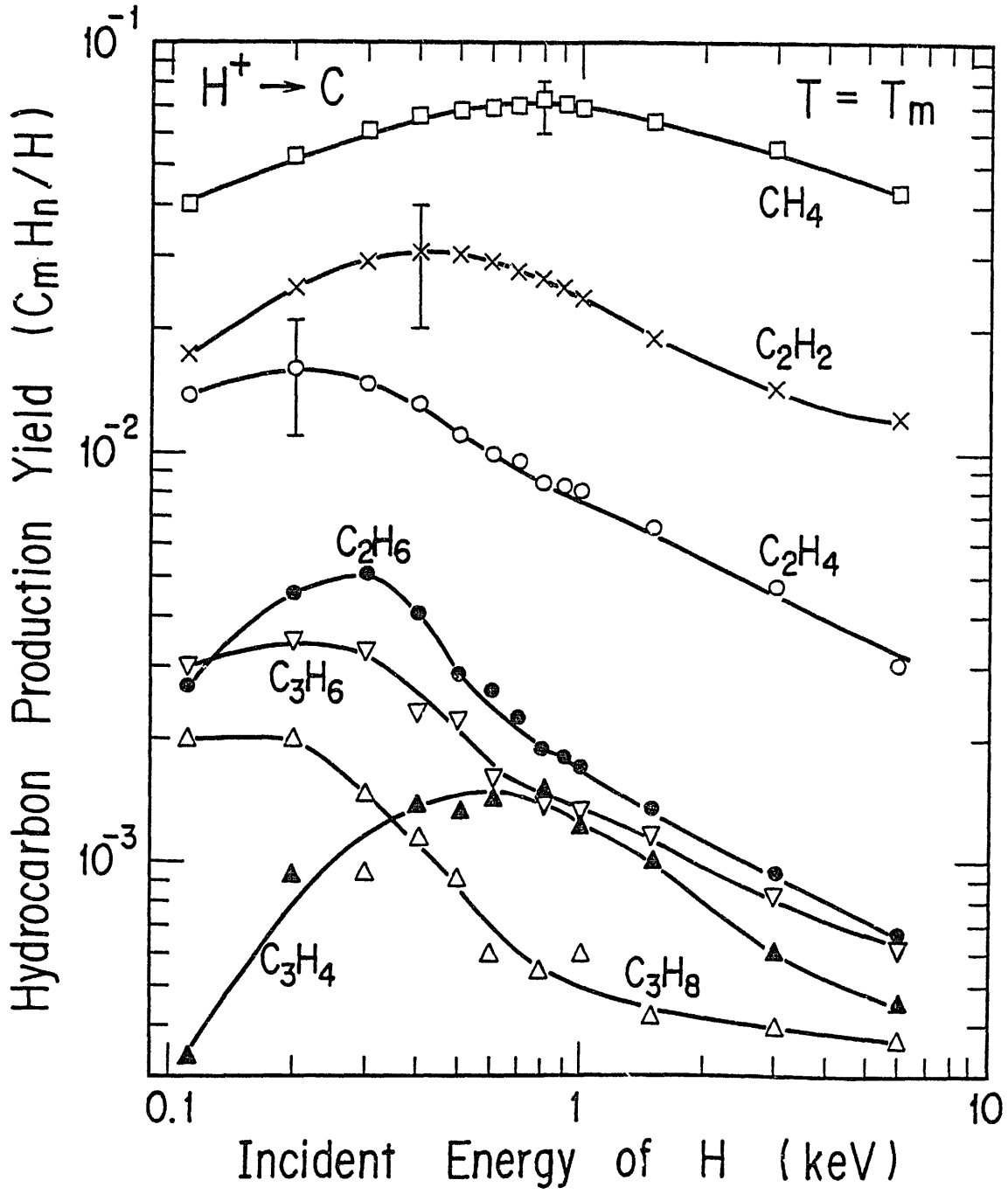

Fig. 2 Energy dependences of estimated C_2 and C_3 hydrocarbon production yields at the peak temperature of T_m. In order to obtain the chemical sputtering yields, the hydrocarbon production yields should be multiplied by the number of the carbon atoms of hydrocarbons. From ref.6

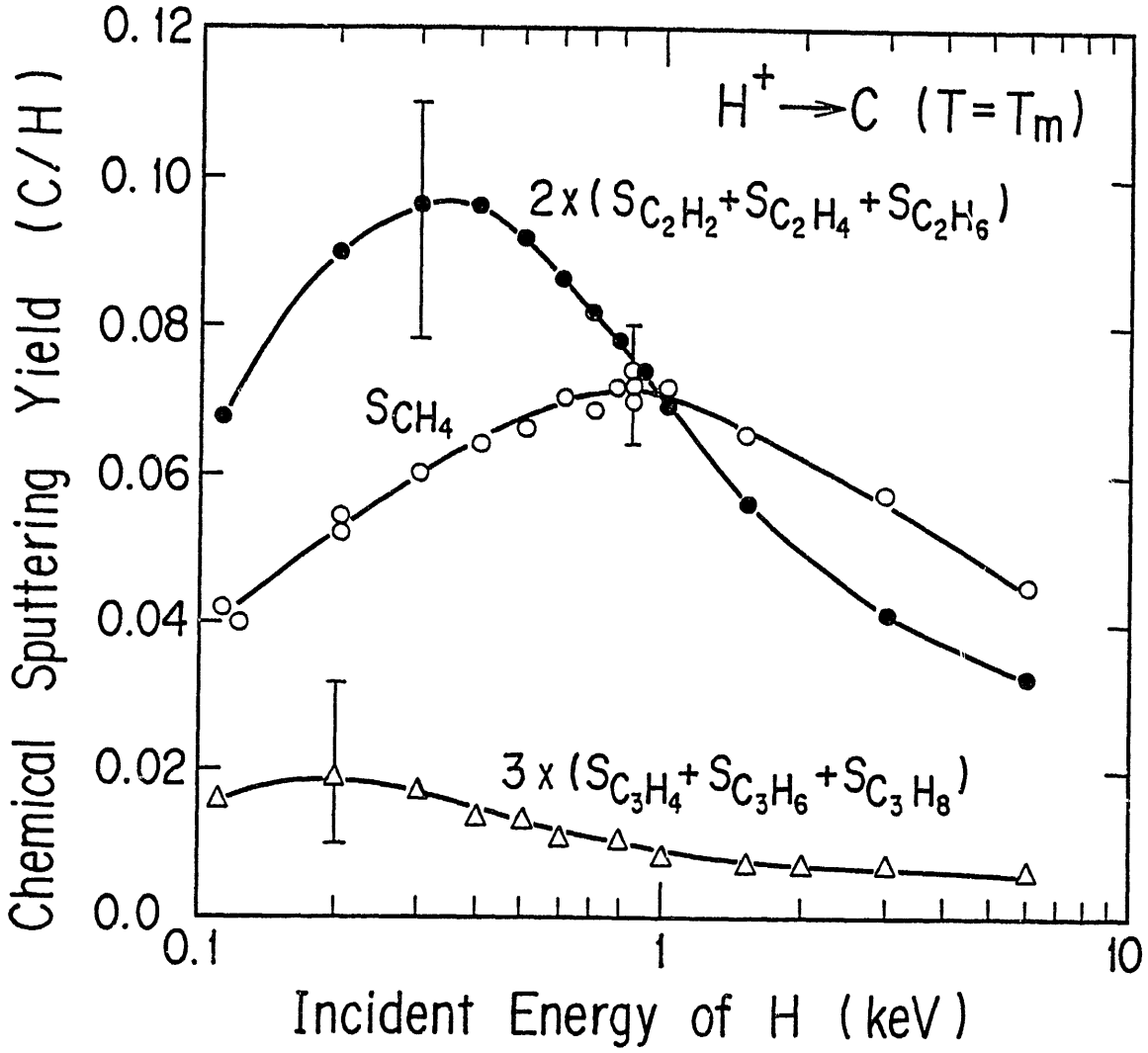

Fig. 3 Energy dependences of estimated chemical sputtering yields (C/H) of C_1, C_2 and C_3 hydrocarbons at the peak temperature of T_m. From ref.6

Chemical Sputtering of Graphite under Hydrogen Ion Irradiation

Y. Horino

Department of Crystalline Materials Science, Faculty of Engineering,
Nagoya University, Furo-cho, Chikusa-ku, Nagoya 464-01, Japan

Abstract

In this paper, several experimental results regarding chemical sputtering of graphite under hydrogen ions irradiation are introduced and a theoretical investigation of the chemical sputtering based on the physical two-step model is reported.

1. Experimental features of chemical sputtering of graphite

The chemical sputtering of graphite, which is a good candidate for plasma-facing materials for fusion reactors, is one of the important problems of plasma-wall interactions. A great deal of experiments have been done[1,2] and, even though experimental results are scattered to some extent from author to author, several following characteristic features of chemical sputtering of graphite have been revealed :

(1) Temperature dependence

(2) Energy dependence

(3) Flux dependence

(4) Synergistic effects

The temperature dependence of chemical sputtering yield of graphite under irradiation with hydrogen ion, which has a peak around 800 K[3], is the most significant feature (Fig. 1). At this

temperature range, the formation of hydrocarbons, whose main species is methane, enhances the sputtering yield relative to physical sputtering that dominates at low temperature. The yield enhancement by a factor of 10-100 has been observed at temperature around 800 K for hydrogen ions in the energy range of 100 eV to 20 keV. Above 1300 K, radiation enhanced sublimation is known to become dominant and the erosion yields of graphite again increase gradually[4].

The energy dependence of the chemical sputtering yield at the temperature around 800 K is shown in Fig. 2[2]. It can be seen that there are two different types of dependence of the chemical sputtering yield on hydrogen ion energy : a weak energy dependence having a peak around 200 eV (Fig. 2a) and a stronger energy dependence having a peak around 2 keV (Fig. 2b). It seems that the two different types of the energy dependence originate in different methods of measuring the chemical sputtering yield. The sputtering yield determined by means of weight loss measurement exhibits the former energy dependence and the yield determined by means of Q-mass spectroscopy which detects CH_4 molecules exhibits the latter. Recently, Yamada[5] has shown that energy dependence of erosion yield of graphite determined by detection of not only methane but also other hydrocarbons by Q-mass spectroscopy measurement has a peak around 200 eV, similar to that observed by means of weight loss.

The flux dependence of the chemical sputtering yield at constant sample temperatures has a peak at a certain hydrogen ion flux density and the yields decrease at both low and high flux densities[3] (Fig. 3). However, as far as maximum yield, Y_M, is concerned, the variation with flux density is much less pronounced[3]. It is known that the temperature T_M at which the yield is the highest, Y_M, varies substantially with flux density[3,5].

The synergistic effects in chemical sputtering, namely the erosion rate under simultaneous irradiation with two kinds of beams is larger than the summation of the erosion rates under irradiation with individual beams, are one of the characteristic features in graphite sputtering and a great deal of investigations have been done. Auciello et al[2,6]. have investigated the methane formation yield under simultaneous irradiation with 3 keV H_3^+ and sub-eV H^0 at around 800 K (Fig. 4). It is shown that the yield under simultaneous irradiation with H^+ and H^0 is larger by a factor of 4 than the yield under irradiation with only H^+. More significant synergism has been observed by Vietzke et al.[4,8] using H^+ and Ar^+ ion beams.

These synergistic effects have been explained by Itoh and Hasebe[9] using their "physical two-step model". Theories of chemical sputtering need to explain synergism as well as other important characteristics of chemical sputtering such as temperature and energy dependences.

2. Model of chemical sputtering

Models for chemical sputtering have been proposed by several authors. The most sophisticated model has been suggested by Balooch and Olander[10]. Their model is essentially based on the kinetics of methane formation through several intermediate states. Because of the existence of several unknown factors, application of their model to real cases is not easy. Erents et al.[11] have suggested a simplified phenomenological scheme that explains the temperature dependence and the relation between T_M and the incident energy. Their model, however, includes parameters for which the physical basis is not clear. Synergistic effects have not been explained in terms of these models.

In the following, we show that the physical two-step model[9], by which the synergistic effects are explicable, can be used to explain several other experimental characteristics of chemical sputtering. Since the experimental results are scattered to some extent from author to author, we do not intend to obtain the best fit parameters for chemical sputtering. We intend to show briefly how the present model can explain semiquantitatively a variety of experimental data regarding chemical sputtering including synergistic effect (The details are given in ref. 13).

The present physical two-step model is based on the assumption that there are two potential minima that govern the reaction between carbon atoms of graphite and implanted hydrogen atoms to form CH_4. The potential energy curve describing the physical two-step model is shown in fig. 5. The initial state of the reaction is a carbon atom in graphite and four hydrogen atoms in vacuum. The final product is a CH_4 molecule. We assume that there are two potential minima M_1 and M_2 between the initial state and the final state. Each minimum represents an intermediate reaction product. Referring to fig. 5, we define the rate constants for transitions between the minima and those from and to the minima as follows. α, β and γ are the rate constants for CH_4 ejection from M_1, for supplying to M_2, and for the reverse reaction from M_2, respectively; k_1 and k_2 are the rate constants for the transitions from M_1 to M_2 and from M_2 to M_1, respectively. We can obtain kinetic equations for the numbers n_1 and n_2 of hydrogen atoms per unit row perpendicular to the surface in M_1 and M_2, reacting with carbon atoms to form the states represented by M_1 and M_2 as follows :

$$dn_1/dt = -(\alpha+k_1)n_1+k_2n_2 \ , \qquad (1)$$

$$dn_2/dt = k_1n_1-(k_2+\gamma)n_2+\beta(n_0-n_2) \ , \qquad (2)$$

where n_0 is the saturation concentration for n_2. A similar saturation concentration may exist for n_1 but practically it needs not be considered, since $n_1 << n_2$. These equations are similar to those in our previous paper[9] for synergestic effects, where the term n_2 is not included.

At steady states, the sputtering rate Q is given by

$$Q = \alpha n_1 = \frac{\alpha\beta\, k_2 n_0}{\alpha k_2 + (\beta+\gamma)(\alpha+k_1)} \quad . \tag{3}$$

For chemical erosion by energetic hydrogen ions, Q divided by the flux, ϕ, gives the sputtering yield Y.

Hysteresis effects have been observed and ascribed to the effect of hydrogen atoms accumulated in the near-surface layers[1]. The hydrogen concentration near the surfaces depends on several factors such as flux, incident energy E, the speed of temperature change and previous history of treatments. In order to avoid complexity, we take the surface fractional concentration as a parameter, denoted by c.

In view of the arguments in our previous paper[13], several conditions have been imposed on the parameters of the kinetic equations as follows.

1) α, γ and k_1 follow Arrhenius equation and γ is also proportional to c ;

2) k_2 is proportional to the number of knockons ;

3) β is proportional to the flux, ϕ.

Fig. 6 shows the temperature dependence of the sputtering yield for several values of the parameter ϕ/c. The absolute value is designated in arbitrary units because of the ambiguity in the parameter values. The maximum values Y_M of the sputtering yield and

the temperature T_M increase as ϕ/c increases. The increase in Y_M with decreasing c arises from the reduction of the rate of the reverse reaction. The dependence on ϕ/c of Y_M, T_M and the half-width T_H of the Y-T curves are shown in figs. 7 and 8.

The Y-T curves for several incident energies are given in fig. 9. The result is consistent with that by Erents et al. : the temperature T_M where the Y-T curve reaches a maximum is independent of the incident energy below about 1 keV, and the maximum yield Y_M increases slightly as the energy increases up to 0.2 keV and then decreases. The energy dependence of Y_M for several values of ϕ/c is shown in fig. 10.

The synergistic effects under simultaneous bombardment with energetic H^+ ions and sub-eV H^0 atoms can be described using eq. (3). In our previous paper[9], H^+ was assumed to be effective on α, k_2 and while H^0 is effective only on α. Alternatively, it may be assumed that H^0 is effective only on β directly and on α indirectly through c. A substantial difference is seen in the Y-T curves under these two assumptions : T_M is independent of the flux of H^0 under the former assumption, while under the latter assumption it increases with increasing H^0 flux. Since several experimental results[12] show a shift of T_M to higher temperatures with increasing H^0 flux, we adopt the latter version in the present paper. We assume $\beta=\phi/N_s$ for thermal hydrogen atoms where N_s is the number of carbon atoms per unit area.

Fig. 11 shows Y-T curves for simultaneous bombardment with H^+ and H^0. The synergistic effects are clearly indicated. Furthermore, T_M is seen to increase with increasing H^0 flux. In fig. 12 we show the relation between the sputtering rate Q and the flux of energetic hydrogen ions and without simultaneous irradiation of thermal energy

hydrogen atoms. Without thermal hydrogen, Q depends on ϕ/c quadratically, while with thermal hydrogen, Q is proportional to ϕ/c when ϕ/c is small. The values of Q with and without the thermal energy hydrogen atoms approach each other when ϕ/c is larger than the flux of thermal energy hydrogen atoms.

3. Summary

In summary, we have shown several characteristic experimental features of chemical sputtering of graphite under hydrogen ion irradiation such as temperature dependence and also have shown that our proposed physical two-step model can explain semiquantitatively several important features of chemical sputtering including synergistic effects. The detailed description of the present model is given in ref. 13.

References

1) J. Roth, Topics in Applied Physics, vol. 52, ed. R. Behrisch (Springer, Berlin, 1983) p.91.

2) O. Auciello, A. A. Haasz and P. C. Stangeby, Radiat. Eff. 89, 63 (1985).

3) J. W. Davis, A. A. Haasz and P. C. Stangeby, J. Nucl. Mater. 145-147, 417 (1984).

4) J. Roth, J. Bohdansky and K. L. Wilson, J. Nucl. Mater. 111/112, 775 (1982).

5) R. Yamada, J. Nucl. Mater. 145-147, 359 (1987). Also see this proceedings.

6) A. A. Haasz, J. W. Davis, O. Auciello, P. C. Stangeby, E. Vietzke, K. Flaskamp and V. Philipps, J. Nucl. Mater. 145-147, 412 (1987).

7) E. Vietzke, K. Flaskamp and V. Philipps, J. Nucl. Mater. 111/112, 763 (1982).

8) E. Vietzke, K. Flaskamp and V. Philipps, J. Nucl. Mater. 128/129, 545 (1984).

9) N. Itoh and Y. Hasebe, J. Nucl. Mater. 139, 77 (1986).

10) M. B. Balooch and D. R. Olander, J. Chem. Phys. 63, 4772 (1975).

11) S. K. Erents, C. M. Braganza and G. M. McCracken, J. Nucl. Mater. 63, 399 (1976).

12) J. B. Roberto and R. Behrisch, J. Nucl. Mater. 128/129, 764 (1984).

13) N. Itoh and Y. Horino, Nucl. Instrum. & Methods B28, 264 (1987).

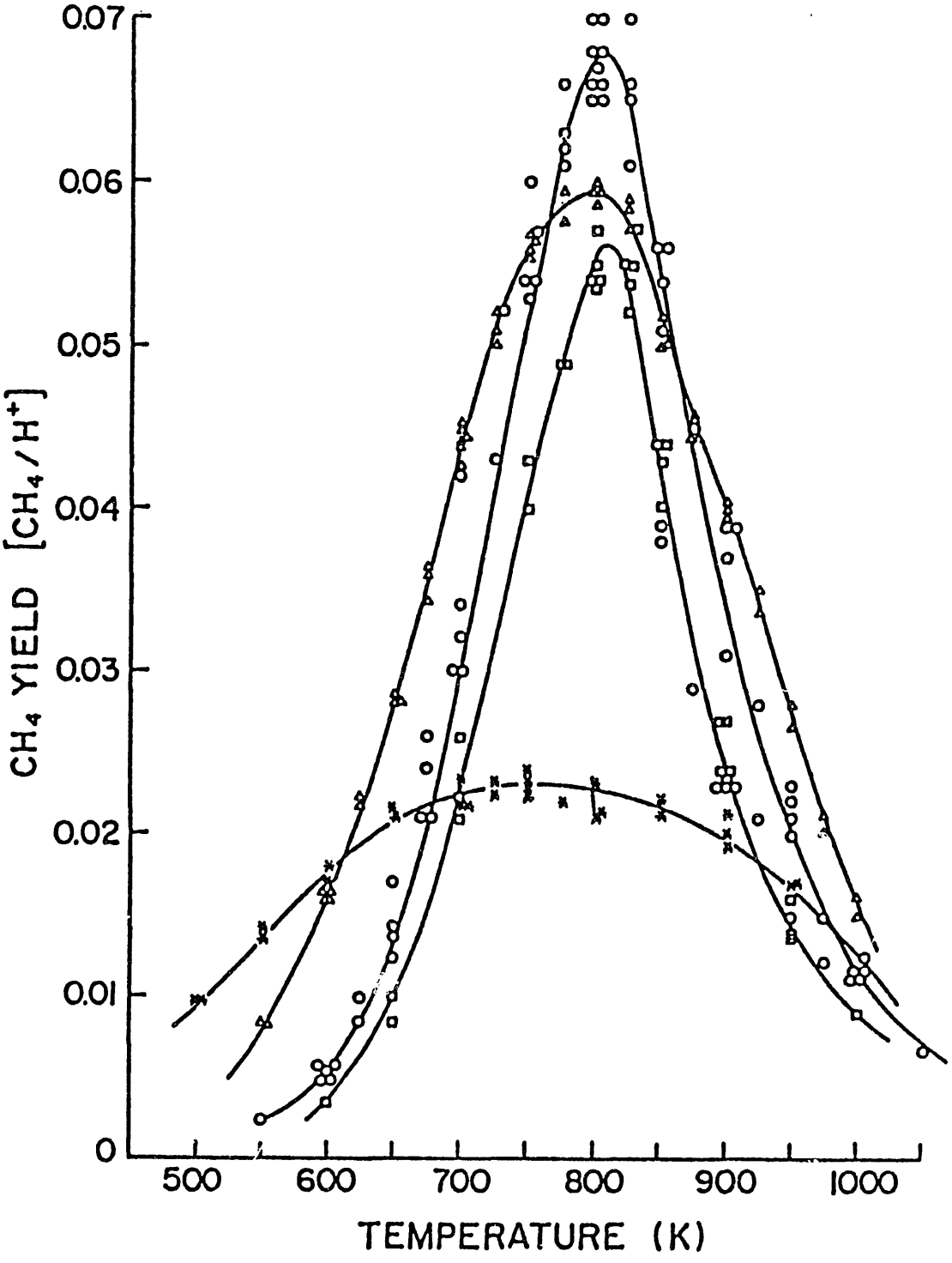

Fig. 1 CH_4 yield as a function of sample temperature :
☆ 300 eV H_3^+; △ 900 eV H_3^+; ○ 3 keV H_3^+ and □ 9 keV H_3^+ (ref. 3).

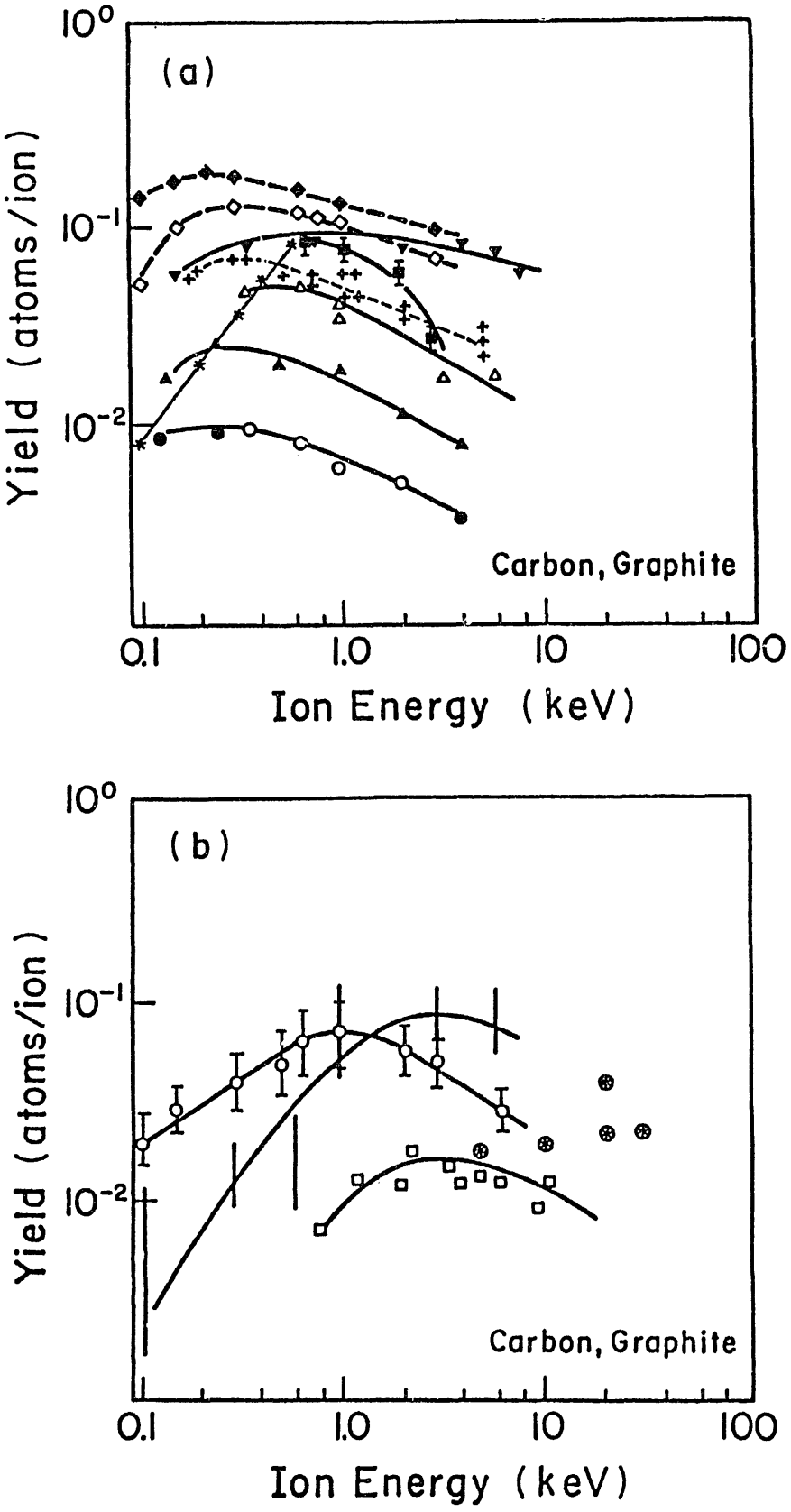

Fig. 2 Experimental sputtering yield as a function of incidence energy obtained by different groups (ref. 2).

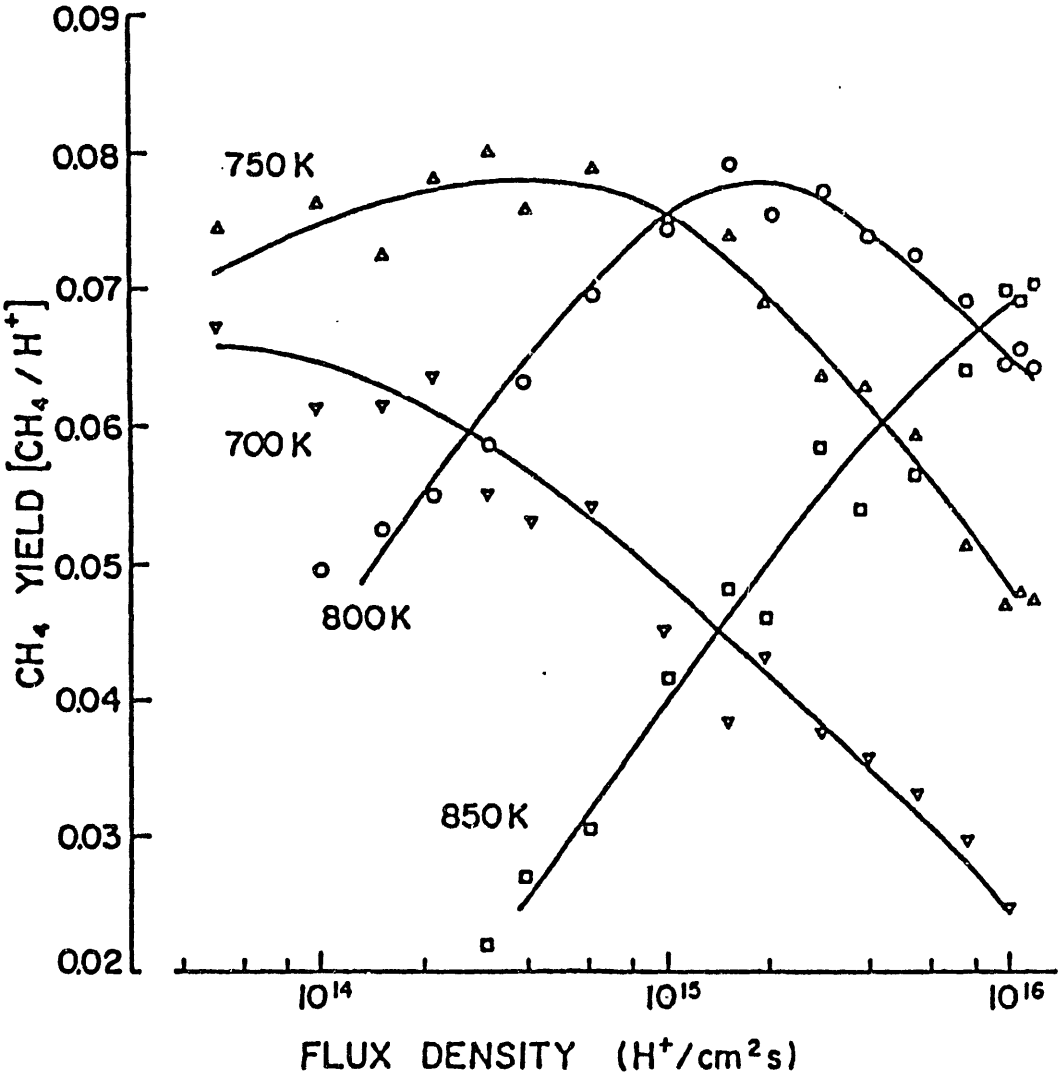

Fig. 3 CH_4 yield as a function of flux density of incidence ions at 700 k(▽), 750 K(△), 800 K(○) and 850 K(□).

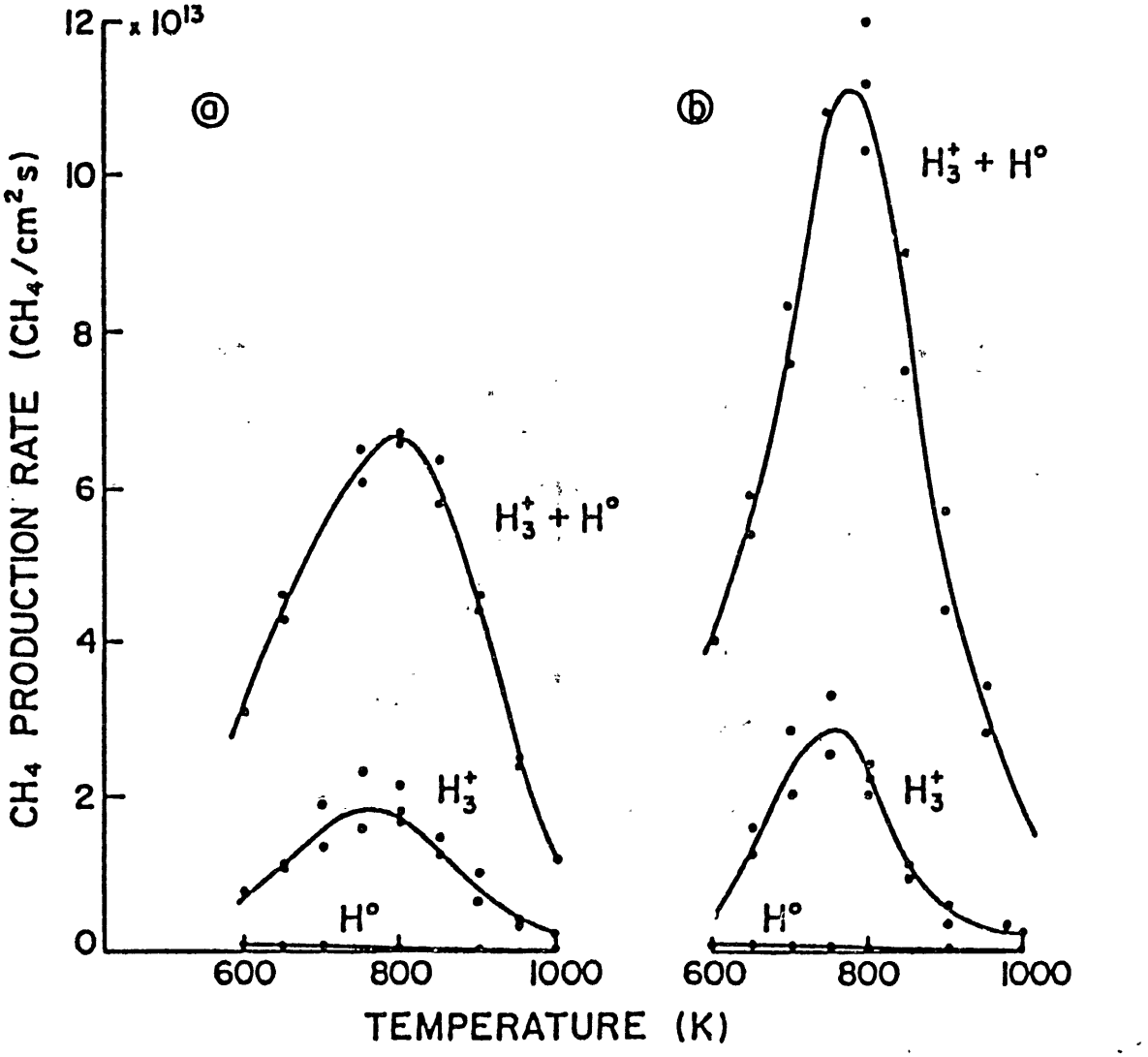

Fig. 4 Temperature profiles for methane production from H^0 atoms alone (1.7×10^{15} $H^0/cm^2 \cdot s$), H^+ ions alone and combined H^+-H^0 bombardment; (a) 900 eV H_3^+, 2.8×10^{14} $H^+/cm^2 \cdot s$ and (b) 3 keV H_3^+, 3.3×10^{14} $H^+/cm^2 \cdot s$ (ref. 6)

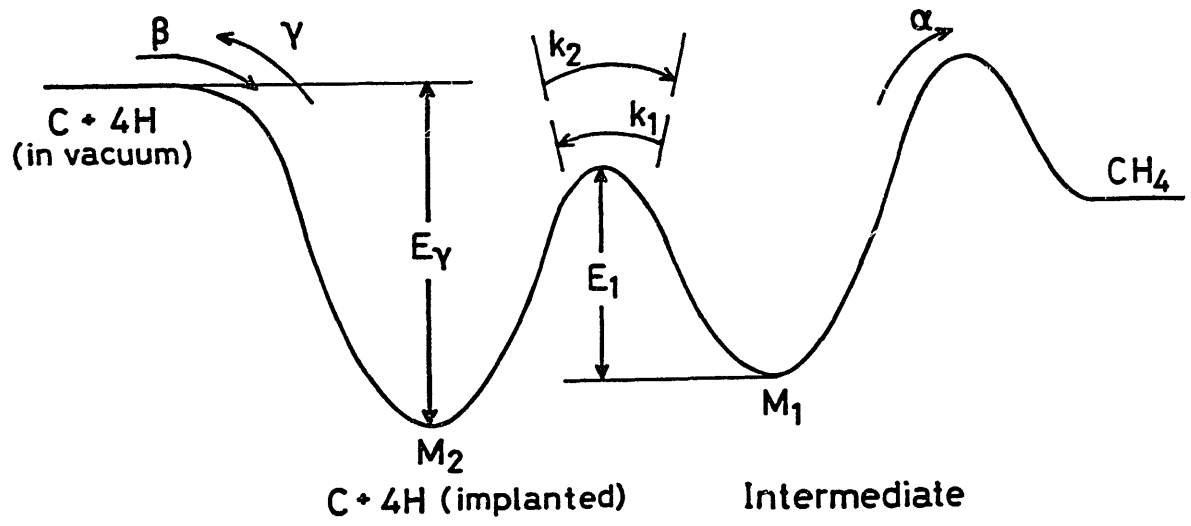

Fig. 5 The physical two-step model for chemical sputtering of graphite.

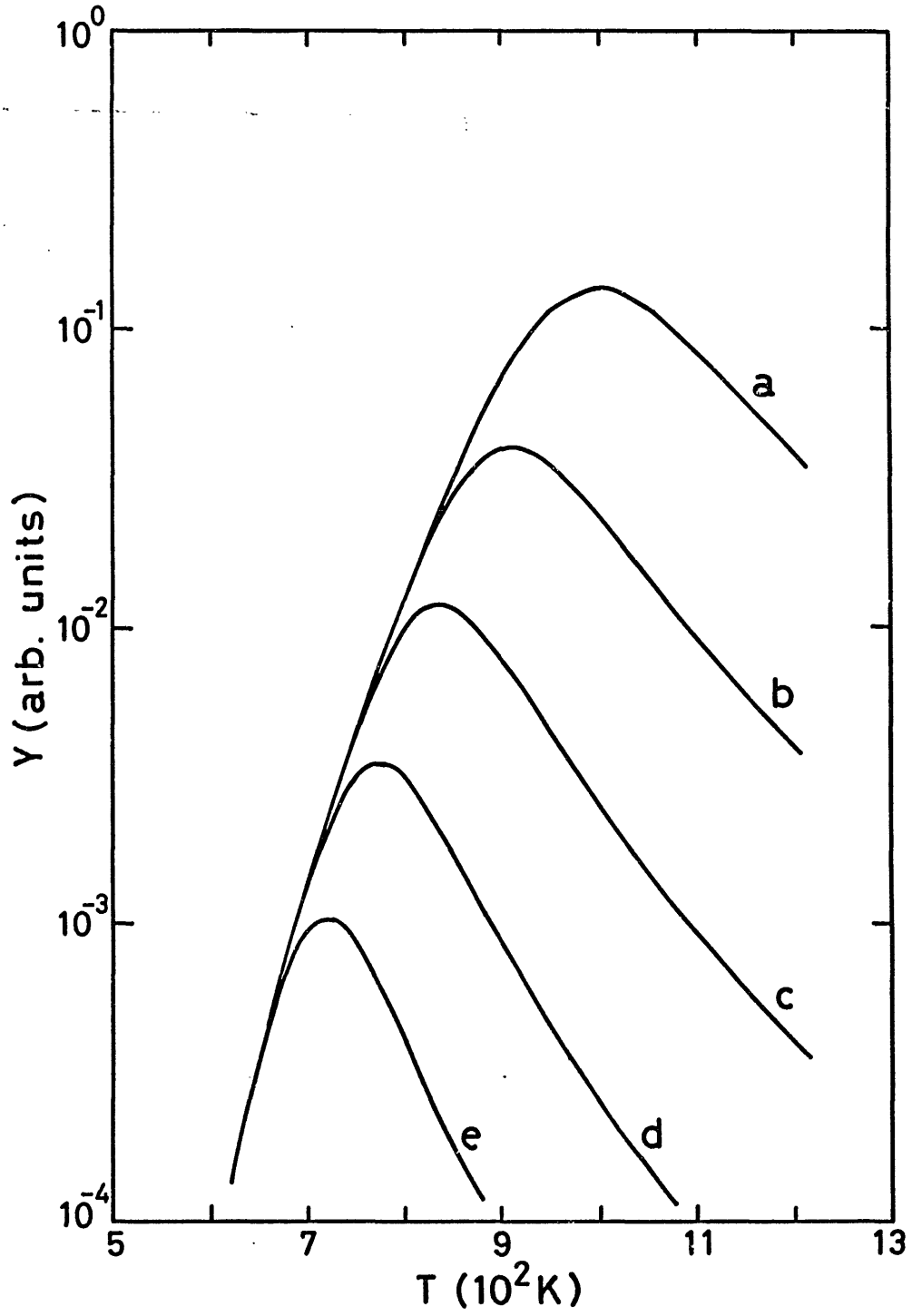

Fig. 6 Y-T relation for ϕ/c values of (a) 10^{19} cm^{-2}, (b) 10^{18} cm^{-2}, (c) 10^{17} cm^{-2}, (d) 10^{16} cm^{-2} and (e) 10^{15} cm^{-2}.

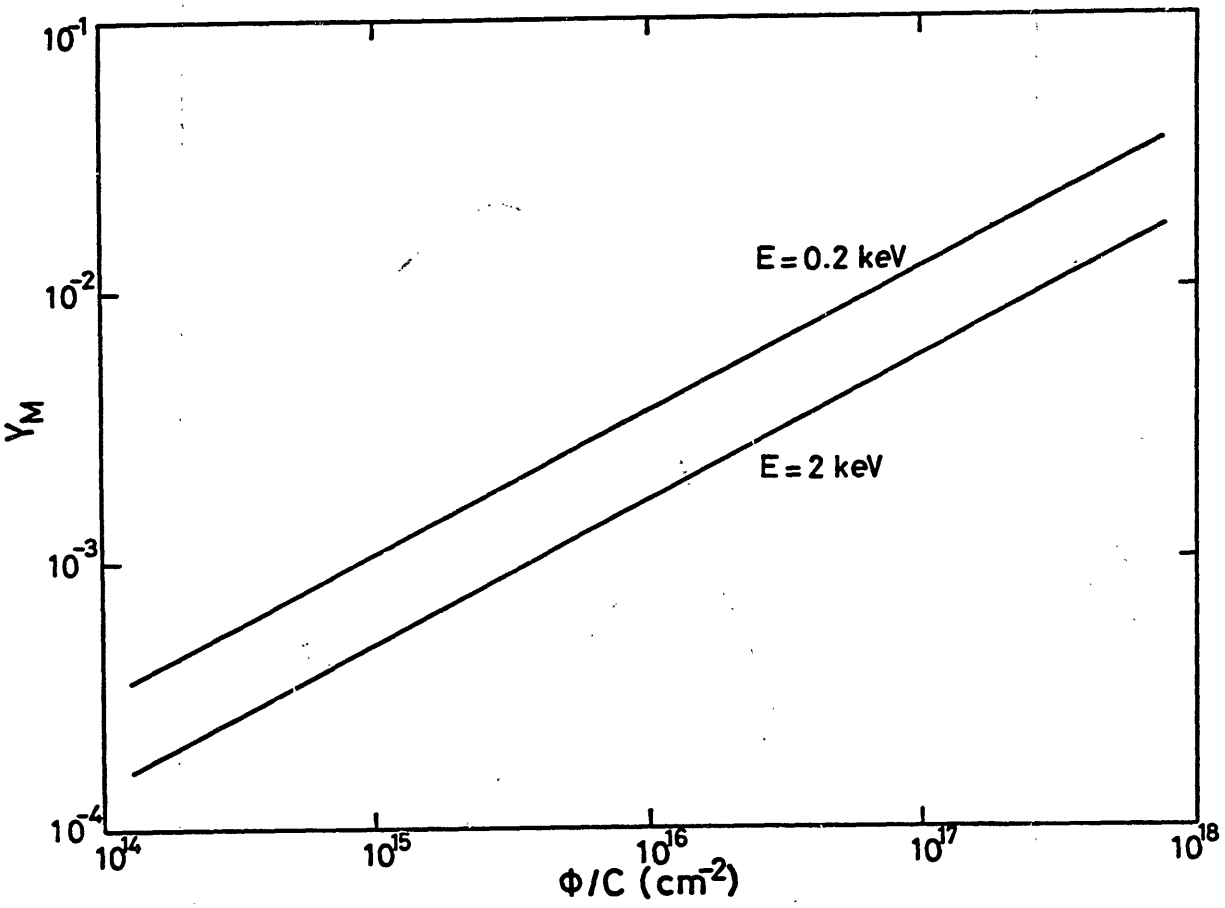

Fig. 7 The relation between the maximum yield Y_M and ϕ/c for incident energies of 0.2 and 2 keV.

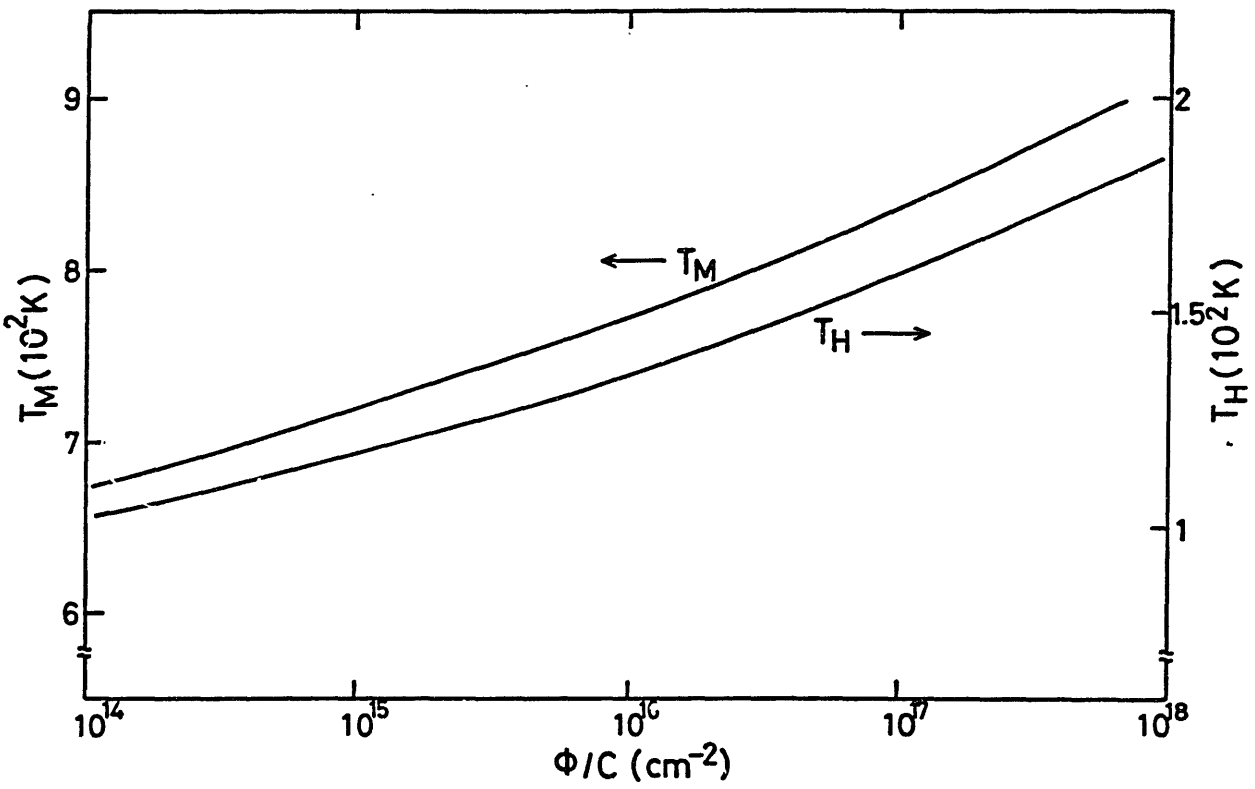

Fig. 8 The ϕ/c dependence of the temperature T_M where the maximum sputtering yield occurs and the full half-width T_M of the Y-T curves, for an incident energy of 0.2 keV.

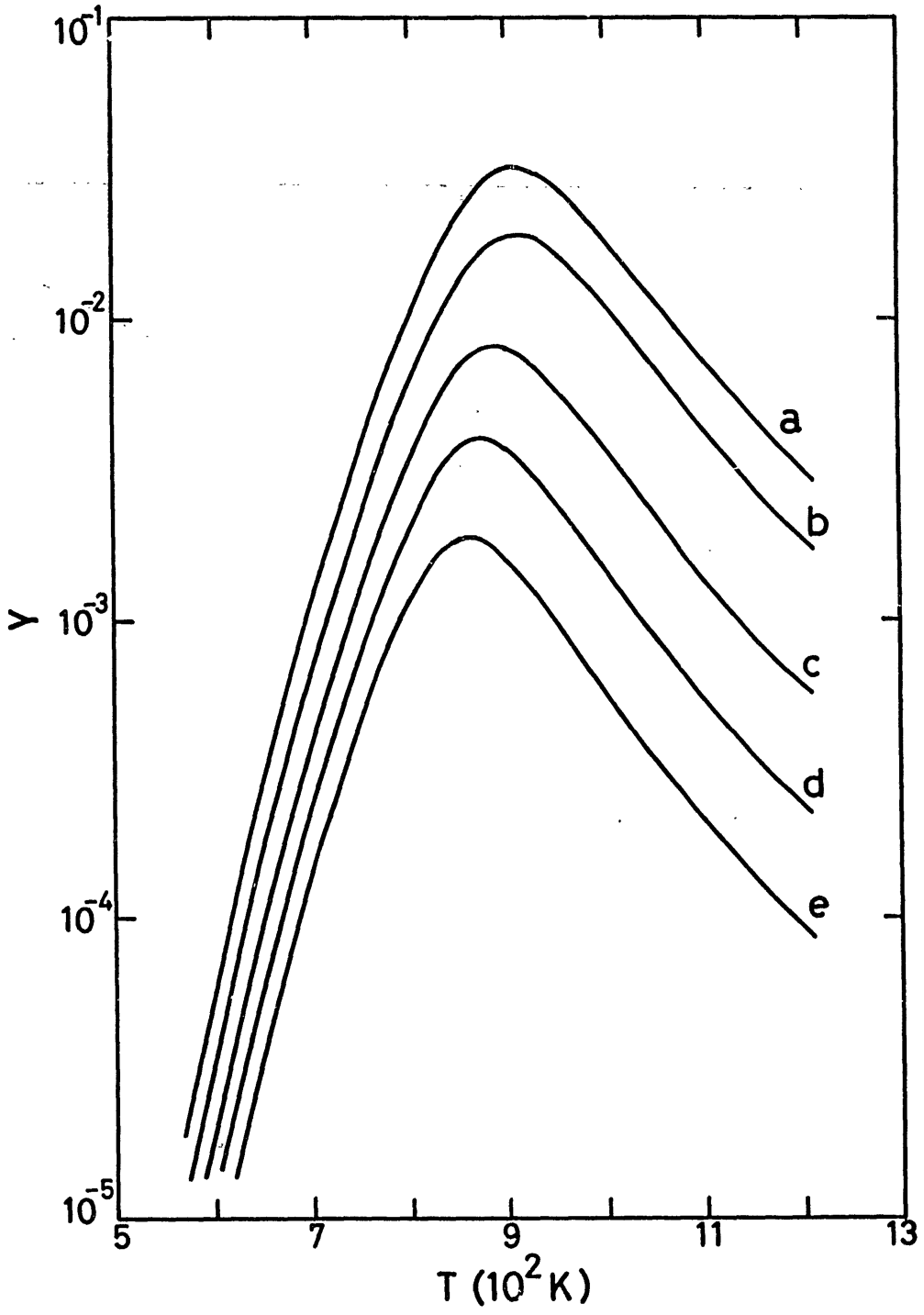

Fig. 9 Y-T curves for incident energy of (a) 0.2 keV, (b) 1 keV, (c) 5 keV, (d) 10 keV and (e) 20 keV.

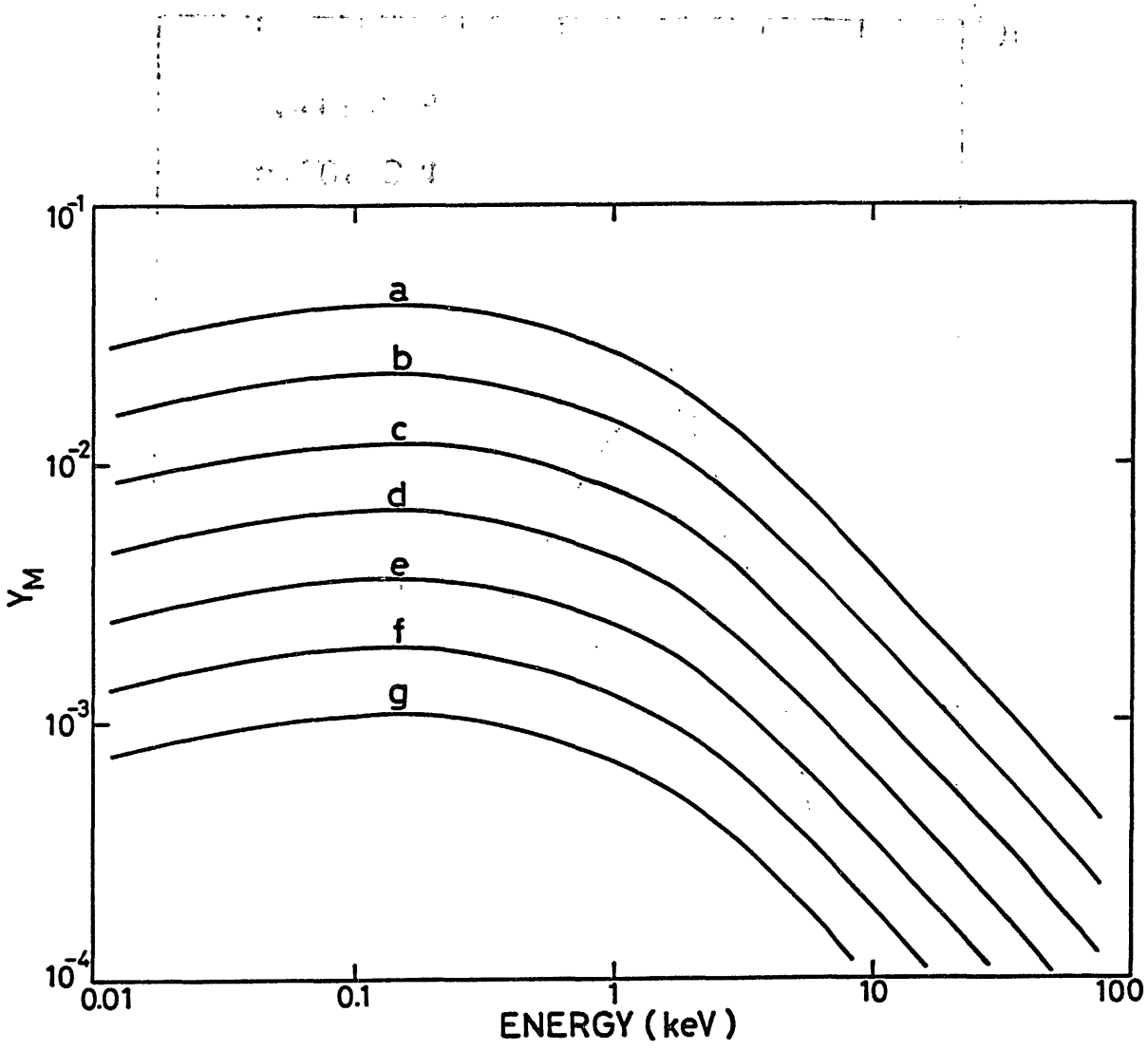

Fig. 10 Energy dependence of the maximum yield for ϕ/c values of (a) 10^{18} cm^{-2}, (b) 3.2×10^{14} cm^{-2}, (c) 10^{17} cm^{-2}, (d) 3.2×10^{16} cm^{-2}, (e) 10^{16} cm^{-2}, (f) 3.2×10^{15} cm^{-2} and (g) 10^{15} cm^{-2}.

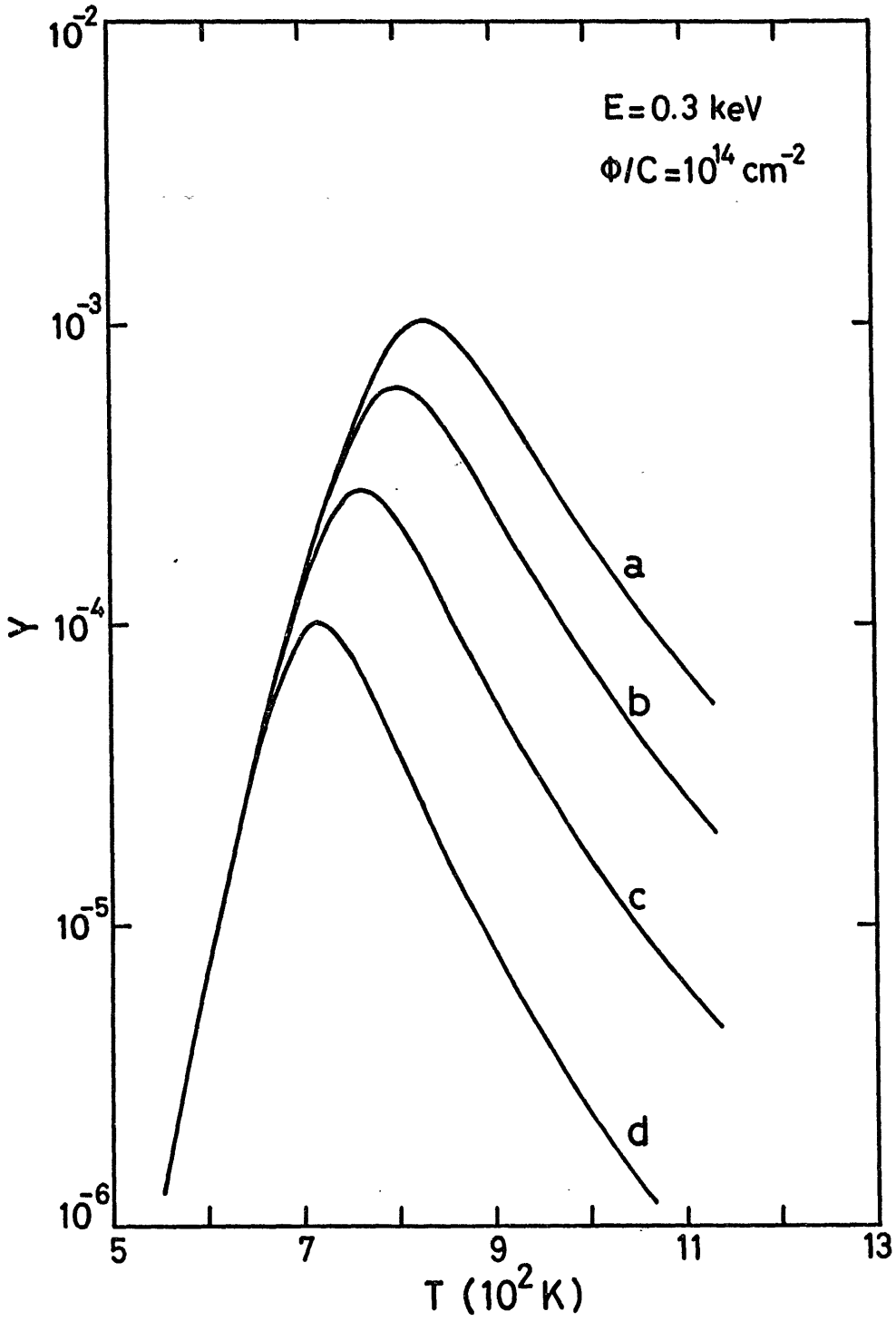

Fig. 11 Y-T curves for simultaneous irradiation of energetic H^+ ions and hydrogen atoms with fluxes of (a) 8×10^{15} cm^{-2}, (b) 3×10^{15} cm^{-2}, (c) 6×10^{14} cm^{-2} and (d) 0 cm^{-2}. The value of ϕ/c for H^+ ions is 10^{14} cm^{-2}.

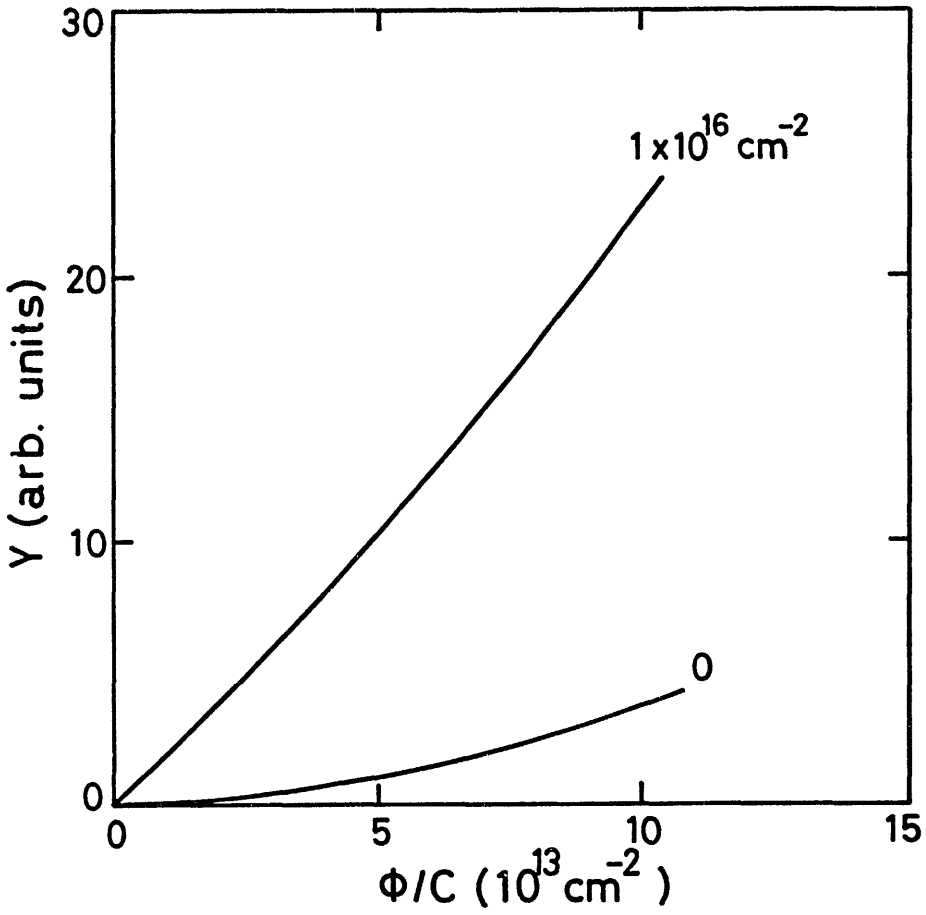

Fig. 12 The relation between the chemical sputtering yield Y and ϕ/c under simultaneous irradiation with a flux of 10^{16} cm^{-2} hydrogen atoms and without a simultaneous irradiation.

The present status of atomic and molecular data for edge plasmas

H. Tawara

Institute of Plasma Physics, Nagoya University

Nagoya 464

A brief review is given on the present situation of atomic and molecular data relevant to diagnostics and modelling of plasmas in or near low temperature edge region.

[1] main consituents in edge plasma region

The constituents in or near the edge plasma region are strongly dependent upon the materials of the first wall facing directly the plasma and their surface conditions[1]. Recently graphites or carbon-coated layers became the most popular and important materials as the first wall in order to reduce the impurities with high atomic numbers expecting to result in the reduction of radiation losses from high temperature plasma. Such graphites, under bombardment of intense hydrogen beams, can produce a series of different hydrocarbon molecules, particularly at high temperatures. This phenomena can be understood to be due to a series of chemical reactions of carbons with active atomic and molecular hydrogens at the elevated temperatures, which are called the chemical sputtering and results in the erosions of the inner surfaces of the wall. In order to reduce materials with high atomic numbers directly facing the plasma, an in-situ carbon-layer coating technique (called carbonization process) is now being developed based upon the deposition of

carbon layers formed through glow discharges or high frequency discharges of CH_4 or C_2H_2 molecules[2]. In fact, this technique is found to result in significant reduction of impurities with high atomic numbers[1].

Up to now, the detailed observation of the constituents and their abundances in the edge plasmas and how they depend upon the plasma operating conditions has not been reported. Furthermore in carbonization processes the detailed mechanisms of carbon layer formation and coating and its properties are still not known and, moreover, the best coating techniques should be developed yet[3]. However, the followings can be the most important constituents :

1) electron (relatively low energies, whose main part has the energy less than 100 eV)
2) photon (including bremsstrahlung and characteristic X-rays from highly ionized impurity ions)
3) H, H^+, H_2, H_2^+, H_3, H_3^+ : main plasma components and related components
4) He, He^+, He^{2+} : products of the burning plasma
5) O_2, O_2^+, O, O^{i+} (i=1-8), H_2O, H_2O^+, H_3O, H_3O^+, OH^+ : mainly originated from water vapor on the surfaces of the wall
6) C, C^{i+} (i=1-6), C_nH_m, $C_nH_m^+$: products from collisions of hydrogens with graphite or carbons and their dissociated products
7) CO, CO^+, CO_2, CO_2^+ : products from collisions of carbons or hydrocarbons with oxygens

8) surfaces (usually not clean but dirty or covered with an unknown amount of the unknown adsobates)

Some more detailed discussion on the present status of atomic and molecular data connected with the edge plasma can be found in a recent paper[4].

[2] Collision(cross section)data

In the plasma edge region occur a large number of the collisions involving different species which contribute to the formation of plasma and the determination of plasma properties. In this section we shall discuss briefly the present situation of atomic and molecular data on the collisions between electron, photon and heavy particle(ion, neutral). The following collision processes should play an important role in the edge plasma region :

1) Excitation processes

The excitation functions (their cross sections as a function of the collision energy) are known to be different, in particular near the threshold or low energy region, among different investigations because of technical difficulties in determining the absolute efficiencies of photon-measuring systems.

A part of the products result in photon emission in decaying into lower states and the other may be autoionized. The branching ratios in the excited states for various species are important for modelling and diagnostics of the edge plasmas.

2) Dissociation processes

The important parameters here are (1) products(branching

ratio resulting into different dissociating channels), (2) their electronic states (ground state or excited states), (3) their energy distribution, (4) their angular distribution and (5)photon emission from different products. In hydrocarbon molecules, some of their charged products from dissociative ionization have been measured. However, their neutral products or those from pure dissociation processes are not known yet.

3) Ionization processes including dissociative ionization
   Important parameters here are (1) products(branching ratio), (2) their electronic states, (3)their energy distribution, (4) their angular distribution, (5) photon emission from different products.

4) Recombination with electrons
   The recombination processes of molecular species results in dissociation or radiation emission (photon emission). AM data for hydrogen species are relatively well known but little is known for hydrocarbon species except for common species such as CH_4. Particularly, data for radicals are practically non-existing.
   It has recently been established that the recombination rates are strongly dependent upon the electronic states of collision species. That is why such information on the electronic states of the collision products is requisite in modelling of plasmas near the edge region.

5) Electron transfer processes
   Even near the edge region where the electron temperatures

are relatively low, a relatively large fraction of highly ionized impurities are present because of strong diffusion from hot plasma regions. A quite large volume of data have been obtained for collisions of these highly ionized impurities with hydrogens up to now. However, little is known for hydrocarbon molecular gases.

6) Particle transfer or chemical reactions

Near the edge region with graphites or carbon layers far more than 100 processes including a number of hydrocarbons may contribute to the formation and destruction of various ions, atoms, molecules and radicals which determine the edge plasma properties, although the number of the most dominant processes may not be so large.

[3] Interactions with surfaces

The interactions or collisions of various species with surfaces near the edge play a far more significant role, compared with purely atomic and molecular collisions between two collision partners. However, only a limited information is available on such collisions involving molecular species with the surfaces.

Sputtering

For example, the physical sputtering of materials by particles are relatively well understood from both theoretical and experimental aspects. However, the chemical sputtering processes have been recognized to be important only very recently in some plasma environments and their understanding is still limited at the moment though some synergistic effects have been found to come into a significant play under hydrogen plasmas[5].

Particularly the sputtering under intense molecular species such as those in the edge region is not yet investigated where such synergistic effects might play a role.

Physical sputtering :

1) The sputtered particles are known to be mostly neutral, with a minor contribution of the charged particles(usually less than a few per cent of total yields).
2) Their threshold behaviors, which are particularly important at low energies corresponding to those near the edge region in order to minimize the sputtering erosion, are well understood theoretically. Yet experimental confirmation for this predicted behaviors has to be made.
3) The angular distributions of the sputtered atoms, which are strongly dependent upon the incident angle, are known well.
4) The energy distributions for neutrals are also relatively known but those for ions is not well established yet, though significant parts of ions are known to have a few eV of the energy.
5) Information of the electronic states of the sputtered atoms and ions is very limited. This is particularly important in determining a fraction of ionized species or the degree of ionization of the plasma near the edge region which seem to be significantly influenced by the electronic states of the sputtered species. Only very recently some experiments have begun using the laser excitation technique, for example, although this can be applied to only some limited species.
6) Only little is known about the effects of the adsorbed species

such as oxygens or water vapors. In some cases, the presence of oxygens has been known to enhance the sputtering yields. In other cases, their presence results in reduction of sputtering yields. This effect of the adsorbates should become particularly significant at the elevated temperatures.

7) The preferential sputtering which is observed in some alloys or compound materials is not well understood yet. This results in modification of the surfaces, which is followed by the enhancement or reduction of the surface saputtering. In some compounds, the segregation processes of some of the constituent atoms onto the surfaces from the inside of bulk materials can result in formation of the self-sustaining layers of coating. This phenomena are now being tried to be used as a coating method when one of the constituents of wall materials tends to have low sputtering yields under hydrogen bombardment.

Chemical sputtering :

1) Chemical sputtering of carbon layers or graphites is enhanced significantly or non-linearly at the elevated temperatures under atomic hydrogen bombardment.
2) Information on the products from such chemical sputtering processes is very limited. Untill up to now, only CH_4 has been assumed to be produced from graphite materials. Recently it has been confirmed that a significant amount of higher order hydrocarbon molecules such as C_2H_2, C_2H_4 are produced in such chemical sputtering processes[6]. These higher order hydrocarbon molecular species should influence plasma

edge modelling itself.

3) In graphites or carbon layers, the production of hydrocarbons, for example CH_4 molecules, is believed to due to successive hydrogenation of carbon atoms through some intermediate species (for example, CH, CH_2) which are probably formed in the radiation-damaged carbon layers as well as in the surfaces. In fact the observed enhancement of sputtering yields at the elevated temperatures from very thin layers are found to be small, compared with those of graphites, indicating that the accumulated number of such intermediate species formed in the radiation-damaged region is small.

Scattering

Backscattering phenomena of atomic species from surfaces are relatively well understood but those of molecules particularly at low energies are still less understood.

Atomic species

1) In the collisions of atomic species, ions or atoms, a lot of information on particle backscattering, reflection or energy reflection has been obtained.
2) It is known that at the present energy range of interest for the edge plasmas the scattered particles are mostly neutrals, with only a fraction of charged ions.
3) However, only little is known on the electronic states of the scattered particles which may influence significantly the succeeding collision processes.
4) Although some calculations indicate that nearly 100 % atoms or

ions are trapped onto the surfaces at very low energies (less than 10 eV), no experimental confirmation is obtained yet. This is one of the most important and urgent problems to be solved in analysis of hydrogen recycling processes through the wall and plasma.

Molecular species

1) It has been confirmed in some collision processes that most of the particles reflected are neutral molecules at the collision energies less than 100 eV and only a part of them are dissociated or charged.
2) However, little is known on their electronic states after collisions with surfaces.
3) Little is also known on the collision products and their electronic states in the dissociation processes after collisions with surfaces.

Chemical reactions at the surfaces

1) It is expected that the surfaces may play a role as catalyzer for some chemical reactions in formation and destruction of hydrocarbon molecules.
2) Then the so-called synergistic processes should be important at the surfaces. Their understanding is only qualitative at best presently.
3) The importance of surface-adsorbed impurities such as oxygens or water vapors should not be forgotten even though the detailed physical and chemical processes involved are not understood quantitatively.

[4] Spectroscopic data

Atomic and ionic species

These spectroscopic data involving the energy levels, the transition energies, their intensities, their transition probabilities are relatively well known and their data are compiled for a number of species including highly charged ions.

Molecule and molecular ion species

Their spectrum shapes (band and line) are relatively well known for common hydrocarbon molecules and CO and CO_2. Sometimes those for some of their ions are also known and summarized. However, the lifetimes of their excited states and metastable states and their transition probabilities are less known. Particularly, these AM data should be noted to be influenced by their electronic states. Also radicals from these products should play a role in photon emission and other processes near the edge.

It should be noted that their electronic states under intense hydrogen plasma environments are believed to be very much different from those investigated in laboratories up to now[7]. This may result in different spectrum shapes. In fact some observations indicate quite different band distribution of rotational states from some hydrocarbon molecules in large plasma devices.

[5] Summaries

1) Not only data of collisions between atomic and molecular species but also those with surfaces are quite important in analysis of the edge plasmas.

2) Relatively well known are data involving atomic species for both collisions bewteen ion/atom/atom and collision with surfaces.

3) Only a little is known for molecular species and radicals.

4) In particular, AM data of some processes for species with different electronic states are known to be significantly different from those of the ground states and thus such effects should be investigated in detail.

5) As a consequence, it should be noted that great care should be exercised when AM data provided from laboratory experiments are going to be used in diagnostics and modelling of the edge plasmas. Indeed data for some processes are different orders of magnitude among different electronic configurations. Otherwise,we might come to serious misunderstanding[8].

[6] References

1) N.Nishino, H.Kubo, A.Sakasai, Y.Koide, T.Sugie, H.Takeuchi and JT-60 Team, this volume p.1.

2) S.Amemiya, this volume p.25.

3) H.Sugai, this volume p.

4) H.Tawara and R.A.Phaneuf, to be published in Comm. At. Mol. Phys.(1988)

5) Y.Horino, this volume p.

6) R.Yamada, this volume p.

7) K.Kondo, K.Okazaki, T.Oda, N.Noda, K.Akaishi, H.Kaneko, T.Mizuuchi, F.Sano, O.Motojima and A.Iiyoshi, this volume p.

8) H.Tawara, to be published in Physics of Atoms and Molecules Series (Plenum Press)

LIST OF IPPJ-AM REPORTS

IPPJ-AM-1* "Cross Sections for Charge Transfer of Hydrogen Beams in Gases and Vapors in the Energy Range 10 eV–10 keV"
H. Tawara (1977) [Published in Atomic Data and Nuclear Data Tables 22, 491 (1978)]

IPPJ-AM-2* "Ionization and Excitation of Ions by Electron Impact –Review of Empirical Formulae–"
T. Kato (1977)

IPPJ-AM-3 "Grotrian Diagrams of Highly Ionized Iron FeVIII-FeXXVI"
K. Mori, M. Otsuka and T. Kato (1977) [Published in Atomic Data and Nuclear Data Tables 23, 196 (1979)]

IPPJ-AM-4 "Atomic Processes in Hot Plasmas and X-Ray Emission"
T. Kato (1978)

IPPJ-AM-5* "Charge Transfer between a Proton and a Heavy Metal Atom"
S. Hiraide, Y. Kigoshi and M. Matsuzawa (1978)

IPPJ-AM-6* "Free-Free Transition in a Plasma –Review of Cross Sections and Spectra–"
T. Kato and H. Narumi (1978)

IPPJ-AM-7* "Bibliography on Electron Collisions with Atomic Positive Ions: 1940 Through 1977"
K. Takayanagi and T. Iwai (1978)

IPPJ-AM-8 "Semi-Empirical Cross Sections and Rate Coefficients for Excitation and Ionization by Electron Collision and Photoionization of Helium"
T. Fujimoto (1978)

IPPJ-AM-9 "Charge Changing Cross Sections for Heavy-Particle Collisions in the Energy Range from 0.1 eV to 10 MeV I. Incidence of He, Li, Be, B and Their Ions"
Kazuhiko Okuno (1978)

IPPJ-AM-10 "Charge Changing Cross Sections for Heavy-Particle Collisions in the Energy Range from 0.1 eV to 10 MeV II. Incidence of C, N, O and Their Ions"
Kazuhiko Okuno (1978)

IPPJ-AM-11 "Charge Changing Cross Sections for Heavy-Particle Collisions in the Energy Range from 0.1 eV to 10 MeV III. Incidence of F, Ne, Na and Their Ions"
Kazuhiko Okuno (1978)

IPPJ-AM-12* "Electron Impact Excitation of Positive Ions Calculated in the Coulomb-Born Approximation –A Data List and Comparative Survey–"
S. Nakazaki and T. Hashino (1979)

IPPJ-AM-13 "Atomic Processes in Fusion Plasmas – Proceedings of the Nagoya Seminar on Atomic Processes in Fusion Plasmas Sept. 5-7, 1979"
Ed. by Y. Itikawa and T. Kato (1979)

IPPJ-AM-14 "Energy Dependence of Sputtering Yields of Monatomic Solids"
N. Matsunami, Y. Yamamura, Y. Itikawa, N. Itoh, Y. Kazumata, S. Miyagawa, K. Morita and R. Shimizu (1980)

IPPJ-AM-15 "Cross Sections for Charge Transfer Collisions Involving Hydrogen Atoms"
Y. Kaneko, T. Arikawa, Y. Itikawa, T. Iwai, T. Kato, M. Matsuzawa, Y. Nakai, K. Okubo, H. Ryufuku, H. Tawara and T. Watanabe (1980)

IPPJ-AM-16 "Two-Centre Coulomb Phaseshifts and Radial Functions"
H. Nakamura and H. Takagi (1980)

IPPJ-AM-17 "Empirical Formulas for Ionization Cross Section of Atomic Ions for Electron Collisions –Critical Review with Compilation of Experimental Data–"
Y. Itikawa and T. Kato (1981)

IPPJ-AM-18 "Data on the Backscattering Coefficients of Light Ions from Solids"
T. Tabata, R. Ito, Y. Itikawa, N. Itoh and K. Morita (1981) [Published in Atomic Data and Nuclear Data Tables 28, 493 (1983)]

IPPJ-AM-19 "Recommended Values of Transport Cross Sections for Elastic Collision and Total Collision Cross Section for Electrons in Atomic and Molecular Gases"
M. Hayashi (1981)

IPPJ-AM-20 "Electron Capture and Loss Cross Sections for Collisions between Heavy Ions and Hydrogen Molecules"
Y. Kaneko, Y. Itikawa, T. Iwai, T. Kato, Y. Nakai, K. Okuno and H. Tawara (1981)

IPPJ-AM-21 "Surface Data for Fusion Devices – Proceedings of the U.S–Japan Workshop on Surface Data Review Dec. 14-18, 1981"
Ed. by N. Itoh and E.W. Thomas (1982)

IPPJ-AM-22 "Desorption and Related Phenomena Relevant to Fusion Devices"
Ed. by A. Koma (1982)

IPPJ-AM-23 "Dielectronic Recombination of Hydrogenic Ions"
T. Fujimoto, T. Kato and Y. Nakamura (1982)

IPPJ-AM-24 "Bibliography on Electron Collisions with Atomic Positive Ions: 1978 Through 1982 (Supplement to IPPJ-AM-7)"
Y. Itikawa (1982) [Published in Atomic Data and Nuclear Data Tables 31, 215 (1984)]

IPPJ-AM-25 "Bibliography on Ionization and Charge Transfer Processes in Ion-Ion Collision"
H. Tawara (1983)

IPPJ-AM-26 "Angular Dependence of Sputtering Yields of Monatomic Solids"
Y. Yamamura, Y. Itikawa and N. Itoh (1983)

IPPJ-AM-27 "Recommended Data on Excitation of Carbon and Oxygen Ions by Electron Collisions"
Y. Itikawa, S. Hara, T. Kato, S. Nakazaki, M.S. Pindzola and D.H. Crandall (1983) [Published in Atomic Data and Nuclear Data Tables 33, 149 (1985)]

IPPJ-AM-28 "Electron Capture and Loss Cross Sections for Collisions Between Heavy Ions and Hydrogen Molecules (Up-dated version of IPPJ-AM-20)
H. Tawara, T. Kato and Y. Nakai (1983) [Published in Atomic Data and Nuclear Data Tables 32, 235 (1985)]

IPPJ-AM-29 "Bibliography on Atomic Processes in Hot Dense Plasmas"
T. Kato, J. Hama, T. Kagawa, S. Karashima, N. Miyanaga, H. Tawara, N. Yamaguchi, K. Yamamoto and K. Yonei (1983)

IPPJ-AM-30 "Cross Sections for Charge Transfers of Highly Ionized Ions in Hydrogen Atoms (Up-dated version of IPPJ-AM-15)"
H. Tawara, T. Kato and Y. Nakai (1983) [Published in Atomic Data and Nuclear Data Tables 32, 235 (1985)]

IPPJ-AM-31 "Atomic Processes in Hot Dense Plasmas"
T. Kagawa, T. Kato, T. Watanabe and S. Karashima (1983)

IPPJ-AM-32 "Energy Dependence of the Yields of Ion-Induced Sputtering of Monatomic Solids"
N. Matsunami, Y. Yamamura, Y. Itikawa, N. Itoh, Y. Kazumata, S. Miyagawa, K. Morita, R. Shimizu and H. Tawara (1983) [Published in Atomic Data and Nuclear Data Tables 31, 1 (1984)]

IPPJ-AM-33 "Proceedings on Symposium on Atomic Collision Data for Diagnostics and Modelling of Fusion Plasmas, Aug. 29 – 30, 1983"
Ed. by H. Tawara (1983)

IPPJ-AM-34 "Dependence of the Backscattering Coefficients of Light Ions upon Angle of Incidence"
T. Tabata, R. Ito, Y. Itikawa, N. Itoh, K. Morita and H. Tawara (1984)

IPPJ-AM-35 "Proceedings of Workshop on Synergistic Effects in Surface Phenomena Related to Plasma-Wall Interactions, May 21 – 23, 1984"
Ed. by N. Itoh, K. Kamada and H. Tawara (1984) [Published in Radiation Effects 89, 1 (1985)]

IPPJ-AM-36 "Equilibrium Charge State Distributions of Ions ($Z_1 \geqq 4$) after Passage through Foils – Compilation of Data after 1972"
K. Shima, T. Mikumo and H. Tawara (1985) [Published in Atomic Data and Nuclear Data Tables 34, 357 (1986)]

IPPJ-AM-37 "Ionization Cross Sections of Atoms and Ions by Electron Impact"
H. Tawara, T. Kato and M. Ohnishi (1985) [Published in Atomic Data and Nuclear Data Tables 36, 167 (1987)]

IPPJ-AM-38 "Rate Coefficients for the Electron-Impact Excitations of C-like Ions"
Y. Itikawa (1985)

IPPJ-AM-39 "Proceedings of the Japan-U.S. Workshop on Impurity and Particle Control, Theory and Modeling, Mar. 12 – 16, 1984"
Ed. by T. Kawamura (1985)

IPPJ-AM-40 "Low-Energy Sputterings with the Monte Carlo Program ACAT"
Y. Yamamura and Y. Mizuno (1985)

IPPJ-AM-41 "Data on the Backscattering Coefficients of Light Ions from Solids (a Revision)"
R. Ito, T. Tabata, N. Itoh, K. Morita, T. Kato and H. Tawara (1985)

IPPJ-AM-42 "Stopping Power Theories for Charged Particles in Inertial Confinement Fusion Plasmas (Emphasis on Hot and Dense Matters)"
S. Karashima, T. Watanabe, T. Kato and H. Tawara (1985)

IPPJ-AM-43 "The Collected Papers of Nice Project/IPP, Nagoya"
Ed. by H. Tawara (1985)

IPPJ-AM-44 "Tokamak Plasma Modelling and Atomic Processes"
Ed. by T. Kawamura (1986)

IPPJ-AM-45 Bibliography of Electron Transfer in Ion-Atom Collisions
H. Tawara, N. Shimakura, N. Toshima and T. Watanabe (1986)

IPPJ-AM-46 "Atomic Data Involving Hydrogens Relevant to Edge Plasmas"
H. Tawara, Y. Itikawa, Y. Itoh, T. Kato, H. Nishimura, S. Ohtani, H. Takagi, K. Takayanagi and M. Yoshino (1986)

IPPJ-AM-47 "Resonance Effects in Electron-Ion Collisions"
Ed. by H. Tawara and G. H. Dunn (1986)

IPPJ-AM-48 "Dynamic Processes of Highly Charged Ions (Proceedings)"
Ed. by Y. Kanai and S. Ohtani (1986)

IPPJ-AM-49 "Wavelengths of K X-Rays of Iron Ions"
T. Kato, S. Morita and H. Tawara (1987)

IPPJ-AM-50 "Proceedings of the Japan-U.S. Workshop P-92 on Plasma Material Interaction/High Heat Flux Data Needs for the Next Step Ignition and Steady State Devices, Jan. 26 – 30, 1987"
Ed. by A. Miyahara and K. L. Wilson (1987)

IPPJ-AM-51 "High Heat Flux Experiments on C-C Composite Materials by Hydrogen Beam at the 10MW Neutral Beam Injection Test Stand of the IPP Nagoya"
H. Bolt, A. Miyahara, T. Kuroda, O. Kaneko, Y. Kubota, Y. Oka and K. Sakurai (1987)

IPPJ-AM-52 "Energy Dependence of Ion-Induced Sputtering Yields of Monatomic Solids in the Low Energy Region"
N. Matsunami, Y. Yamamura, N. Itoh, H. Tawara and T. Kawamura (1987)

IPPJ-AM-53 "Data Base on the High Heat Flux Behaviour of Metals and Carbon Materials for Plasma Facing Components – Experiments at the 10 MW Neutral Beam Injection Test Stand of the IPP Nagoya"
H. Bolt, C. D. Croessmann, A. Miyahara, T. Kuroda and Y. Oka (1987)

IPPJ-AM-54 "Final (n, ℓ) State-Resolved Electron Capture by Multiply Charged Ions from Neutral Atoms"
N. Shimakura, N. Toshima, T. Watanabe and H. Tawara (1987)

IPPJ-AM-55 "Atomic Data for Hydrogens in Collisions with Electrons – Addenda to IPPJ-AM-46"
H. Tawara, Y. Itikawa, H. Nishimura and M. Yoshino (1987)

IPPJ-AM-56 "Total and Partial Cross Sections for Electron Capture for C^{q+} (q= 6–2) and O^{q+} (q=8–2) Ions in Collisions with H, H_2 and He Atoms"
H. Tawara (1987)

IPPJ-AM-57 "Atomic Models for Hot Dense Plasmas"
K. Fujima (1988)

IPPJ-AM-58 "Recommended Data for Excitation Rate Coefficients of Helium Atoms and Helium-Like Ions by Electron Impact"
T. Kato and S. Nakazaki (1988)

IPPJ-AM-59 "Atomic and Molecular Processes in Edge Plasmas Including Hydrocarbon Molecules"
Ed. by H. Tawara (1988)

Available upon request to Research Information Center, Institute of Plasma Physics, Nagoya University, Nagoya 464, Japan, except for the reports noted with*.